



If you have discovered material in AURA which is unlawful e.g. breaches copyright, (either yours or that of a third party) or any other law, including but not limited to those relating to patent, trademark, confidentiality, data protection, obscenity, defamation, libel, then please read our [Takedown Policy](#) and [contact the service](#) immediately

STRUCTURAL BEHAVIOUR AND DESIGN  
OF LOAD-BEARING FALSEWORK

D. HINDSON

A THESIS SUBMITTED FOR THE DEGREE OF  
DOCTOR OF PHILOSOPHY

JULY 1978

# STRUCTURAL BEHAVIOUR AND DESIGN OF LOAD BEARING FALSEWORK

DAVID CHARLES HINDSON

A THESIS SUBMITTED FOR THE DEGREE OF DOCTOR OF PHILOSOPHY

JULY 1978

## SUMMARY

The object of this research was to investigate the behaviour of birdcage scaffolding as used in falsework structures, assess the suitability of existing design methods and make recommendations for a set of design rules. Since excessive deflection is as undesirable in a structure as total collapse, the project was divided into two sections. These were to determine the ultimate vertical and horizontal load-carrying capacity and also the deflection characteristics of any falsework. So theoretical analyses were developed to ascertain the ability of both the individual standards to resist vertical load, and of the bracing to resist horizontal load. Furthermore a model was evolved which would predict the horizontal deflection of a scaffold under load using strain energy methods. These models were checked by three series of experiments. The first was on individual standards under vertical load only. The second series was carried out on full scale falsework structures loading vertically and horizontally to failure. Finally experiments were conducted on scaffold couplers to provide additional verification of the method of predicting deflections.

This thesis gives the history of the project and an introduction into the field of scaffolding. It details both the experiments conducted and the theories developed and the correlation between theory and experiment. Finally it makes recommendations for a design method to be employed by scaffolding designers.

KEY WORDS : FALSEWORK, SCAFFOLDING, BUCKLING, DEFLECTION

## ACKNOWLEDGEMENTS

I wish to express my sincere thanks to my supervisors for their support, understanding and guidance during the course of this research, namely :

Professor M. Holmes, Ph.D., D.Sc., C.Eng., F.I.C.E.,  
Head of Department of Civil Engineering,  
University of Aston

Mr. C.F. Turner, M.I.Struct.E., M.I.Weld.E.,  
Technical Director, Rapid Metal Developments Ltd.

Mr. M.K. Hussey  
I.H.D. Department, University of Aston

Also to the many people who to a greater or lesser extent have assisted me at various times during this project, including :

R.M.D. for their financial support and especially  
Mr. K.J. Cadman, all employees of R.M.D. regardless  
of the size of their involvement, the technicians of the  
Civil Engineering Department, The University of Aston in  
Birmingham, and the staff of the I.H.D. Department.

# STRUCTURAL BEHAVIOUR AND DESIGN OF LOAD BEARING FALSEWORK

	<u>Page</u>
Title page	1
Summary	2
Acknowledgements	3
Contents page	4
Preface	6
1. INTRODUCTION	7
2. RESEARCH PAST AND PRESENT	9
2.1 Glossary of terms	10
2.2 Structural and other differences between U.P. scaffolding and tube and fittings	13
2.3 Review of current and recent scaffolding research	16
3. SUMMARY OF THE PROJECT	20
3.1 History of the project	21
3.2 Details of experiments carried out during the project	24
4. INTRODUCTION TO THE THEORETICAL ANALYSIS EMPLOYED AND ASSUMPTIONS MADE	29
4.1 Introduction to the theoretical analysis	30
4.2 Assumptions made and their justification	32
4.3 List of symbols used	38
5. THE DEFLECTION OF U.P. SCAFFOLDING UNDER LOAD	40
5.1 The importance of deflections	41
5.2 Comparison between observed characteristics and elastic behaviour	43
5.3 The prediction of horizontal deflections using a strain energy method	49
5.4 Correlation between theory and experiment	53

	<u>Page</u>
6. THE LOAD CARRYING CAPACITY OF A BRACED FRAME	58
6.1 Externally and internally generated horizontal loads	59
6.2 The ultimate load carrying capacity of a braced bay	72
6.3 Correlation between theoretical and recorded slip load of a coupler	78
7. THE BUCKLING OF STANDARDS	80
7.1 The determination of effective length	82
7.2 The determination of buckling load	107
7.3 Correlation between theory and experiment on buckling of a standard	113
8. CONCLUSIONS AND RECOMMENDATIONS	118
8.1 Recommendations for design procedure	119
8.2 Effects of the project	119
8.3 Recommendations for further work	121
9. REFERENCES	123
10. DRAWING	
Fig. 3.2 - General arrangement of full scale assembly experiments	
11. SUMMARY OF FULL SCALE ASSEMBLY EXPERIMENTAL RESULTS	

## PREFACE

This project has been realised through the Interdisciplinary Higher Degree Scheme at the University of Aston. The scheme enables private companies or public bodies to sponsor research which is of particular interest to them. This is done by employing a graduate who works both at the University and within the sponsors' own organisation. The two groups jointly supervise the project, a main supervisor being drawn from the former to ensure academic content and an industrial supervisor from the latter to ensure continued relevance to the company's needs. The student works for three years, during which time he attends lectures and courses on various management topics. At the end of the period he will normally be awarded a Ph.D. and hopefully be equipped to solve real world problems.

The sponsor for this particular project was Rapid Metal Developments Ltd., (R.M.D.), of Aldridge. This medium sized company was formed in 1948 and is a member of the R.M. Douglas group of companies. It designs and supplies construction equipment, particularly proprietary formwork and scaffolding systems. The company's export success was marked in 1975 with the presentation of the Queens Award to Industry.

## INTRODUCTION

It is an unfortunate truth that many engineering advances are only made as a result of catastrophic failures. The famous example, of course, is that of the Tay Bridge whose collapse brought about a full investigation into the magnitude of wind loading on a structure. More recently the inadequacies of suspension bridge decks and box girders were brought to light in the same way. As far as scaffolding is concerned, it took the collapse of a bridge deck falsework over the River Loddon and the death of three men, in October 1972, to attract the attention of the engineering profession.

Under pressure from the construction Unions, the Secretary of State for Employment appointed an expert committee to look into safety levels of temporary structures and at site responsibilities. This was the Bragg Committee. As often happens under these circumstances, debate was not confined to the appointed group. Problems were identified and discussed throughout the industry. Seminars and lectures were organised by professional bodies and research establishments. One result of this attention was that scaffolding suppliers began to question their design methods which were, and in many cases still are, based on BS 449 - Specification for the use of structural steel in buildings. The main inference of the approach is that the failure load of the strut is related to the vertical distance between horizontal members.

So it was that Rapid Metal Developments Ltd. approached the University of Aston with a view to sponsoring research on their own proprietary scaffolding, the Trade Name of which is U.P. Scaffold (Universal Purpose). Many areas were identified for investigation but the scope



was soon limited to a study of the behaviour of the scaffold under known loads and the formulation of rules for design purposes.

This meant that the work would not duplicate any of the known research either past or present. Rather it would be complementary to the work that other establishments were preparing at that time.

# 2

## RESEARCH PAST AND PRESENT

This chapter is in three sections. Firstly a glossary of terms used throughout the thesis and indeed, throughout the industry. Secondly a survey of the different types of proprietary scaffolds available and in particular a description of the type studied in this report. This section also includes a discussion of the differences between such a proprietary scaffold and the traditional tube and fittings scaffolding. Finally, there is a review of research past and present in the scaffolding field.

## 2.1 GLOSSARY OF TERMS

Below is a list of terms used in this thesis. A more complete list can be obtained from reference 3. (See also Fig. 2.1)

Base, Adjustable Base	The bottom member which transmits the load from the standard to the ground. It normally contains some method of adjustment for erection of scaffold on rough terrain.
Bay, Bay size	The plan distance between standards in a given frame.
Brace, Bracing	A system of tubes and couplers designed to prevent excessive horizontal deflection.
Clevis	That part of the proprietary joint connected to the ledger or transom (see lug).
Coupler	A device for connecting two scaffold tubes together.
Cross Brace	Bracing arrangement when two braces are in the same bay and lift.
Falsework	That part of a temporary structure which supports the formwork.
Foot Tube	A scaffold tube joining the bases of adjacent standards in the same frame.

Forkhead	A member with a 'U' shaped top to support the formwork and transmit the load to the standard. It sometimes contains an adjusting mechanism for sloping soffits.
Formwork	The timber or steel surface which encloses and thus determines the final shape of concrete.
Frame	The scaffolding along one grid line. Sometimes called a fence.
Head Tube	A scaffold tube joining the forkheads of adjacent standards in the same frame.
Header Beam	A steel or timber beam spanning between forkheads and which supports the formwork.
Ledger	A long horizontal member (see Transom).
Lift, Lift height	The vertical distance between ledgers or transoms.
Lug	That part of the proprietary joint which is connected to the standard (see Clevis).
Lug Cluster	A set of four lugs connected to the standard all at the same level but at 90° to each other.
Spigot	Proprietary joint which locates one standard on top of another.

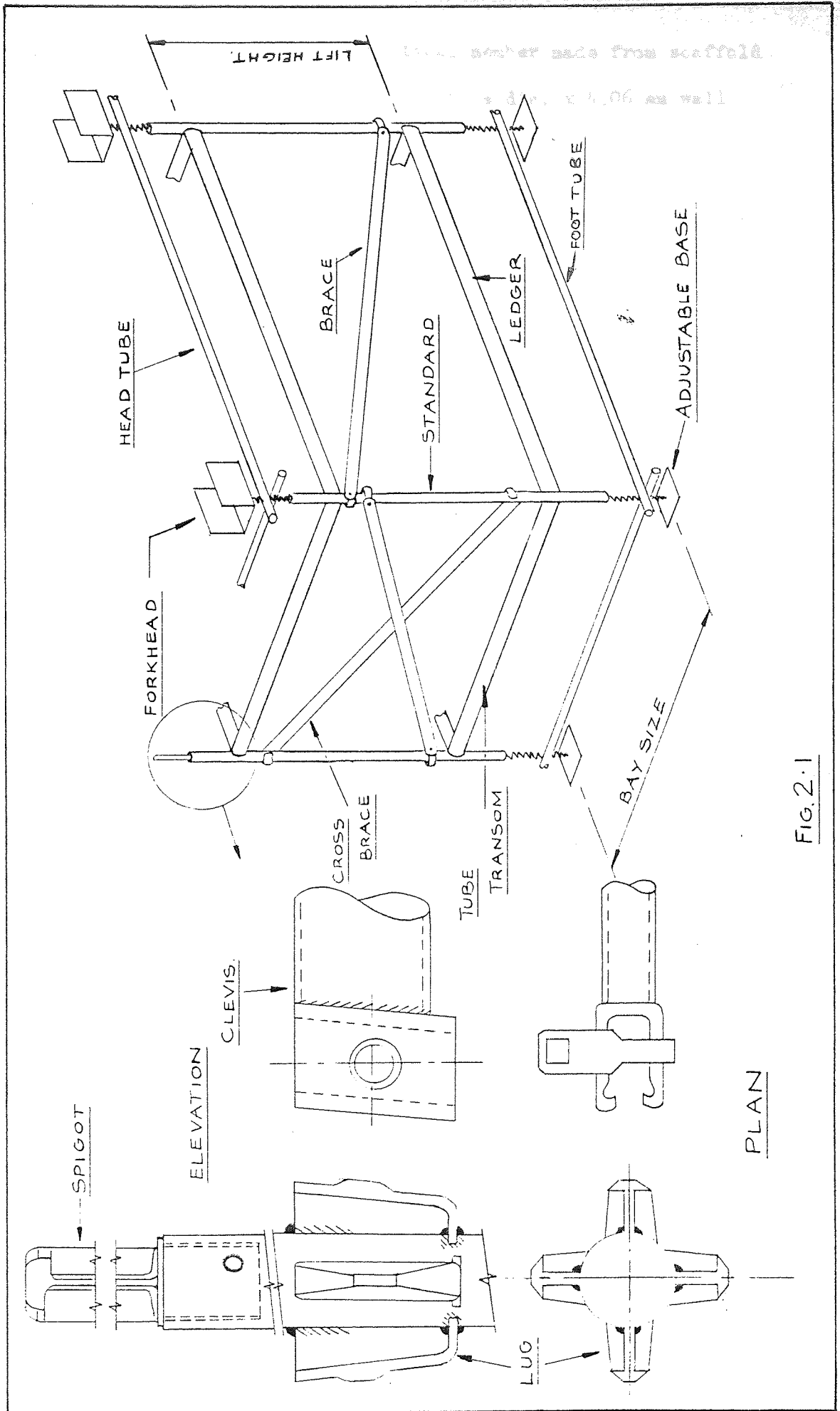


FIG. 2.1

Standard	A vertical member made from scaffold tube (48.4 mm dia. x 4.06 mm wall thickness).
Transom	A short horizontal member (see Ledger).

## 2.2 STRUCTURAL AND OTHER DIFFERENCES BETWEEN U.P. SCAFFOLDING AND TUBE AND FITTINGS

Originally all scaffolding structures were built of timber cut into rectangular sections and nailed or lashed together. About 1920 tubular steel scaffolding began to appear and because of its obvious advantages over timber, the latter soon died out. Much later proprietary systems were introduced and these have gradually been taking more and more of the market.

There are many types of proprietary scaffolds which various people have attempted to classify. According to Brand's (ref.4) classification, U.P. scaffolding is a 'tube component modular system.' According to Obbard (ref.5) it falls into Category 2, a 'non-triangulated H frame.'

The system is composed of standards and ledgers which are connected by means of a patented joint. As can be seen from Fig. 2.1, one part of the joint (the lug) is welded to the standard in clusters of four. These clusters are spaced at 1'7 $\frac{1}{2}$ " (496 mm) centres along the tube. The other part of the joint (clevis) is welded to the ledger which is available in fixed lengths of 8'0" (2440 mm) and 6'0" (1830 mm) or to a transom, (4'2" or 1270 mm). Obviously there are differences both practically and structurally. These can be summarised as follows :

### Practical Differences

- (a) Proprietary systems have few, if any, loose fittings. This saves erection time and loss of components on site.
- (b) It is difficult to erect proprietary systems incorrectly and so they may be erected by semi-skilled labour. Tube and fittings are normally erected by trained scaffolders; to avoid omission of members and ensure proper tightening of joints.
- (c) Tube and fittings are more versatile. Proprietary systems are most efficient when used over a large orthogonal area so that the modules fit conveniently.
- (d) The material cost of tube and fittings is less than that of a proprietary system. This must be weighed against the fact that for reasons given above a proprietary system is cheaper to erect.

### Structural Differences

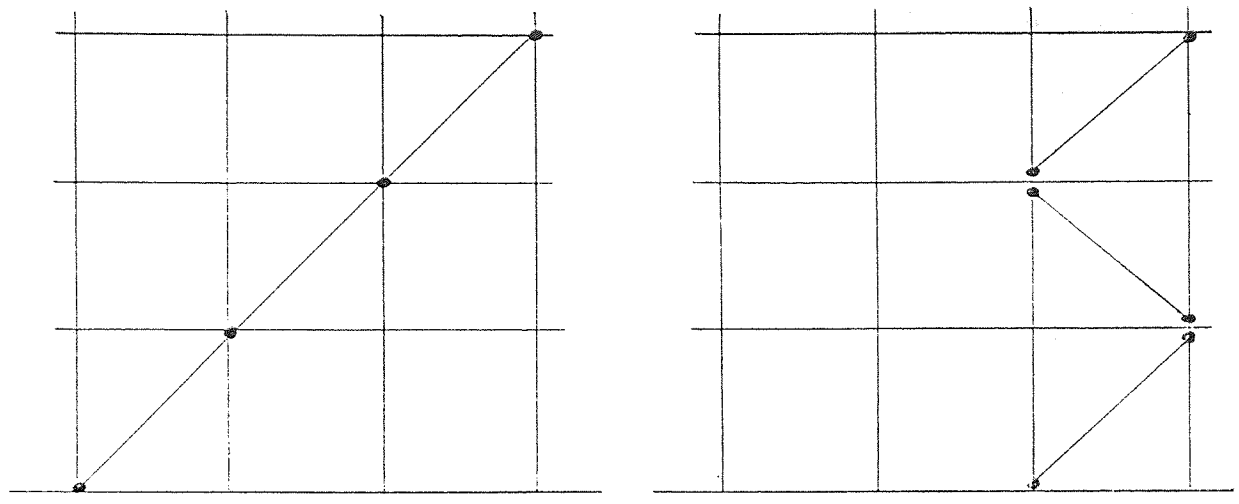
- (e) Traditional scaffolds are built from 21' (6.5m) scaffold tubes and this has two effects. Firstly a horizontal may span between three or four verticals and this continuity means a greater plan stiffness than one would expect from a system scaffold where horizontals only span between two verticals. Secondly, vertical members also have more continuity and thus buckling modes for proprietary systems and tube and fittings would be different.
- (f) The patented joints of a proprietary system are generally stiffer than those used in traditional scaffolds. Although

this makes little difference to the overall frame stiffness of a properly braced structure, it can affect the buckling load of an individual standard.

- (g) In system scaffolds the lift height is limited to a multiple of the distance between lug clusters. Often, therefore, the distance between ledgers is less than the optimum lift height for the loads the structure is to carry.
- (h) In some ways proprietary systems can be erected more accurately than tube and fittings. The distance from centre to centre of standards is set automatically by ledger length and so once one standard is erected plumb, all the others must be plumb. This is not the case with tube and fittings. Other imperfections such as eccentricity of loading are of course applicable to both.
- (j) With proprietary systems braces and ledgers tend to be connected to the standard very close together. This is better structurally since it reduces local bending in the standard.
- (k) The method of bracing tends to differ between the two types of scaffold (see Fig. 2.2). In tube and fittings scaffold a long continuous brace is used to minimise the number of connections whereas in proprietary systems one bay is usually braced using a special member.



including, including a  
of the problem



TUBE & FITTINGS SCAFFOLD

PROPRIETARY SCAFFOLD.

FIG 2.2

2.3 A REVIEW OF CURRENT AND RECENT SCAFFOLDING RESEARCH

N. Birch (Birmingham University)

The work of Mr. Birch's team has been confined to adjustable steel props. He has tested new and old props in three different ways and made recommendations for safe working loads. His work is relevant in that he carried out site surveys to determine how the equipment was actually used. In particular he analysed the frequency and magnitude of out-of-plumb erection and eccentricity of loading. It could be argued that the latter is typical of the way proprietary systems are used.

See reference 6.

R.E. Brand (formerly of Thames Polytechnic)

Mr. Brand has been working in the scaffolding field for some time. His work has mainly been on tube and fittings type structures, and includes the following :

Firstly, a general introduction into scaffolding, including a review of the equipment available and some of the problems associated with design. Secondly, tests on the stability of full scale sub-assemblies. Thirdly, stability tests on  $\frac{1}{4}$  scale model structures of timber and steel. He has also done some work on the characteristics of couplers and, more recently, published a book on scaffolding.

See references 3, 4 and 7.

#### John Laing Research and Development

John Laing Research and Development have been busy in the field of scaffolding in recent years. Firstly, they carried out a literature survey and from this determined what research they considered necessary to meet the needs of the industry. They concluded that manufacturers of proprietary equipment were not giving enough guidance in the use of their equipment. Secondly, they conducted site surveys in which, using a specially designed gauge, they measured loads in standards during concreting operations.

See reference 8.

#### E. Lightfoot (Oxford University)

Doctor Lightfoot has been involved in the theoretical and practical aspects of scaffolding in his work at Oxford University. On the theoretical side his team has developed two computer programmes. One programme derives the maximum load from the condition that at this load the determinant of stiffness matrix is zero. The second is a finite element programme which assumes elastic connections.

On the experimental side he has measured the characteristics of

couplers on a purpose designed rig and tested full size towers under vertical load. His findings have been published in a number of papers, but his work has been confined to tube and fittings scaffolding.

See reference 9 - 16.

#### Tarmac Construction Ltd.

Under a contract from B.R.E., Tarmac have recently completed an investigation into the site usage of scaffolding. They have studied both falsework and access scaffolds in both proprietary systems and tube and fittings. They have measured such features as out-of-plumb erection and eccentricity of loading.

#### Basic Research

Certain basic engineering research is, of course, relevant to scaffolding. Perhaps the most important advances recently have been in the field of strut buckling theory, and in particular, buckling of tubes. Proposals for a new unified European code for steelwork take into account the difference between tubes and other sections, and thus will supersede the existing Perry-Robertson formula of BS.449. See reference 21.

#### Capt. R.C. Obbard (Royal School of Military Engineering)

Captain Obbard has developed a design method which involves calculating the stiffness of a scaffold structure in three planes. It is based on the assumption that vertical frames have uniform flexibility per unit height and are held by elastic restraints. This restraint is provided on every frame by either tying in or bracing, and on intermediate frames by continuity of horizontal members. It is his use of this plan continuity which

makes the method unsuitable for proprietary systems.

See references 5, 17, 18.

#### Transport and Road Research Laboratory

The T.R.R.L. became involved in falsework at the time of the Loddon collapse. At that time they tested components similar to those used in the bridge deck falsework. Since then their main involvement has been the letting of contracts to Doctor Lightfoot at Oxford. They have also contributed significantly by developing a strain gauge suitable for scaffold tube. This has been used to monitor loads under site conditions on falsework structures along the M27.

See references 19, 20.

#### Building Research Establishment

The B.R.E. have not yet done any 'in-house' research of their own. They have in the past let contracts to Doctor Lightfoot and to Tarmac. However, they intend to institute a test programme to study wind loading on scaffolding.

## SUMMARY OF THE PROJECT

# 3

Chapters one and two give an account of the events which led to the setting up of the Bragg Committee and the reaction of industry to its inception. Having given an account of the work of various researchers it is now possible to discuss how the aims of this project were formalised and what steps were taken to achieve those aims. This is done here in Chapter three.

### 3.1 HISTORY OF THE PROJECT

In order to give R.M.D. a worthwhile return for their money, the intention was to produce a series of design rules for use in the company's drawing office. At the start of the project it was envisaged that this would require work which could be categorized as shown below although obviously there would be interaction between these three areas :

- Collection and examination of existing information
- Collection of site data
- Theoretical analysis and experimental work

It was expected that the aims of the project and methods used to achieve those aims would vary with time and just how they varied is explained below.

#### 3.1.1 Collection and examination of existing information

It was hoped that a survey of existing information and of research past and present would generate ideas for a theoretical analysis of scaffold under load. Within a few months of the start of the project this survey was substantially complete. However, almost all the "relevant" published research was either concerned with tube and fittings scaffolding or else was very general work such as column design for buildings. R.M.D.'s own in-house research was confined to tests on individual components, and the effects of their interaction was unknown. The survey then was not very helpful and so it was decided to move on to the next area of work.

#### 3.1.2 Collection of site data

In the early stages of the project, site visits were thought to be

necessary for a number of reasons.

- a. To collect data on how the equipment was actually used compared to the ideal, (i.e. measure out-of-plumb, eccentricity of load, tightness of joints, etc.). This data would be a necessary input for design work.
- b. To determine the loads actually applied to the scaffold both vertically and horizontally. This again would be a necessary input for design work for no-one really knows the loads actually applied to falsework. For instance, how much overloading takes place during concrete laying operations when concrete is emptied from a skip? Nor does anyone know whether C.P. 3 chV (Basic data for the design of buildings : Part 2 - Wind Loads) is really applicable to scaffolding. For it is thought that it does not make proper allowance for shielding effects due to a multiplicity of tubes.
- c. To determine how the scaffold behaves under load. For instance to monitor distribution of load, deflection characteristics, etc. This would be necessary to test the theoretical model.

But although the site survey would undoubtedly have yielded valuable information, it would have taken a considerable amount of time with the limited resources available. So when it was learnt that other organisations, (e.g. Tarmac. John Laing R & D) were carrying out such surveys, then it seemed pointless duplicating the work. In these circumstances the final area of work was concentrated upon.

### 3.1.3 Theoretical Analysis and Experimental Work

Since a site survey seemed out of the question it was decided to limit the investigation to the developing and testing of a mathematical model which could predict the ultimate load carrying capacity and deflection characteristics of U.P. in any birdcage scaffold. Then from the site survey being carried out elsewhere, values for the various imperfections, (e.g. eccentricity of load, out-of-plumb) could be inserted to discover the ultimate load carrying capacity and hence safe working load.

It was envisaged that the experimental work would be in two parts. Firstly a series of experiments on individual components to ascertain the relevance, if any, of B.S. 449 which was then, and still is, in use throughout the industry. Secondly a series of experiments on full scale assemblies to observe failure modes and deflection characteristics. These two sets of experiments are described in detail in the next section but their effect on the project as a whole was as follows.

The first series of experiments on individual standards was carried out in the laboratories of the University of Aston. Very little correlation was observed between the theoretical failure load using B.S. 449 and the measured failure load. But having doubted its validity, few alternative ideas sprang immediately to mind.

By this time the preliminary work on the design of the rig for experiments on full scale assemblies had been done, and it was becoming increasingly apparent that these experiments would take many months to prepare and carry out. And so it was agreed that preparations should begin at once and that the theoretical work be



made to fit into periods when the workload was light. But the programme of seven experiments took fifteen months to arrange and carry out during which time, in fact, very little work on the theoretical analysis was completed. The effect of this was that when the mathematical model was eventually developed, experimental results were already available. This had the effect that very little time was wasted in determining the best assumptions on which to base that model.

When all the above theoretical and experimental work was complete there was, however, still one final series of experiments required. It was thought necessary to check the theory for the deflection of a scaffold under horizontal load other than by comparison with the full scale assembly. So a small rig was developed which was in effect a shear panel and simulated one lift of a single bay of scaffolding. This was used to verify the coupler characteristics obtained from the full scale assemblies.

Having given a chronological account of the project it is now possible to give more details of the three sets of experiments listed above.

### 3.2 DETAILS OF EXPERIMENTS CARRIED OUT DURING THE PROJECT

#### 3.2.1 Experiments on individual standards

These were carried out in the laboratories of the University of Aston in the period March-May 1976. The general arrangement was as shown in Fig. 3.1 and Plates 3.1 and 3.2. It consisted of a central 9'9" (3 m) standard which was restrained by means of four transoms at a number of levels. These transoms connect it to a fairly stiff

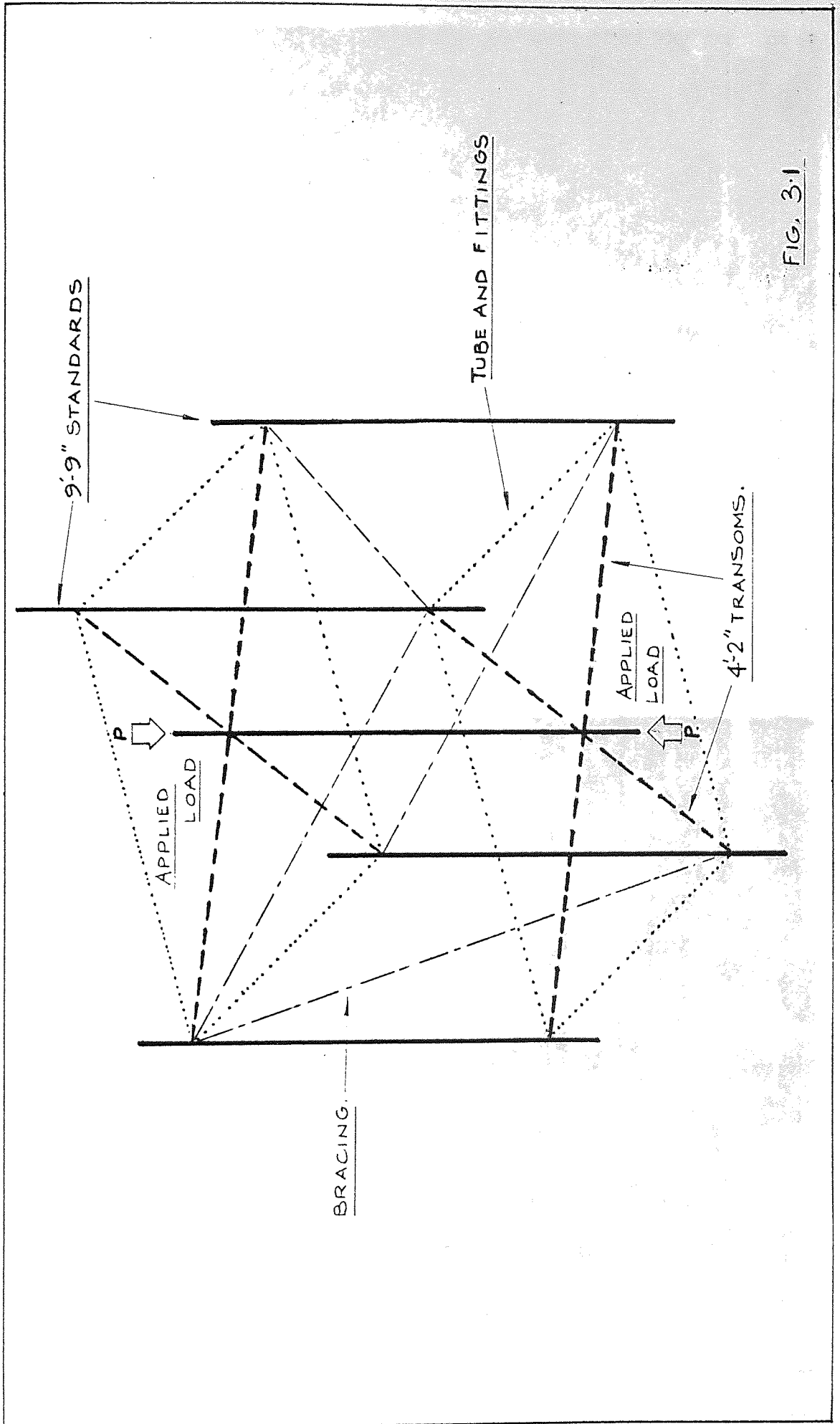


FIG. 3.1

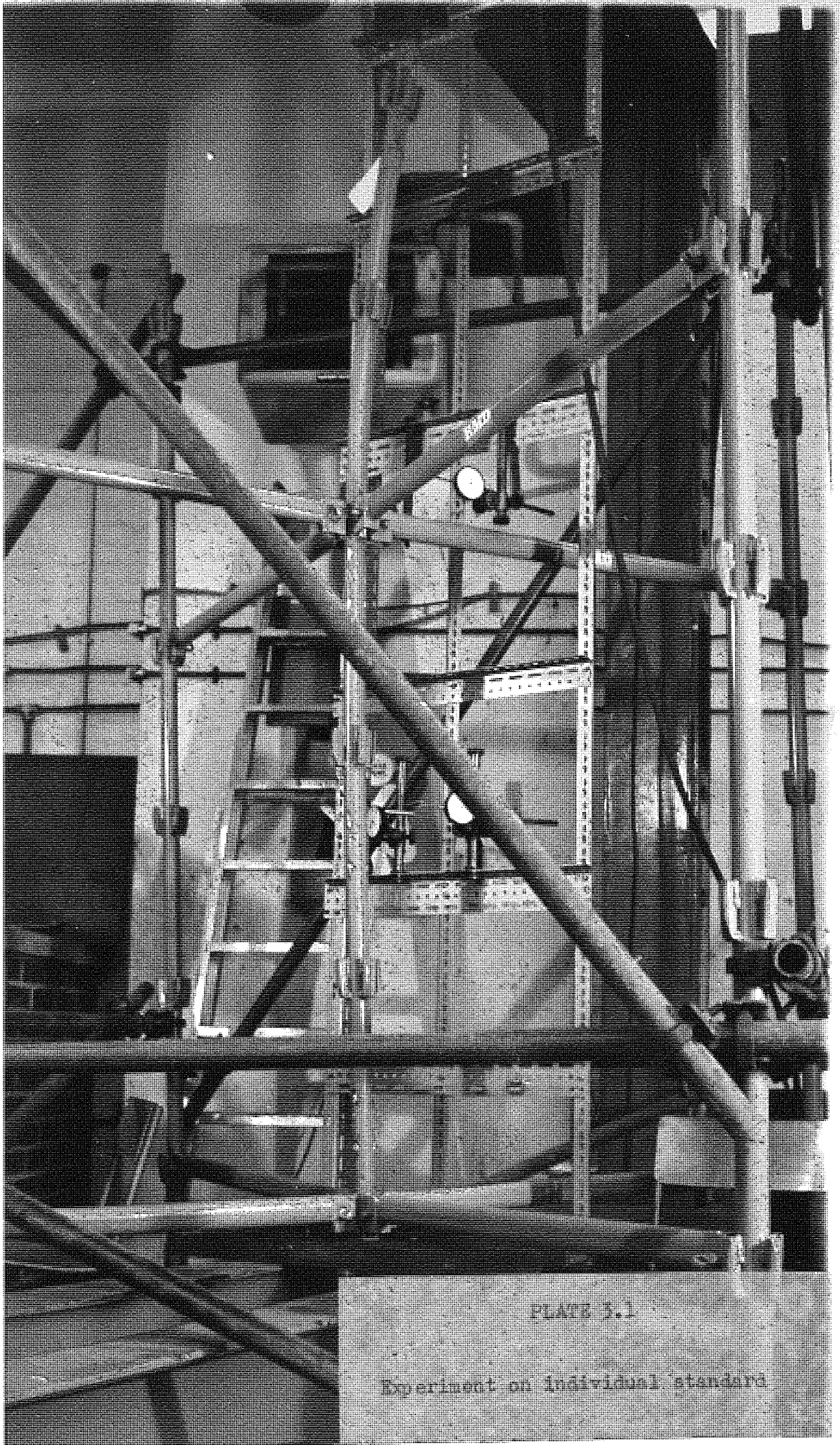
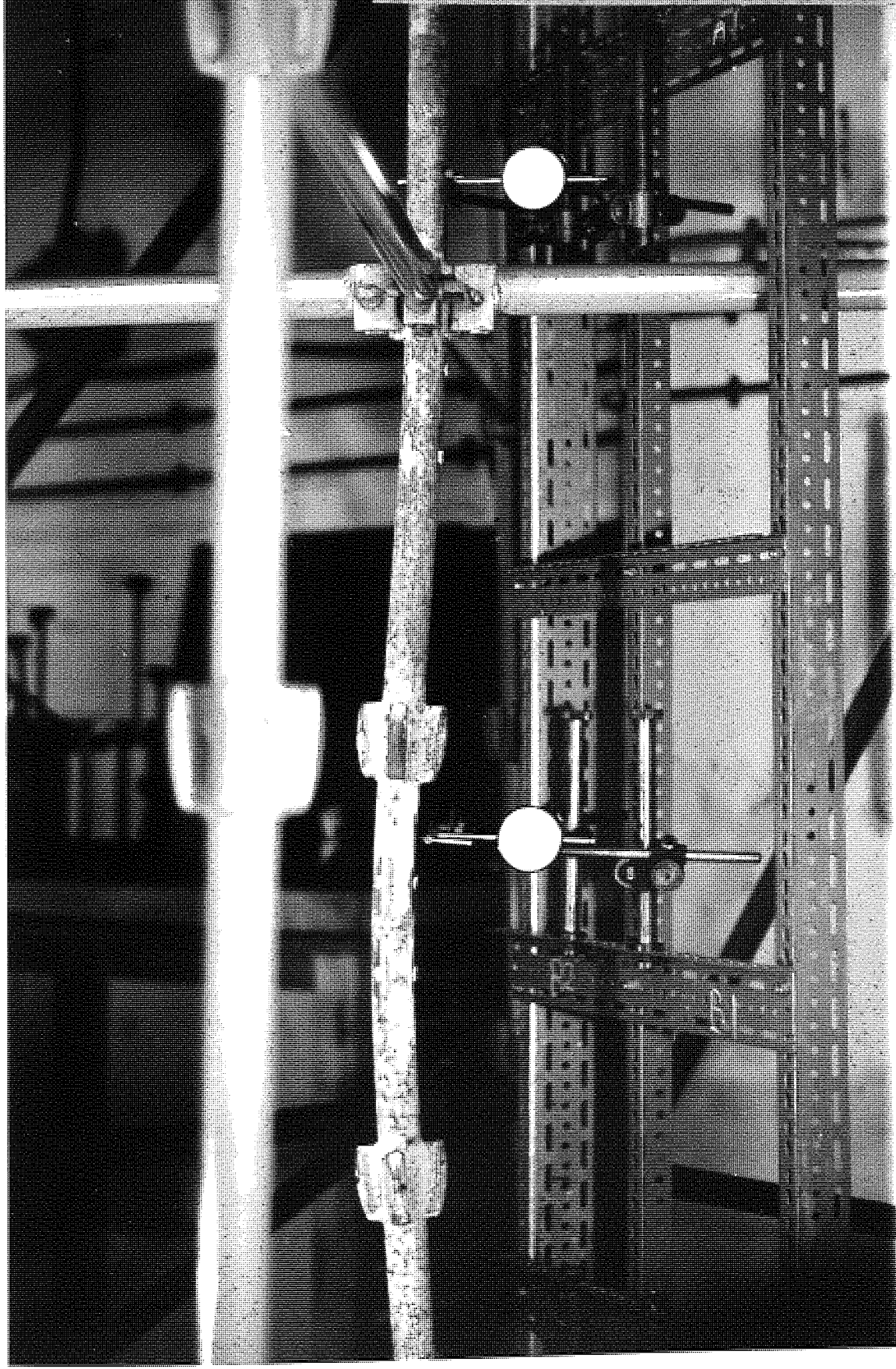


PLATE 3.1

Experiment on individual standard

PLATE 3.2

Experiment on individual standard



surrounding frame also built from scaffolding.

During the experimental programme various modifications were made to the arrangement shown. The position of the ledgers was varied and in some experiments a spigot was introduced into the central standard. The central standard was erected out-of-plumb in certain experiments and the load applied eccentrically in others. Also some standards with an initial curvature of up to 25 mm were tested.

At this time it appeared that for the arrangements used, the existing design method based on B.S. 449 underestimated the strength of the standards. But later it was possible to show that this was a feature of the test and in fact the existing design method could overestimate the strength of certain struts.

Various other items of experimental work were completed at this time including a study of the distribution of stresses in an axially loaded standard. It was found that there were areas of high stress on the surface of the tube above and below lugs. It also appeared that near to the spigot joint, high stresses were concentrated on the inside of the tube. This work was of use later when positioning strain gauges on the scaffolding for the experiments on full scale assemblies.

### 3.2.2 Experiments on full scale assemblies

These were planned and carried out in the period June 1976 - August 1977 at R.M.D.'s premises at Aldridge. The general arrangement was as shown in Fig. 3.2 (at the end of this thesis) and Plates 3.3 to 3.9. The rig consisted of a birdcage scaffold built of U.P. and of similar dimensions to a typical bridge type structure. It was 4 bays long by

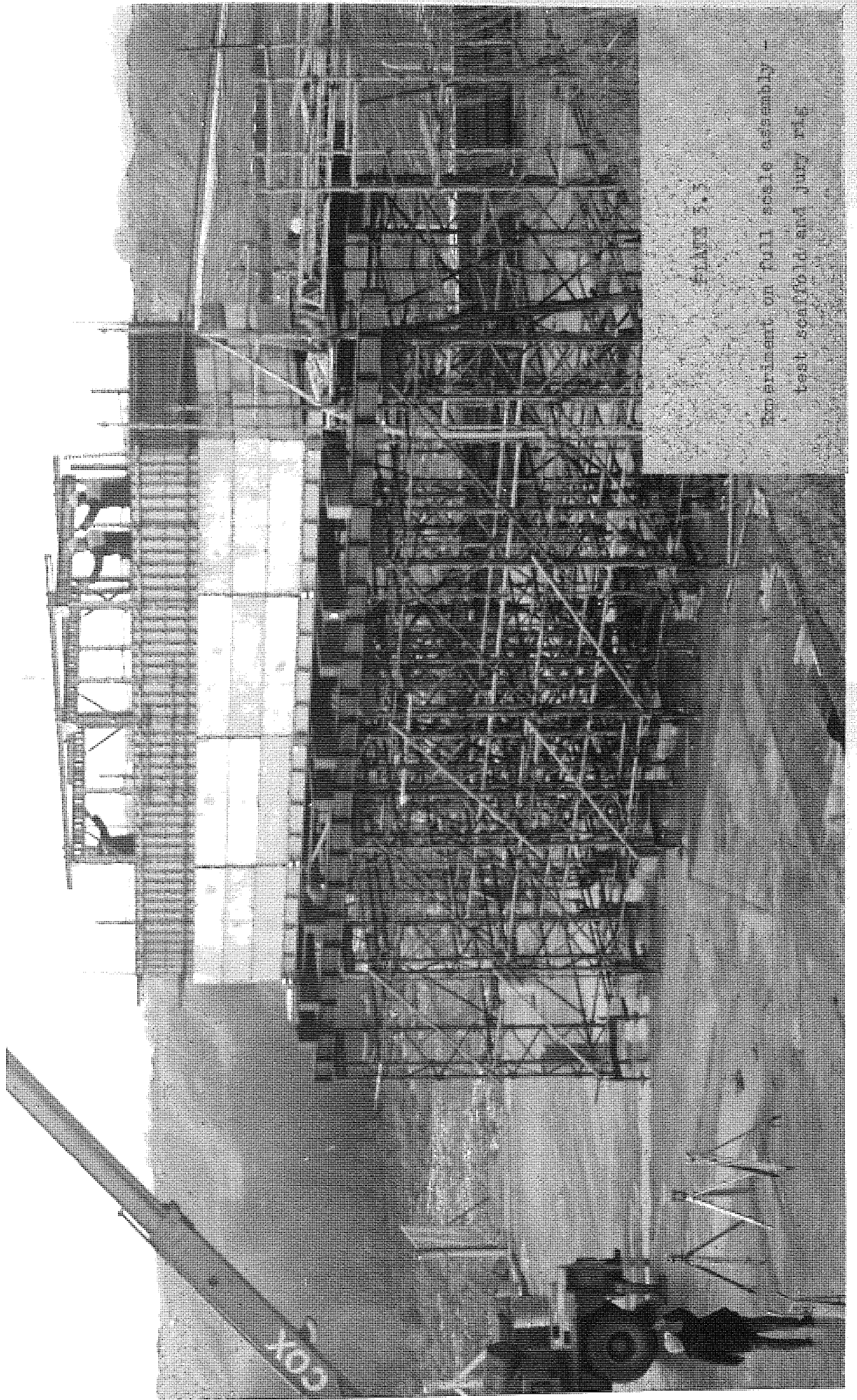


Figure 15.3

Exterior view of full scale assembly -  
test scaffolding and July 1971

COX



PLATE 3.4

Experiment on full scale assembly -  
test scaffold only



PLATE 3.5

Slide of a brace through a coupler



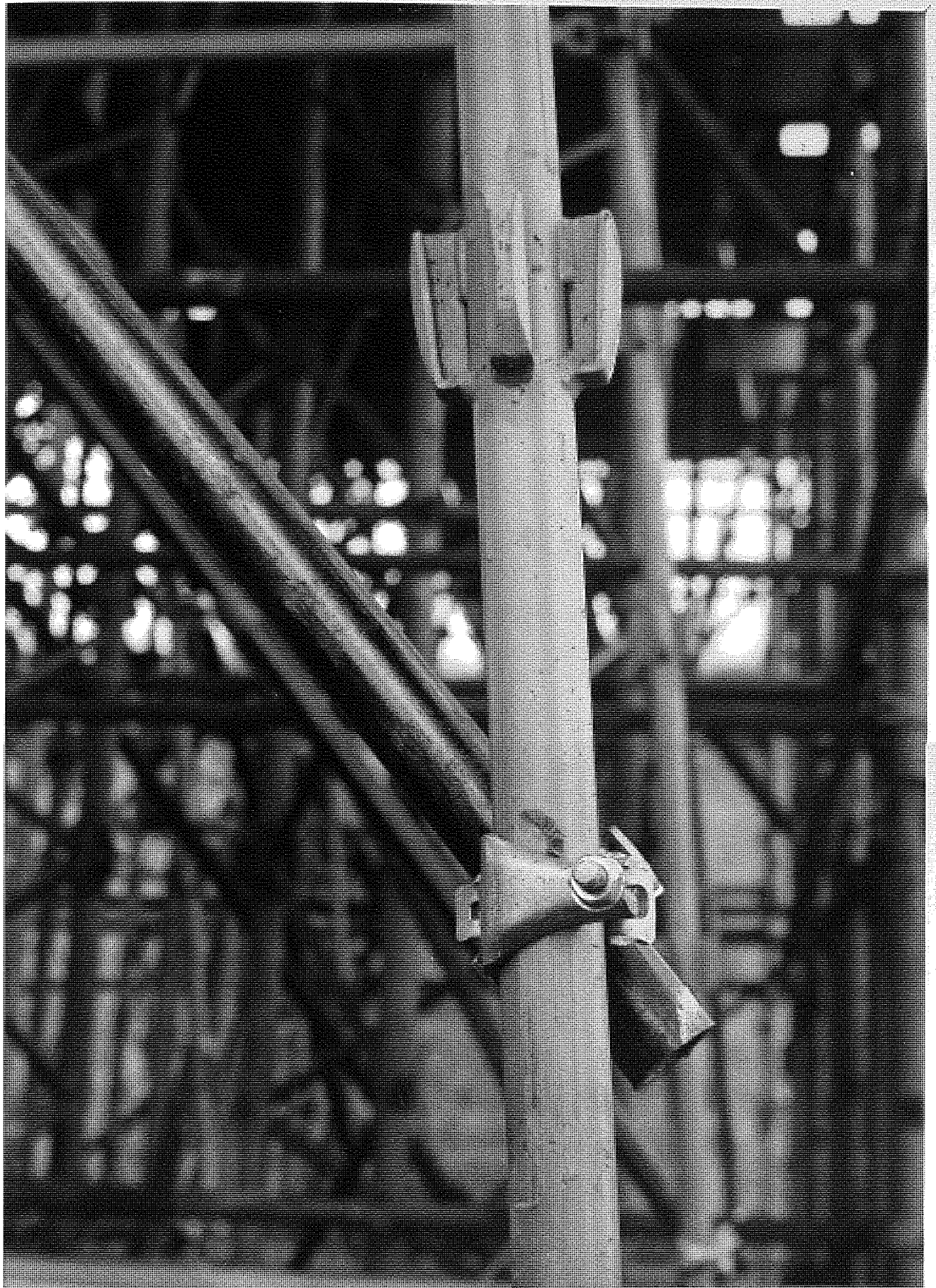
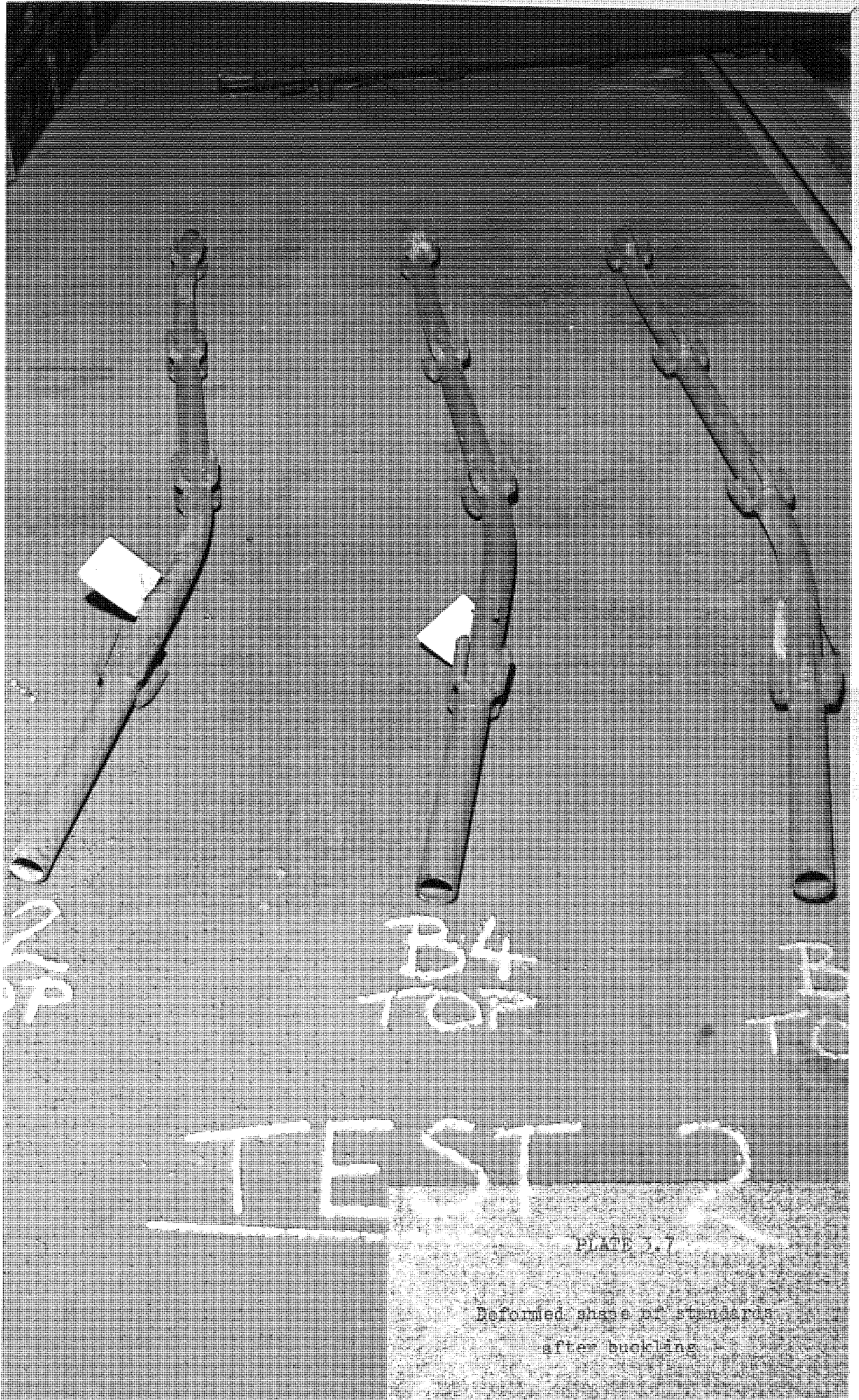


PLATE 3.6

Slip of a coupler along a standard



21P

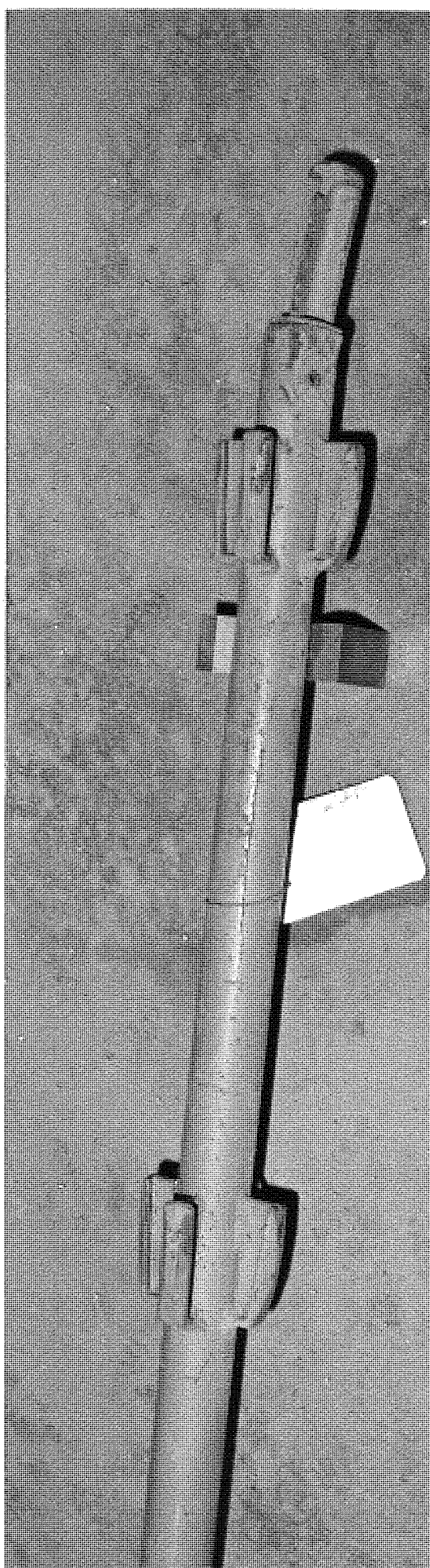
B4  
TOP

TOP

TEST 2

PLATE 3.7

Deformed shape of standards  
after buckling



TEST 2  
B2  
BOTTOM

PLATE 3.8

Deformation of spigot due to  
buckling of standard above.

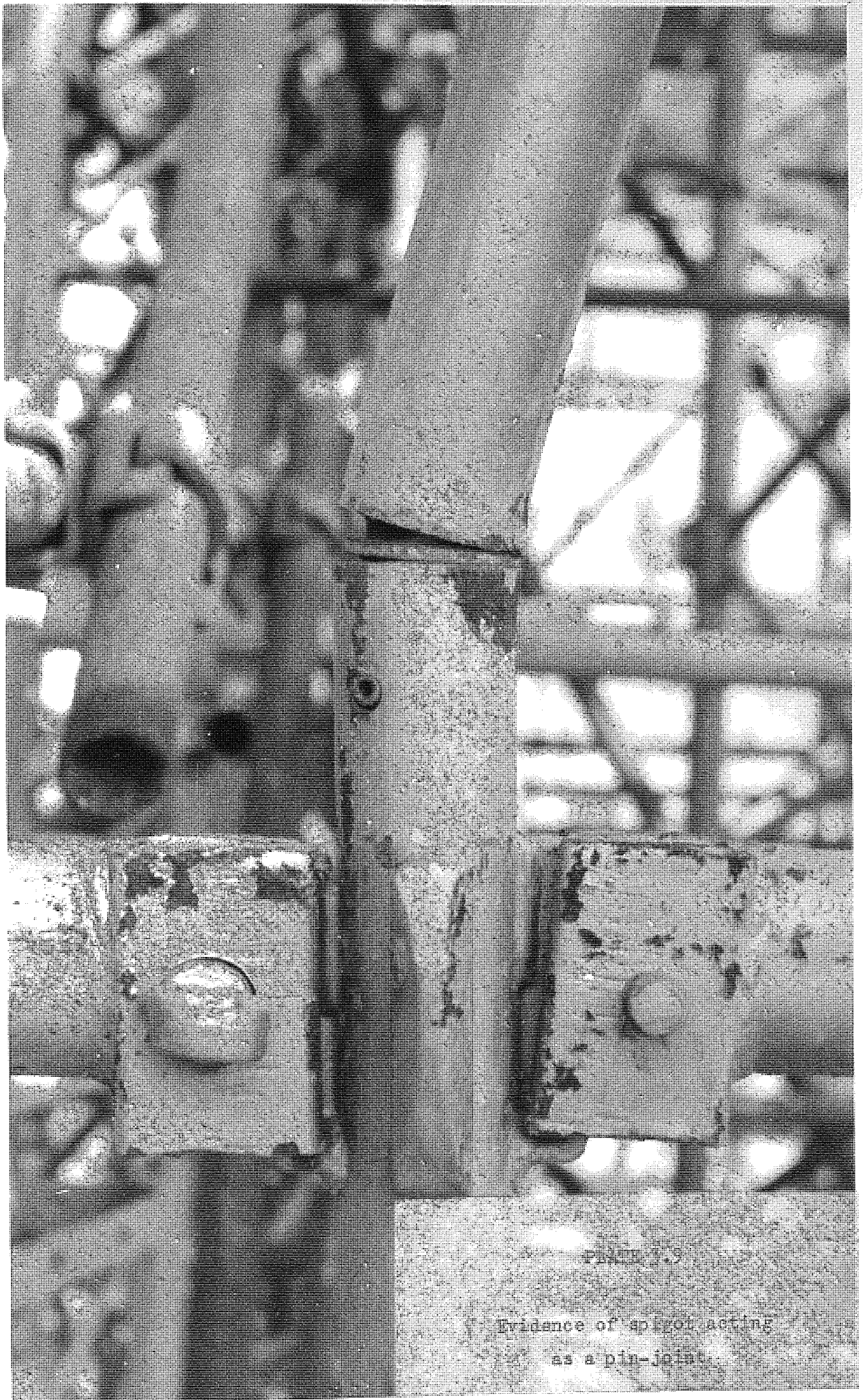


FIGURE 10

Evidence of spigot acting  
as a pin-joint.

3 bays wide giving overall plan dimensions of 32' (9.81 m) long by 12'6" (3.81 m) wide. In elevation it consisted of an adjustable base, 2 standards each 6'6" (2.00 m) long and an adjustable forkhead. Both the forkhead and base had a  $1\frac{1}{2}$ " (38 mm) threaded adjustment and were fully extended. In the forkheads were placed 8" x  $5\frac{3}{4}$ " (203 mm x 133 mm) header beams onto which the kentledge was lifted by mobile crane. It should be noted that this arrangement gave six central fully loaded standards.

The kentledge provided vertical load and consisted of concrete blocks which were placed in three layers each layer applying 30kN to a fully loaded standard. Thus the concrete provided rough adjustment of load. On top of any layer of blocks a tank could be placed which was gradually filled with water to give the fine adjustment of load.

The scaffold was also loaded horizontally by means of two hydraulic jacks. These were laid on a platform with the ram in contact with the scaffold at header beam level. The reaction of the jack was taken back to the nearby canal bank by means of a trishore acting as a horizontal strut.

One obvious requirement of the rig was that when failure took place the entire system did not collapse completely endangering those working nearby. So a safety scaffold was designed which supported the U.P. when the header beams were lowered by more than 50 mm.

A series of seven experiments were carried out on the rig with various features such as extension of forkheads and bracing arrangement being altered, although only one feature was changed at a time. The results

of these experiments and the correlation between these results and the theoretical model are presented at the appropriate point in subsequent chapters.

### 3.2.3 Experiments to determine load deflection characteristics of couplers

Once a model to determine the load-deflection characteristics of the complete structure had been formulated, it was thought necessary to check it by means of a simple test. So the small rig shown in Fig. 3.3 and the Plates 3.10 and 3.11 was devised. It simulates a single lift of one bay of scaffolding. A shear force is applied to the panel by means of the hydraulic jack shown. Because the members are so short deflections due to axial shortening or bending effects are small and the frame distorts mainly because of the movement of couplers. By positioning pointers and dial gauges it is also possible to show how movement of the coupler in different directions influences the overall frame distortion.

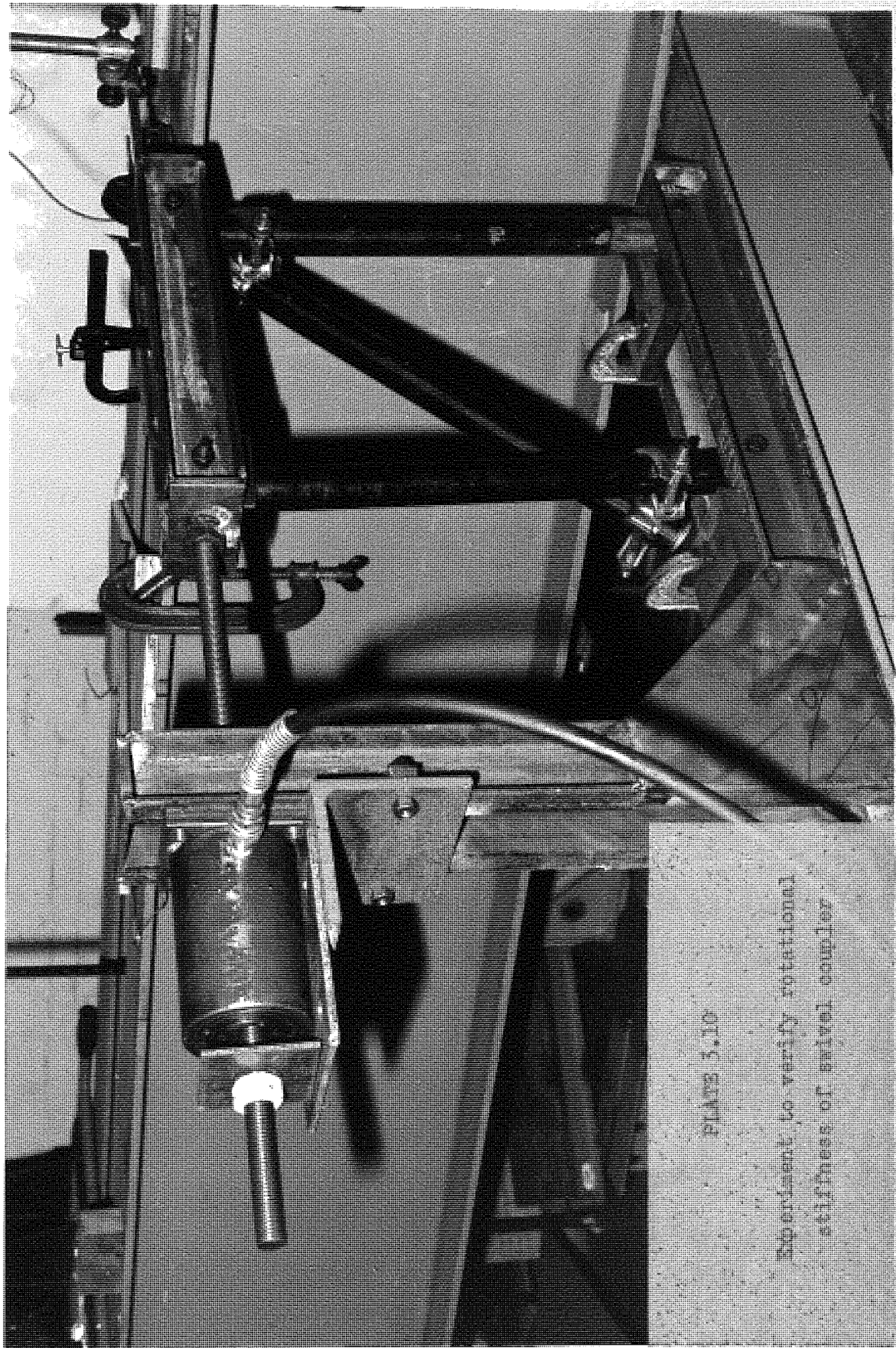


PLATE 5.10

Experiment to verify rotational stiffness of universal coupler.

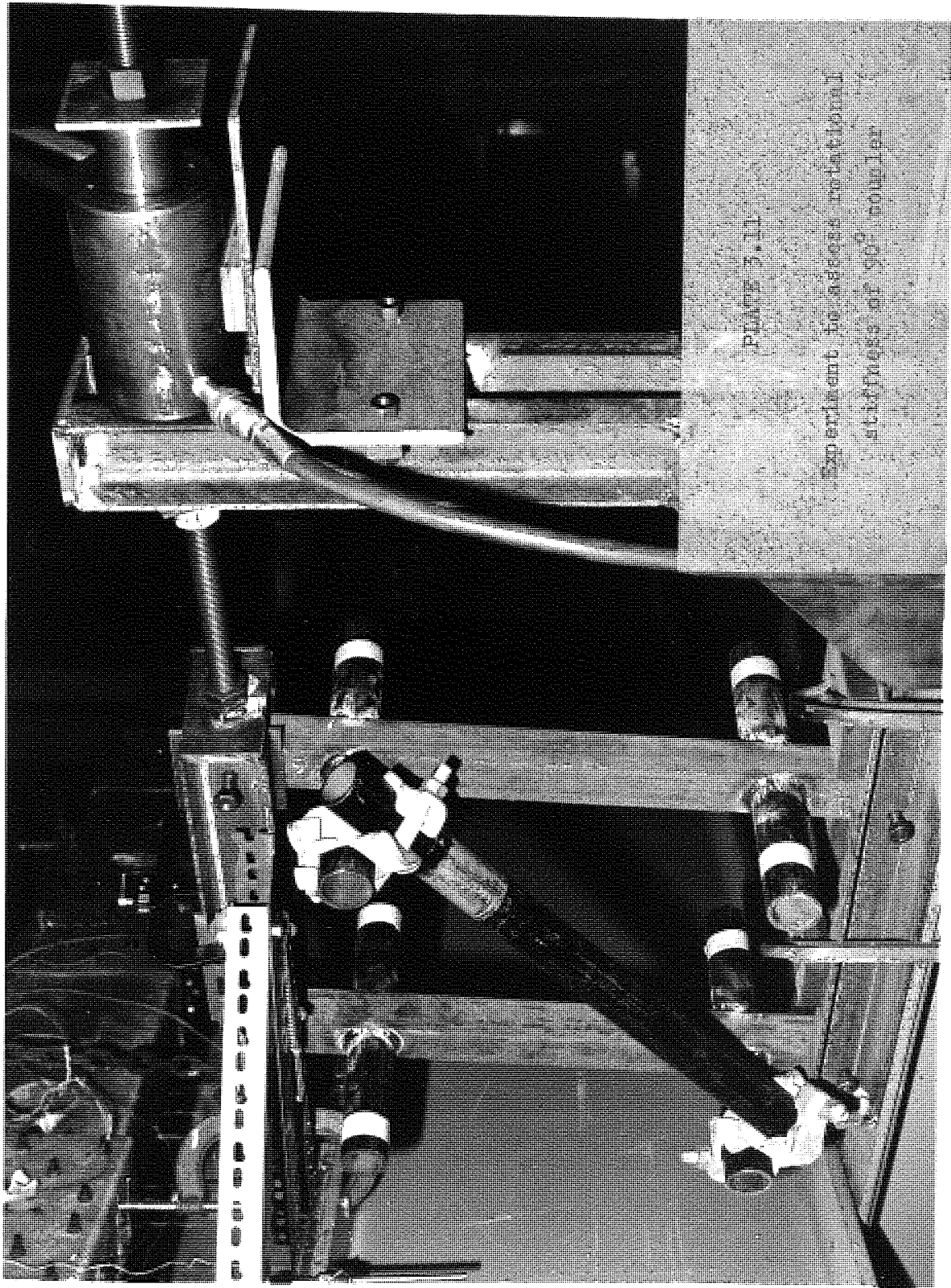


PLATE 3.11

Experiment in stress rotation  
at University of Cambridge



INTRODUCTION TO THE THEORETICAL ANALYSIS  
EMPLOYED AND ASSUMPTIONS MADE

# 4

Having discussed the project in general terms, Chapters 5 - 7 go on to detail the analysis which was developed to describe the observed characteristics of the scaffold best. Before going into such detail this chapter has three main functions. Firstly, there is a discussion of the type of analysis used and its advantages over other, perhaps more modern, methods. Secondly, it lists the assumptions made in subsequent chapters and justifies them. Finally, it defines the symbols used in those chapters and their units.

#### 4.1 INTRODUCTION TO THE THEORETICAL ANALYSIS

Scaffolding, whether it be tube and fittings or a proprietary system has two main uses. The first is for access purposes, for instance to allow tradesmen to work on the outside of a building. This is the most common way in which a scaffold is used. The second is falsework where the scaffold is used to support the formwork for a floor slab or bridge deck for instance. Structurally there are differences between the two, perhaps the most significant being the method of bracing, (see Fig. 4.1). For access scaffolds there can be no bracing in the plane normal to the building for this would hinder movement along the platform. Instead, the scaffold must be tied to the building at regular intervals. Another important difference is that generally support scaffolds are more heavily loaded. It is important to note these differences for this project is only concerned with falsework structures.

The analysis used can be solved by fairly simple mathematics and does not require the use of a computer. An analysis of this sort was a particular requirement of the sponsor for several reasons. Firstly, a very general approach was required so that should any pieces of equipment in the U.P. system be modified, then the method would be equally applicable and only certain constants would need to be altered. This means that the analysis is applicable to a wide range of braced systems and so could form the basis of a design method to be used throughout the industry.

A second reason for adopting this approach is that few, if any, scaffolding contractors use a computer for their design work. It is normally undertaken by technicians and, in smaller companies, not

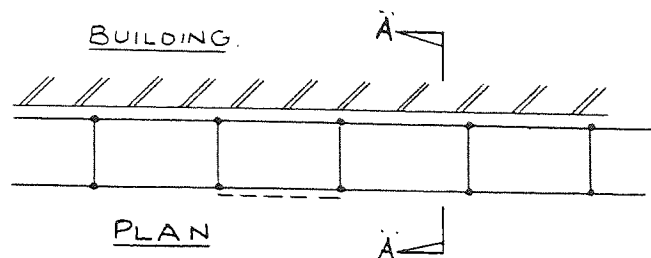
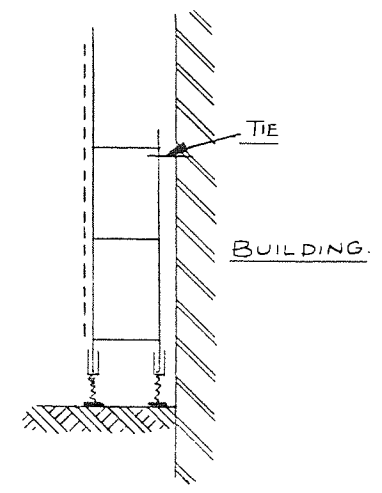
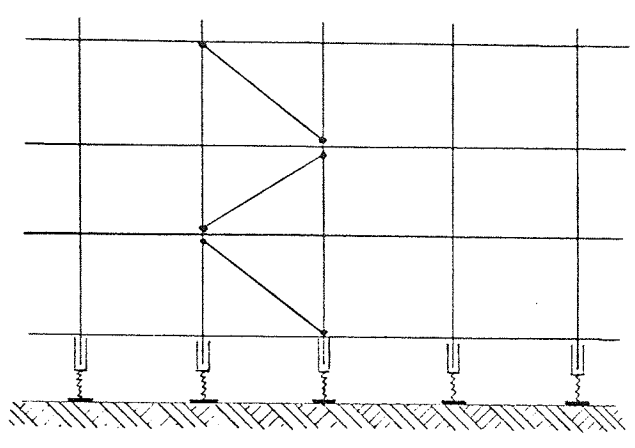
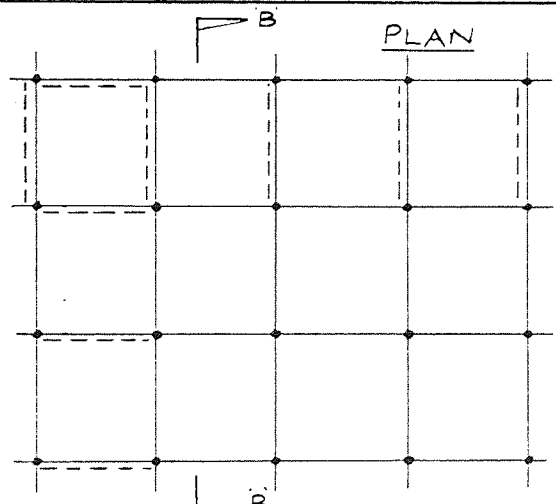


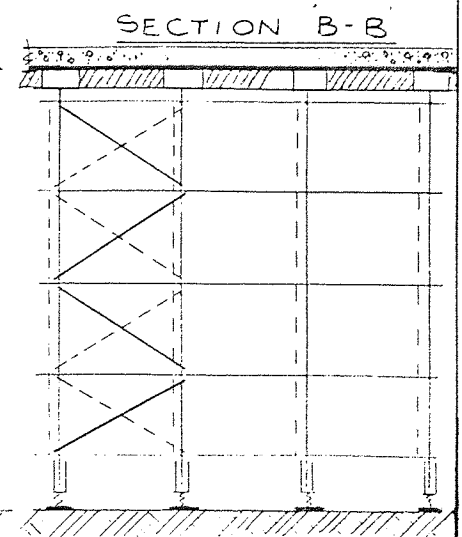
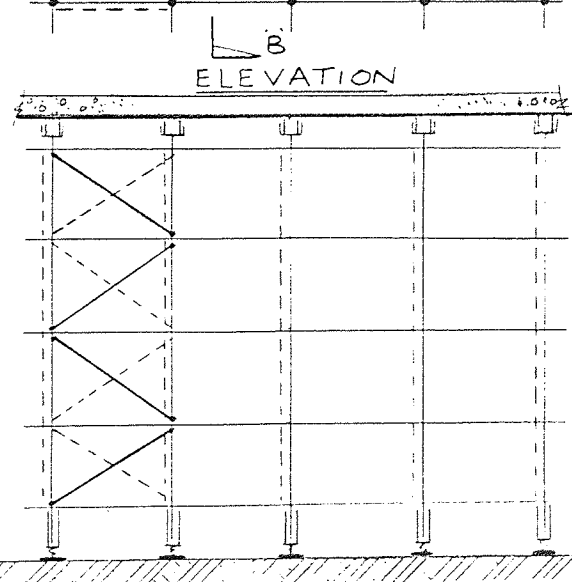
FIG. 4.1



BRACING ON TYPICAL ACCESS SCAFFOLD



BRACING ON  
TYPICAL FALSEWORK



even checked by an engineer.

This explains why the analysis is in its present form. Let us now discuss the assumptions made.

#### 4.2 ASSUMPTIONS MADE IN THE ANALYSIS AND THEIR JUSTIFICATION

1. It is assumed that each frame acts independently and, therefore, each frame can be analysed separately. This implies that no loads are transferred by torsion or lateral bending of ledgers (this is discussed further in paragraph 6 below). The main justification for this comes from the fact that the plan stiffness of the formwork is very high compared with that of scaffolding. Thus, the horizontal deflection at the top of all frames will be the same. Since each frame is identically braced, it is likely that the deflection profile of each frame will be the same and, thus, no forces will be transferred between frames. This assumption is commonly made in the analysis of building frames.
  
2. Each frame is in a single plane and remains so when it deflects. Whether this is true or not depends very much on where the horizontal load is applied. In the full scale assembly tests it was observed that at different levels the scaffold rotated in plan resulting in the scaffold becoming non-planar. This is thought to be a manifestation of the phenomena illustrated below. Suppose a force is applied to an object. If the line of action of that force passes through the centre of stiffness of the object, then the object will move directly along that

line (Fig. 4.2a). If, however, the line of action does not pass through the centre of stiffness, the object will also rotate because of the couple that is formed (Fig. 4.2b). If the object is pushed, then this process accelerates, because the distance between the applied force and reaction increases as the object moves (Fig. 4.2c). If, however, it is pulled then the process is self correcting, since that distance decreases (Fig. 4.2d). For a scaffold structure there are so many unknowns that it is almost impossible to predict its behaviour in this respect. These unknowns include the ratio of positive pressure to suction on the windward and leeward side of the scaffold respectively. Another difficulty is determining the exact position of the line of action of the resultant wind forces. In any event, it is likely that the eccentricity of loading shown in Fig. 4.2b will be very small so that little or no rotation will take place in practice.

3. Each frame is considered to be built up from two units. These are the individual standard and the braced bay. A simple calculation will show that the braced bay is many times stiffer than the individual standard in resisting horizontal load. It is, therefore, assumed that all horizontal loads are resisted by the braced bay. It will be shown in subsequent chapters that it will fail by excessive deflections due to the movement of the couplers.
4. Members are unstressed at zero load and behave elastically until failure. The only point where this assumption is not used is when considering the buckling of individual standards.

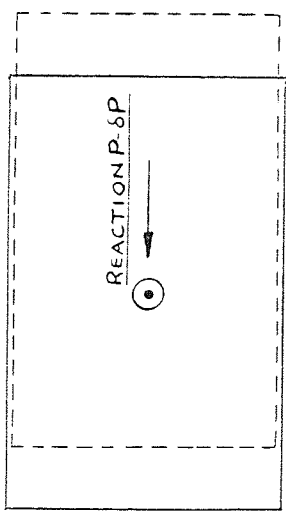


Fig 4.2a. LINE OF ACTION THROUGH CENTRE OF STIFFNESS - LATERAL MOVEMENT ONLY.

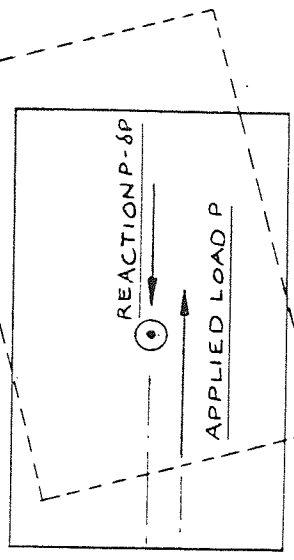


Fig 4.2b. LINE OF ACTION ECCENTRIC TO CENTRE OF STIFFNESS - LATERAL MOVEMENT PLUS ROTATION

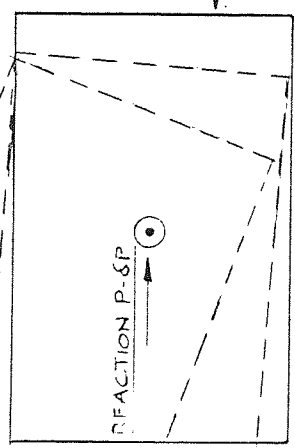
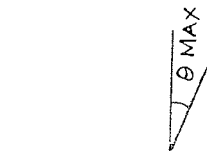


Fig 4.2c. PUSHING CAUSES ACCELERATION OF ROTATION - θ CONTINUOUSLY INCREASING.

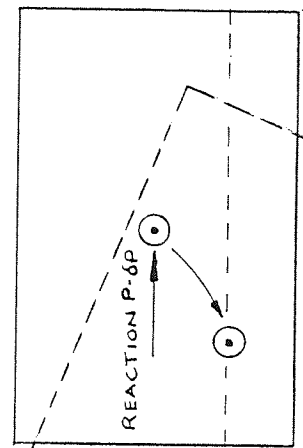


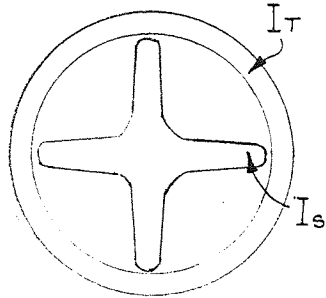
Fig 4.2d. PULLING CAUSES DECELERATION OF ROTATION UNTIL θ REACHES θ MAX WHEN CENTRE OF STIFFNESS IS ON LINE OF ACTION OF FORCE

FIG 4.2

Here, if using the modified Perry formula discussed by Dwight in Ref.22, account is taken of the stresses locked in by the manufacturing process.

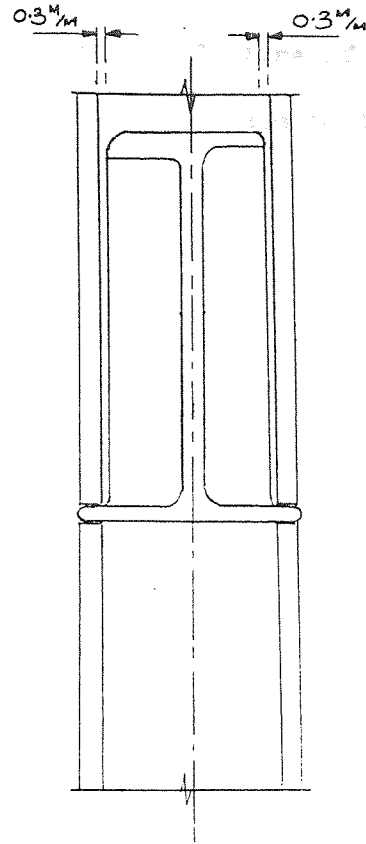
5. In considering the buckling of an individual standard, two assumptions are made. Firstly, the spigot joint acts as a pin. This can be justified both theoretically and experimentally. Theoretically because the spigot has only 20% of the stiffness of the parent tube. Also, because there is play between the tube and spigot, necessary to permit easy erection, some rotation can take place at zero moment (see Fig. 4.3). Experimentally because in the full scale assembly tests when the mode of failure was predominantly buckling, distortion of the spigot and rotation of the standard at this level was observed (see Plates 3.7, 3.8 and 3.9).
6. The second assumption made when considering the buckling of standards concerns the restraint provided by ledgers. It is assumed that the standard is restrained only by bending of the ledgers in the frame under consideration and not by torsion of transoms between frames (see Fig. 4.4). This is really a simplification for in practice there must be a certain amount of torsional restraint, although it is likely to be small because of the plan weakness of the clevis. Conversely, it is assumed that the ledger - standard connection is infinitely stiff and this again is a simplification. However, these two assumptions when considered together provide a model closer to the actual case than either considered in isolation.

RATIO OF SPIGOT  
STIFFNESS TO TUBE  
STIFFNESS.



$$\frac{I_s}{I_T} = 0.21.$$

FIG 4.3



ACTUAL CONDITION

ASSUMED CONDITION

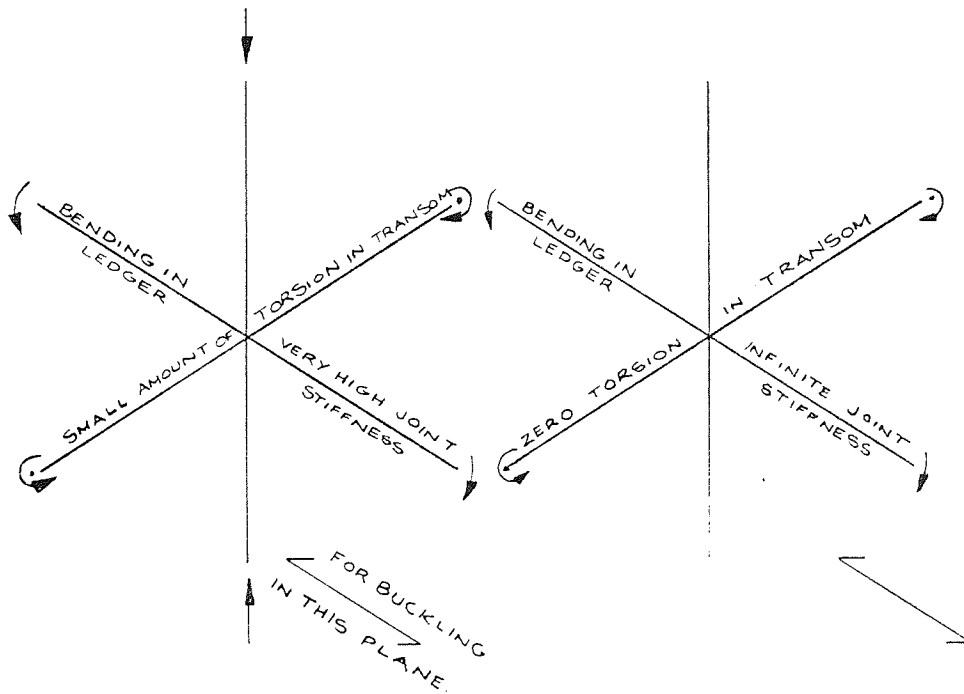


FIG 4.4



7. When considering the deflection and ultimate failure of a braced bay it is assumed that frame deflections due to the bending of members are small. The members have large slenderness ratios (95 and above) and thus only deflections due to axial shortening of members and movement of couplers are considered.
  
8. When considering the movement of couplers it is assumed that they can be modelled by analogy with a helical spring wrapped around the standard. This is an assumption which appears to predict the movement of the scaffolding within certain limits.

### 4.3 LIST OF SYMBOLS USED

A	Cross-sectional area
A,B,C	Constants of integration
a,b	Lengths (could be with subscript, e.g., $a_1$ length of section 1)
D	Tube diameter
E	Young's modulus, modulus of elasticity
e	Eccentricity of load at forkhead Eccentricity of brace on standard at coupler
F	Axial load in member
f	Friction force between coupler and standard - circumferential to standard
H	Applied horizontal load
h (x-a)	Heavyside step function = 0 for $x \leq a$ = 1 for $x > a$
I	2nd moment of area, moment of inertia (normally of standard - I' refers to ledger)
K	Spring constant in coupler analogy
k	$\sqrt{\frac{V}{EI}}$
L	Member length (L' length of ledger, $L_e$ effective length)
M	Applied moment

N	Number (e.g. number of couplers in frame)
P	Horizontal component of load in brace
r	Radius of gyration ( $r_y$ - about y-y axis)
U	Strain energy ( $U_{ax}$ strain energy in axial load, $U_R$ strain energy in rotation of coupler)
V	Applied vertical load
W	Applied load at point where deflection is required
x,y	Directional axis
$\Delta$	Deflection
$\eta$	Constant in Perry-Robertson formula  $\eta = 0.3 \left(\frac{1}{100r}\right)^2 \text{ for lower bound curve}$ $\eta = 0.001 \left(\frac{1}{r}\right) \text{ for average failure load curve}$
$\theta$	Rotation of coupler around standard
$\alpha$	Angle between scaffold and vertical
$\phi$	Slope of brace
$\sigma$	Stress ( $\sigma_e$ - Euler buckling stress = $\frac{\pi^2 E}{\left(\frac{1}{r}\right)^2}$ ;  $\sigma_y$ - yield stress)

# 5

## THE DEFLECTION OF U.P. SCAFFOLDING UNDER LOAD

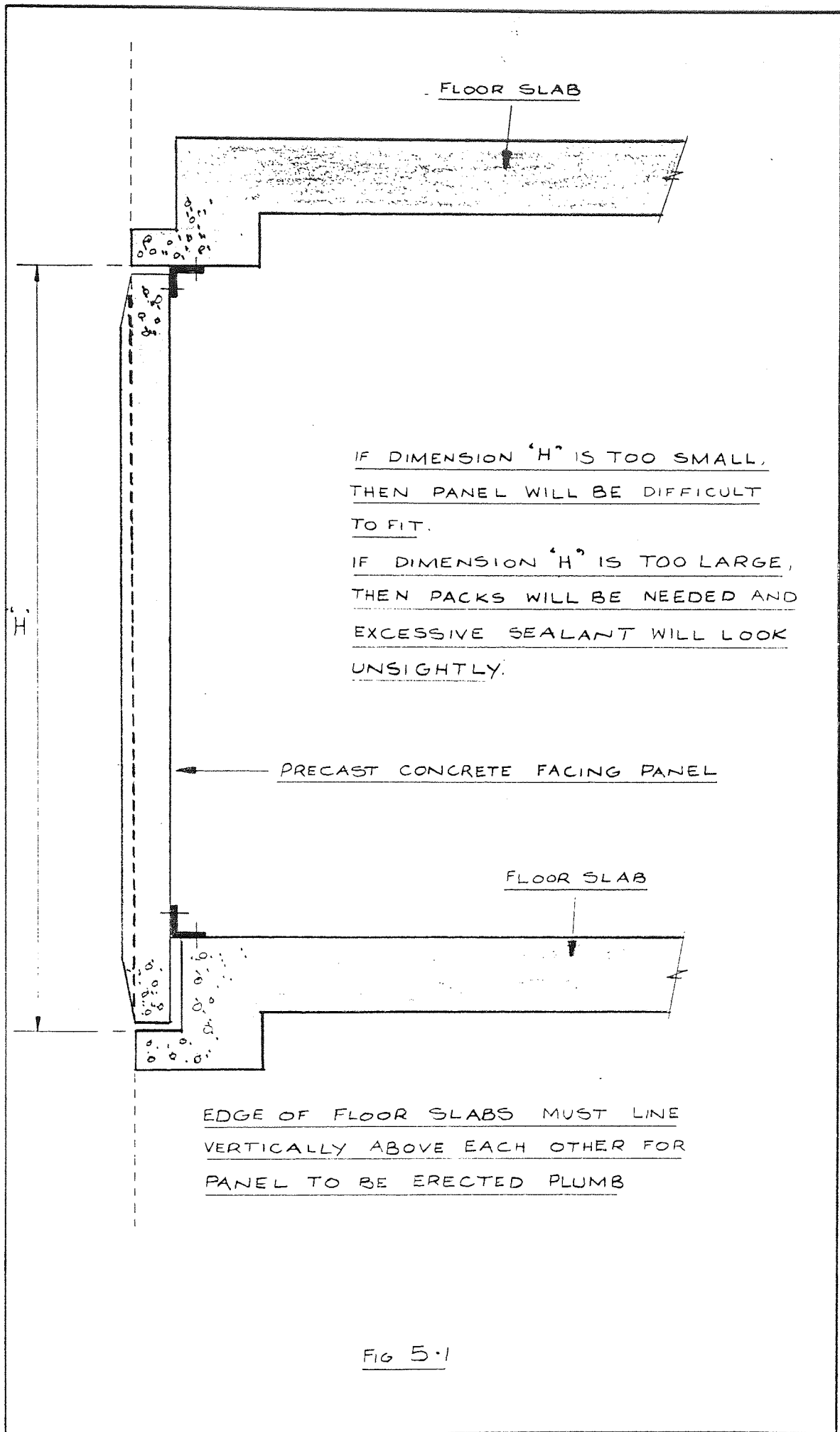
Having idealised the structure by means of the assumptions made in Chapter 4, it is now possible to look at it in more detail. Chapter 5 looks at the horizontal deflections of the scaffolding under load and assesses the importance of such deflections. It should be remembered that all horizontal loads are considered to be resisted by the braced bay (see 4.2, paragraph 3). Conversely, a study of the horizontal deflections of the whole scaffold should be thought of as a study of the horizontal deflections of that braced bay.

## 5.1 THE IMPORTANCE OF DEFLECTIONS

Before studying the prediction of horizontal deflections it is helpful to know why they are so important. There are two main reasons.

Firstly, a scaffold is relatively flexible and fairly large horizontal movements can take place under small loads. One effect of this is that the member forces in the deformed structure are different from those in the underformed structure. Furthermore, the members whose loads are increased most by the deformation are those with the lowest load factor in the underformed structure. These are the strut at the bottom of the compression side of the braced bay and the bracing itself. Excessive deflection can, therefore, reduce the load factor of these members to an unacceptable level. For instance, an increase of 15% in the axial load of a brace, which is not an unrealistic figure, reduces the load factor from 2.0 to 1.74. This is discussed in Chapter 6.

The second reason for studying deflections is that contractually there is almost always a tolerance on the position of the finished concrete. Typically, for a bridge the centre line has a tolerance of  $\pm 6$  mm in level and  $\pm 13$  mm in line. For building work the tolerance is likely to be tighter and in some cases the contractor may set his own limits. The reason for this is that other operations are dependant on the accurate placing of concrete, and errors have to be corrected at the contractors expense by chipping away excess concrete or filling gaps with steel or timber packs. Examples of operations which are thus dependant include the fixing of precast concrete facing panels, windows or proprietary office partitions (see Fig. 5.1).



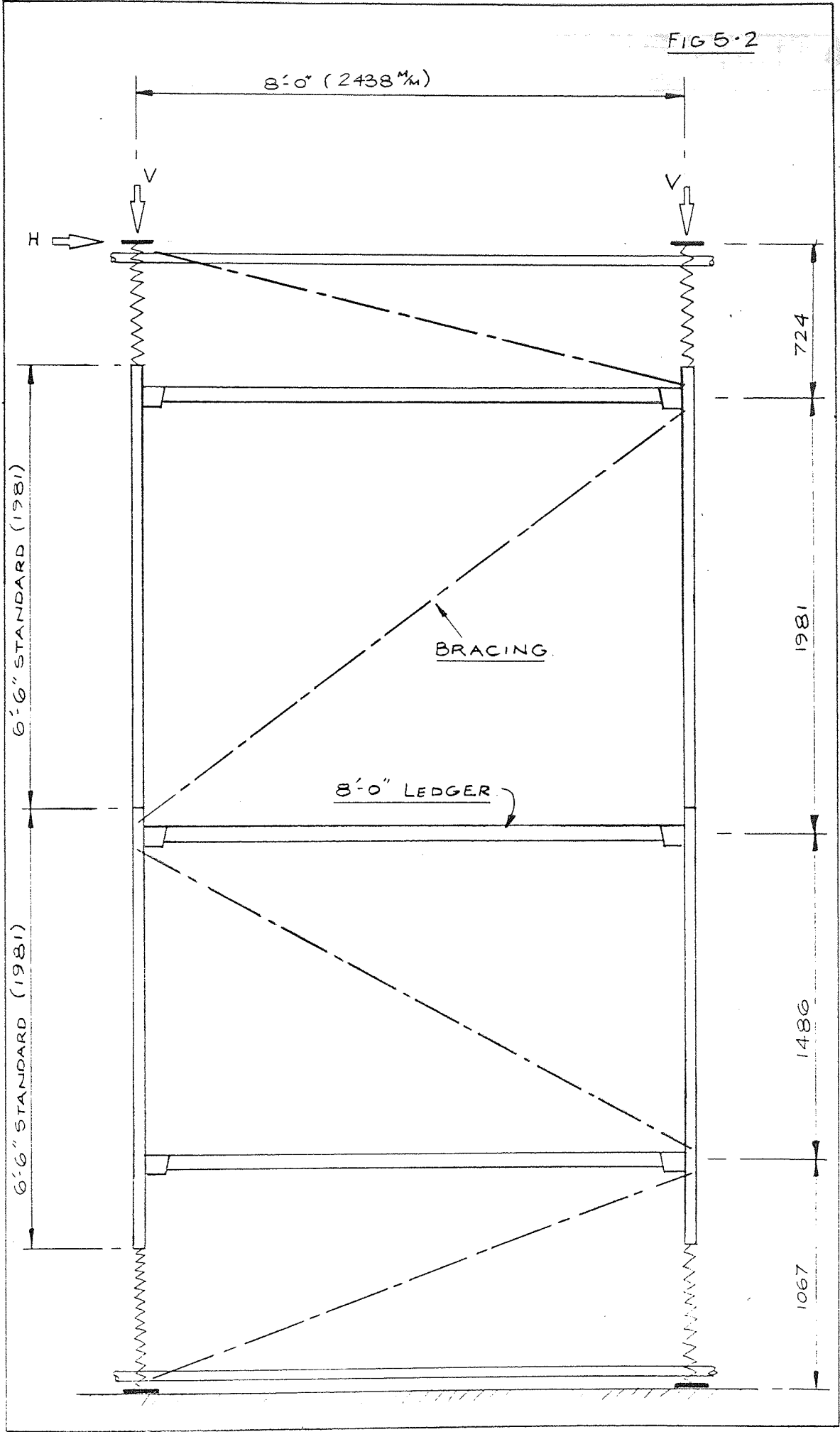
Obviously then, both horizontal and vertical deflections are important for line and level respectively. Unfortunately, in this project only horizontal deflections have been considered. To look at vertical deflections would have required a very tall scaffold assembly and it was not considered worthwhile for the extra costs which would have been involved. But to extrapolate from the structure actually used which was only two standards high, would involve considerable error, so it is hoped that measurements can be taken on a tall scaffold on site when the opportunity arises.

## 5.2 COMPARISON BETWEEN OBSERVED CHARACTERISTICS AND ELASTIC BEHAVIOUR

For the braced frame shown in Fig. 5.2 it was thought that deflection would be solely attributable to axial shortening and extension of members and that because of their large slenderness ratios (95 and above) then deflections due to bending could be ignored. This is a common engineering assumption based on the fact that bending stresses are small compared with axial stresses.

However, Fig. 5.3 shows that the theoretical deflection was very small compared with the deflection measured in the experiments on full scale assemblies. In fact, at the point at which experiment No.4 was halted the measured deflection (61 mm) was approximately twelve times the elastic deflection (5.05 mm) calculated using strain energy methods and allowing only for extension and contraction of members. So modifications to this theory were devised. These modifications allowed for the movement of bracing couplers as the frame deflected. The basic movements were thought to be (see Fig. 5.4) :

FIG 5-2





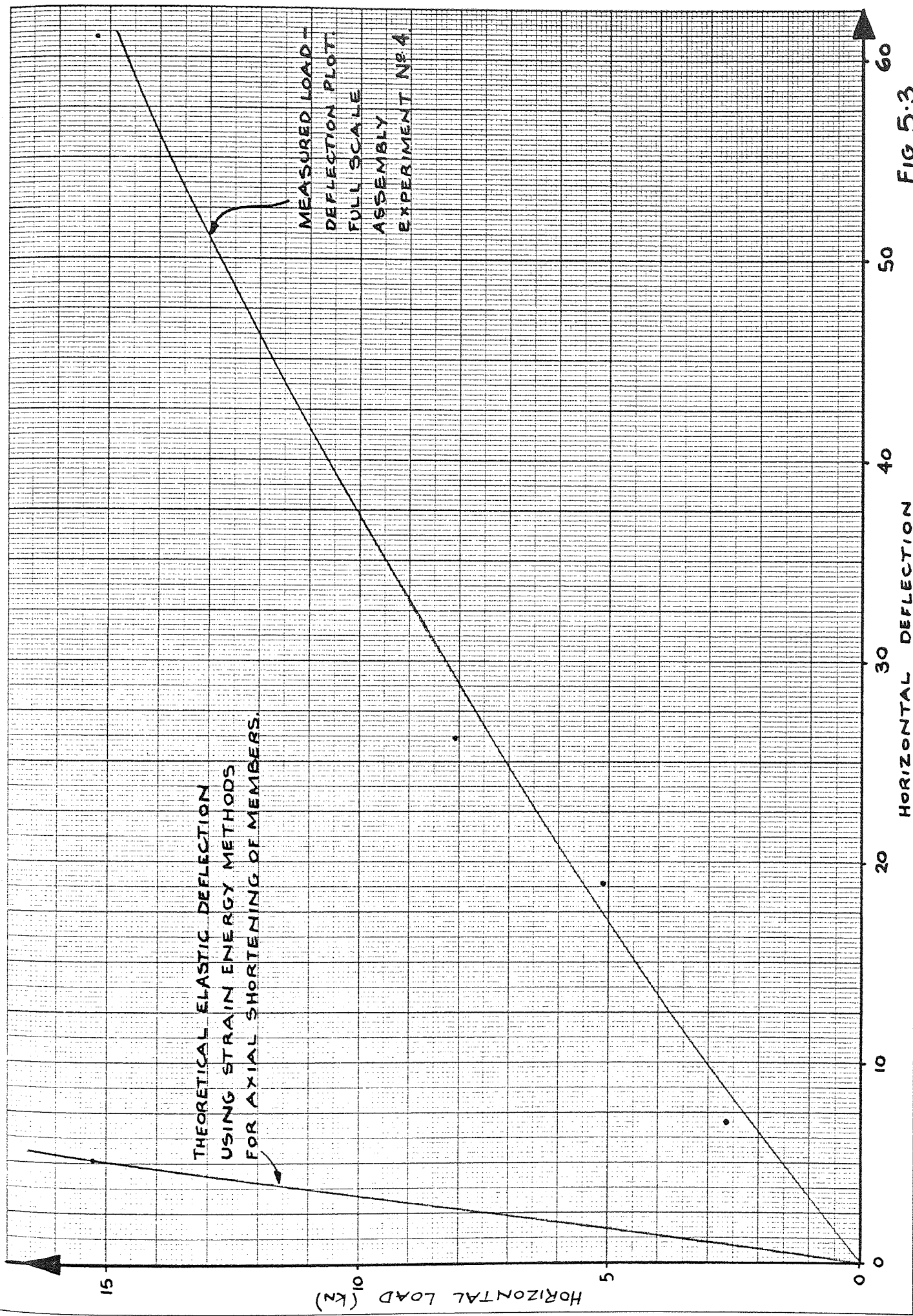


FIG 5.3

1. Rotation of the coupler around the standard. This is dependent on the value of P.
2. Sliding of the brace through the coupler. This is dependent on the value of  $\frac{P}{\cos \phi}$  and is the mode of failure by which the strength of a coupler is assessed (see Ref. 23, clause 17).
3. Sliding of the coupler along the standard. This is dependent on the value of  $P \tan \phi$ .
4. Distortion of the coupler and in particular of the rivet. This is dependent on the value of  $\frac{P}{\cos \phi}$ .

The investigation was then concentrated on determining to what extent each of these influenced overall frame movement. This was no easy task since their relative magnitude depended on many factors such as the relative tightness and frictional properties of the two halves of the coupler, the slope of the brace, the strength of the rivet and the surface condition of the standard and brace. But it was hoped to gain an overall picture without defining these variables too closely. Therefore, the apparatus described in Section 3.2.3 was devised.

Using this rig it was soon established that there was little, if any, slip of the brace through the coupler or of the coupler along the standard. So pointers were fixed to the half of the coupler which was attached to the standard (see Fig. 5.4). By positioning dial gauges at the end of these pointers it was possible to measure the plan rotation of the couplers as the frame deflected, and thus calculate the proportion of the frame deflection attributable to rotation. The

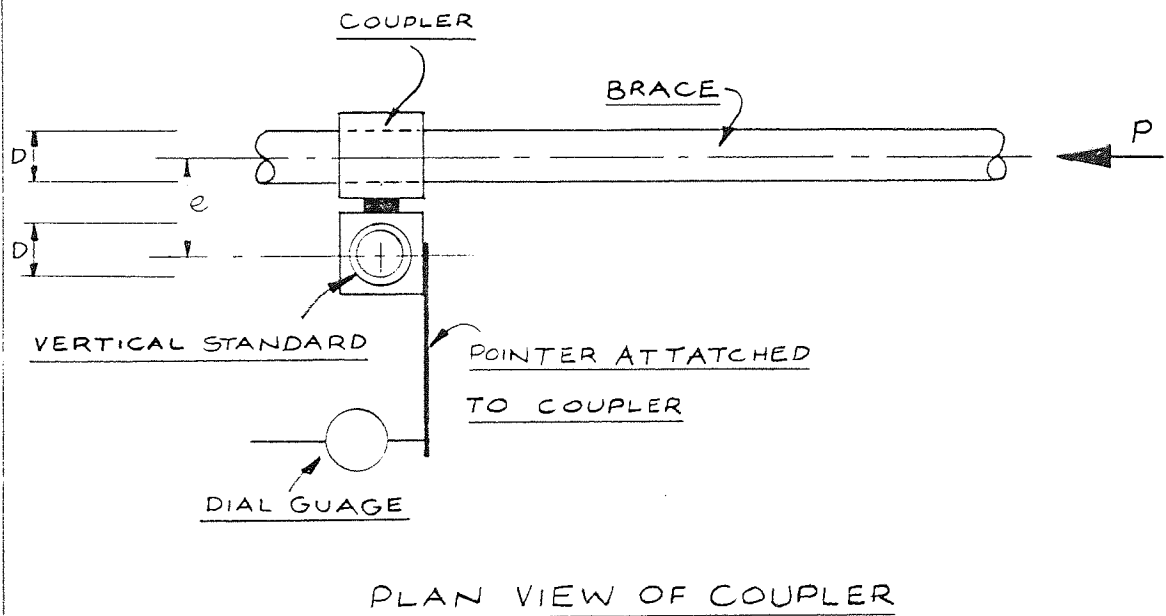
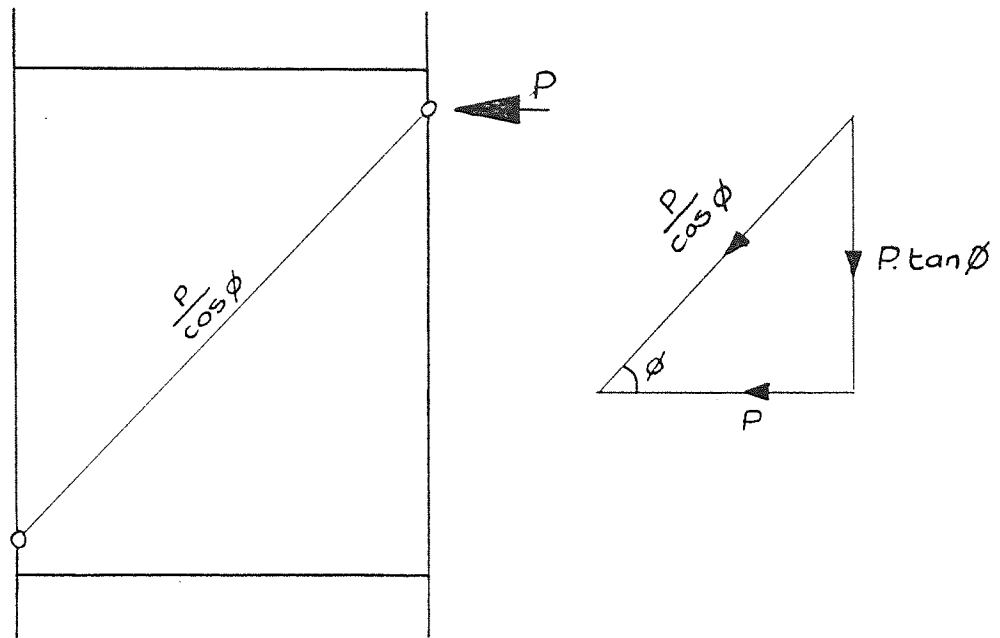
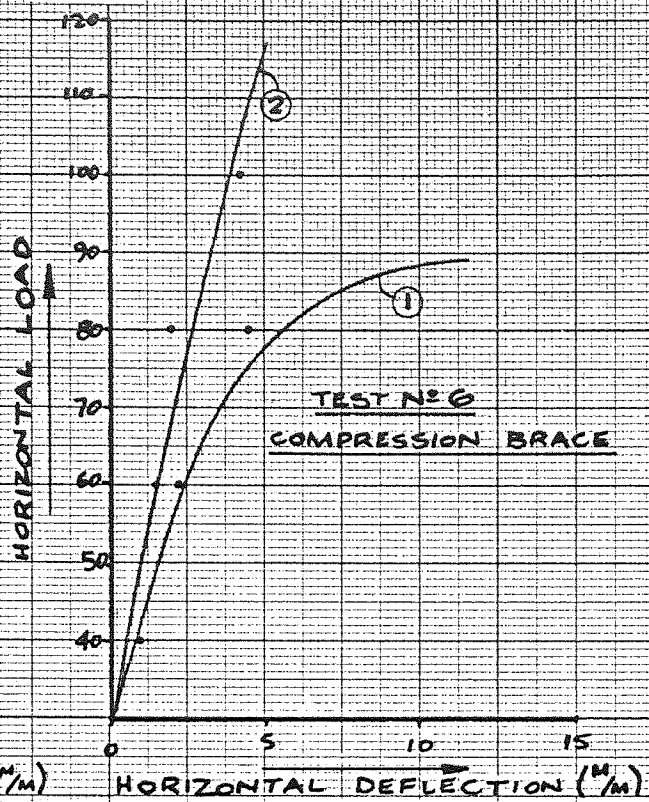
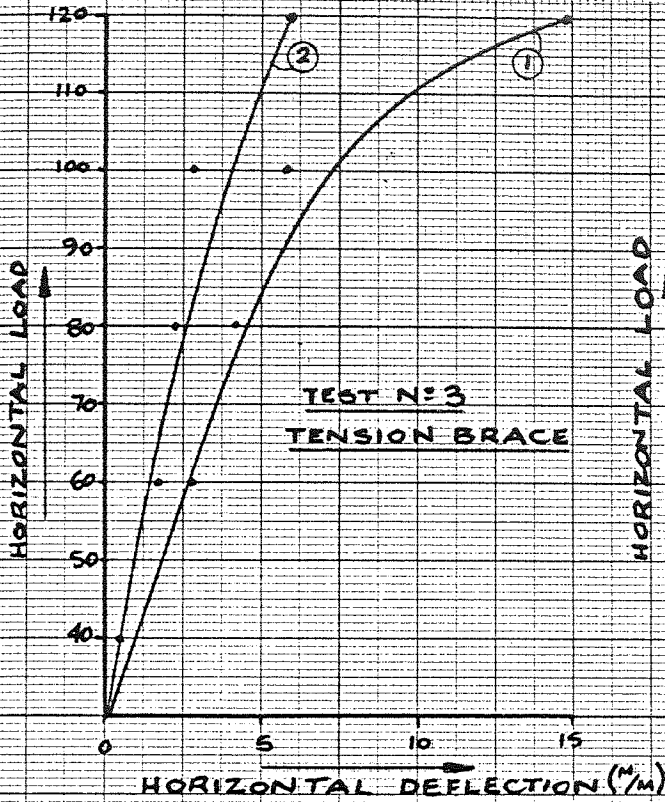
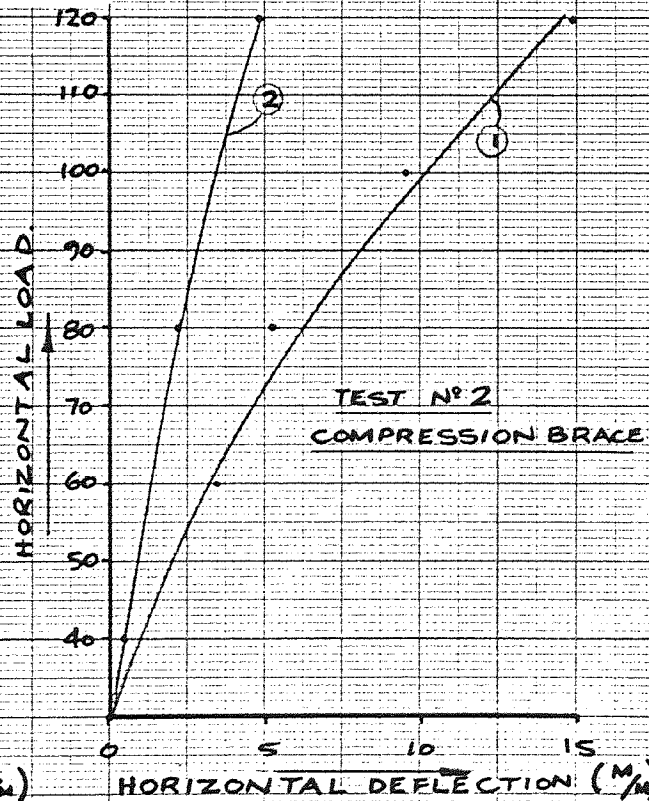
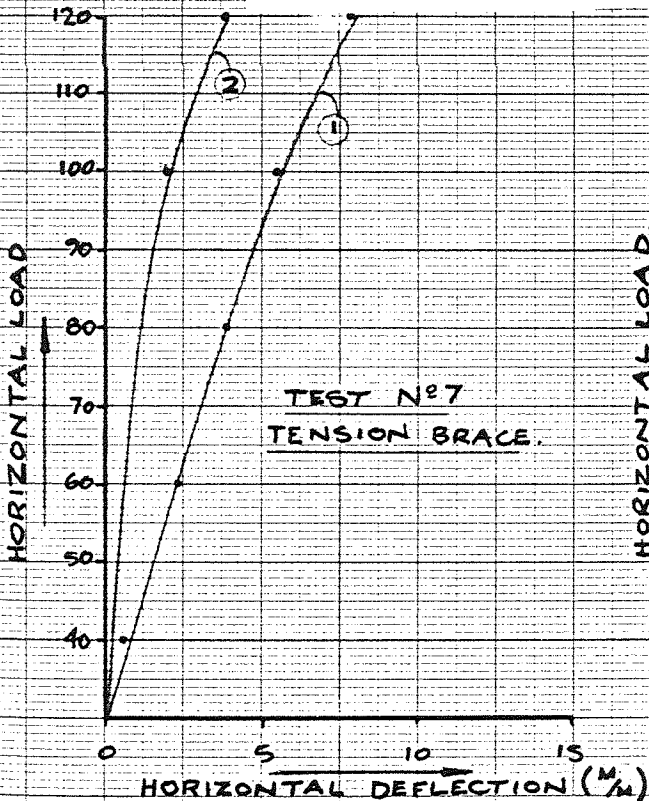


FIG 5.4

### COUPLER TYPE 'A'



### COUPLER TYPE 'B'



CURVE N° 1 ① - TOTAL DEFLECTION OF FRAME.

CURVE N° 2 ② - DEFLECTION ATTRIBUTABLE TO ROTATION OF COUPLER

FIG 5.5

results of some of these tests are shown in Fig. 5.5.

These show that proportion of deflection attributable to rotation was variable both for the same coupler at different loading stages and between different couplers of the same type. However, the graphs shown are typical and indicate that coupler rotation accounts for, on average, about 60% of frame movement below the working load of the coupler and a decreasing percentage above working load. At this point other movements of the coupler became predominant.

### 5.3 THE PREDICTION OF HORIZONTAL DEFLECTIONS USING A STRAIN ENERGY METHOD

It is assumed in this analysis that the coupler can be modelled by analogy with a helical spring wrapped around the standard. Thus the deflection can be found by using the strain energy of that spring.

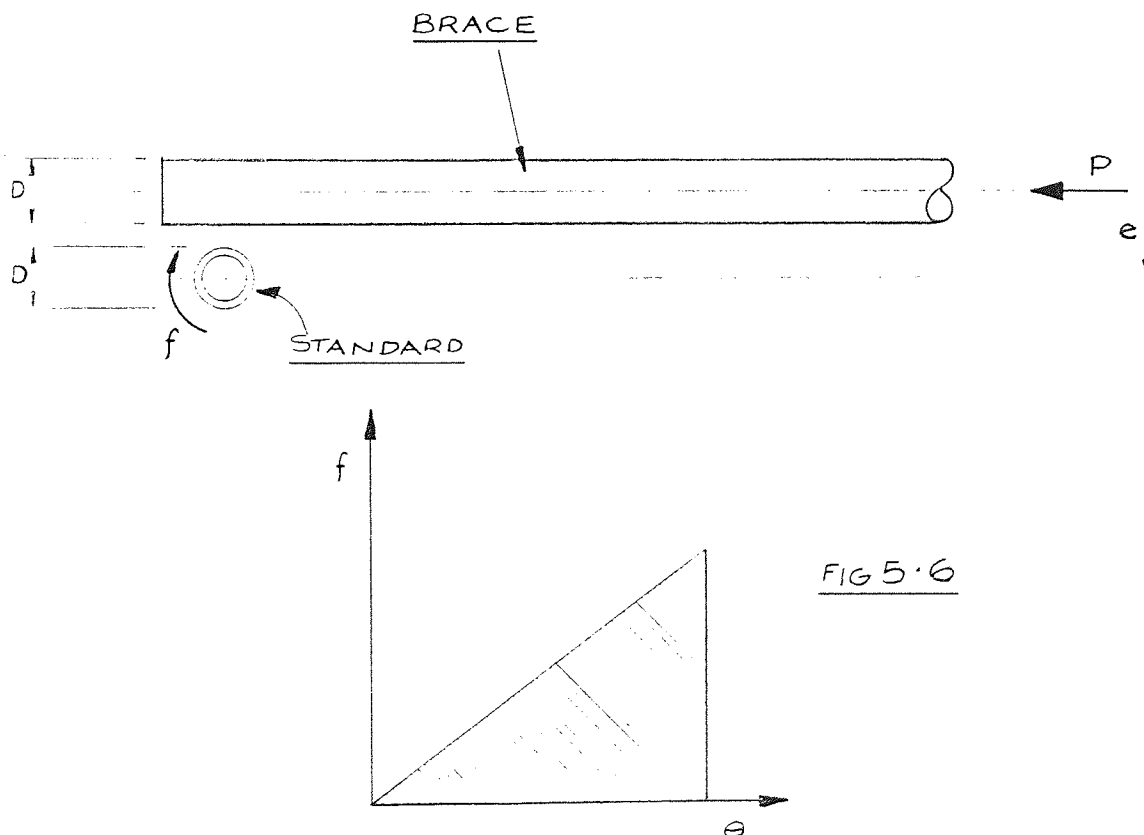


FIG 5.6

$$\text{Strain energy in rotation} = U_R$$

$$U_R = \frac{1}{2} \cdot f \cdot \frac{\theta D}{2} \quad \dots 5.1$$

If the coupler acts as a spring, then

$$f = K \cdot \theta \quad \dots 5.2$$

This assumes that the spring is linear-elastic. This is only an assumption, but seems reasonable from Figs. 5.3 and 5.5.

Substituting 5.2 into 5.1 gives :

$$U_R = \frac{f^2}{K} \cdot \frac{D}{4} \quad \dots 5.3$$

Taking moments about the polar axis of the standard gives :

$$f = \frac{2e}{D} \cdot P \quad \dots 5.4$$

Substituting 5.4 into 5.3 gives :

$$U_R = \frac{P^2}{K} \cdot \frac{e^2}{D}$$

Now total strain energy for the system is the sum of strain energy in rotation of the couplers plus strain energy in axial shortening or lengthening of members :

$$\begin{aligned} U &= U_{AX} + U_R \\ &= \frac{1}{2} \sum \frac{F^2 L}{AE} + \frac{e^2}{D} \sum \frac{P^2}{K} \end{aligned}$$

$$\therefore \Delta = \frac{\partial U}{\partial W} = \sum \frac{FL}{AE} \cdot \frac{\partial F}{\partial W} + \frac{2e^2}{D} \sum \frac{P}{K} \frac{\partial P}{\partial W} \quad \dots 5.5$$

where : F is member force

P is the component of the brace load normal to the standard which for a properly braced frame is the shear in the panel

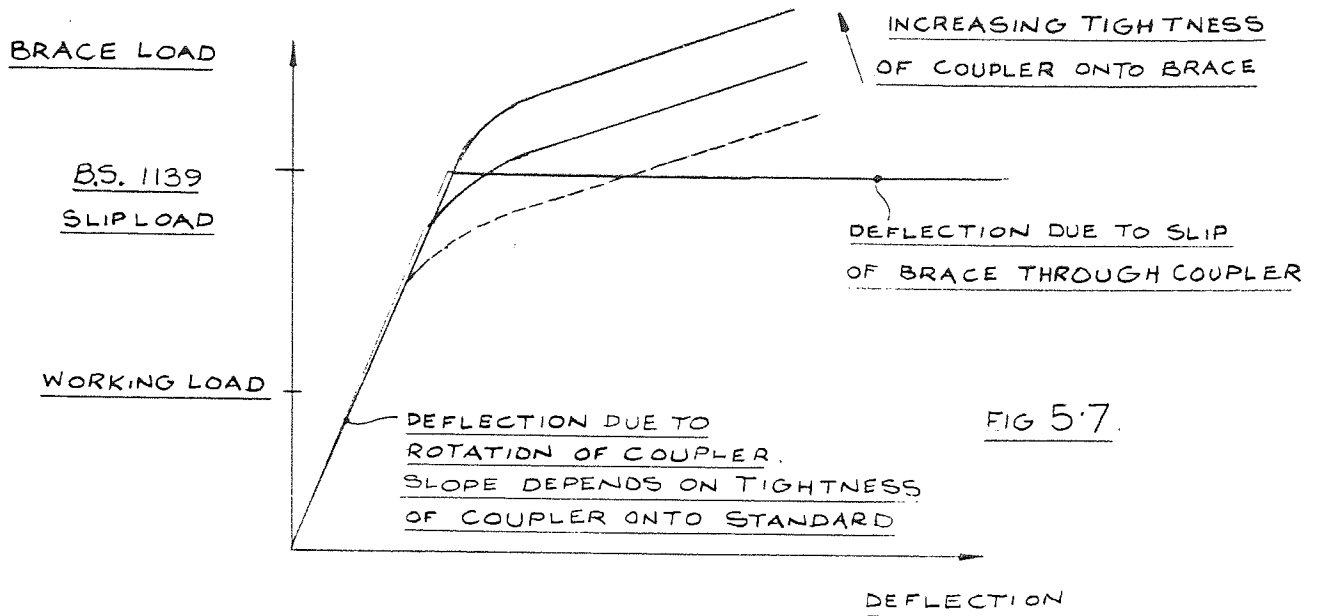
W is the load applied where deflection is to be found.

For the rotational portion of this equation it should be noted that the expression  $\frac{2e^2}{D}$  relates to the physical dimensions of the coupler and emphasises the importance of eccentricities in controlling deflections. The constant K relates to the frictional properties of the coupler and tube and its value must be determined by experiment.

Now the model described by equation 5 states that the structure will deform linearly under horizontal load because the plan rotation of the coupler and axial deformation of the frame are both assumed to be linear-elastic phenomena. This will continue until the load in the brace reaches the slip load of the coupler as laid down by B.S. 1139. The brace will then slide through the coupler at constant load.

However, experiments have shown that the coupler in fact behaves somewhat differently to this (see Fig. 5.7).

The load deflection curve remains linear until the brace load reaches a certain point which is normally above working load of the coupler. Above this point deformation takes place by sliding of the brace through the coupler but not at constant load for this section of the



curve has a slight gradient. This is caused by the fact that the coupler tends to gouge the surface of the bracing tube. The point of transition between the two types of deformation depends on the tightness of that half of the coupler connected to the brace whereas the slope of the first part of the curve depends on the tightness of the coupler on the standard. Under ideal circumstances the tightness of the coupler can be controlled by using a torque-wrench but in the real world this is open to all sorts of errors.

The fact that the model differs from the observed coupler characteristics does not automatically invalidate it for it gives good results in the working range of the coupler. This is discussed in the next section.



#### 5.4 CORRELATION BETWEEN THEORY AND EXPERIMENT

Now in the experiments on full scale assemblies only one design of coupler was used. The value of K for this coupler was obtained from Fig. 5.3 and found to be :

$$K = 715 \text{ KN/rad.}$$

It was thought that this value should be checked so the apparatus described in paragraph 3.2.3 was devised. The calculation for this is shown below :

$$\Delta_R = \frac{2e^2}{D} \leq \frac{P}{K} \frac{\partial P}{\partial W}$$

From Fig. 5.8

$$\text{LOAD IN BRACE} = \frac{W}{\cos \phi} \cdot \frac{b + 2a}{b}$$

$$\therefore P = W \cdot \frac{b + 2a}{b}$$

$$\therefore \frac{P}{W} = \frac{b + 2a}{b} = 1.565$$

$$\text{now } e = 70 \text{ mm}$$

$$D = 48.4 \text{ mm}$$

$$\text{therefore if } W = 5 \text{ KN}$$

$$P = 7.825 \text{ KN}$$

$$\therefore \Delta_R = \frac{2(70)^2}{48.4} \times 2 \times \frac{7.825}{715} \times 1.565 = 10.91 \text{ mm}$$

It should be noted that this rig is much smaller than a full size scaffold and so it differs in two ways. Firstly the deflection due to axial shortening or lengthening of members is small :

$$\Delta_{AX} = \sum \frac{FL}{AE} \frac{\partial F}{\partial W}$$

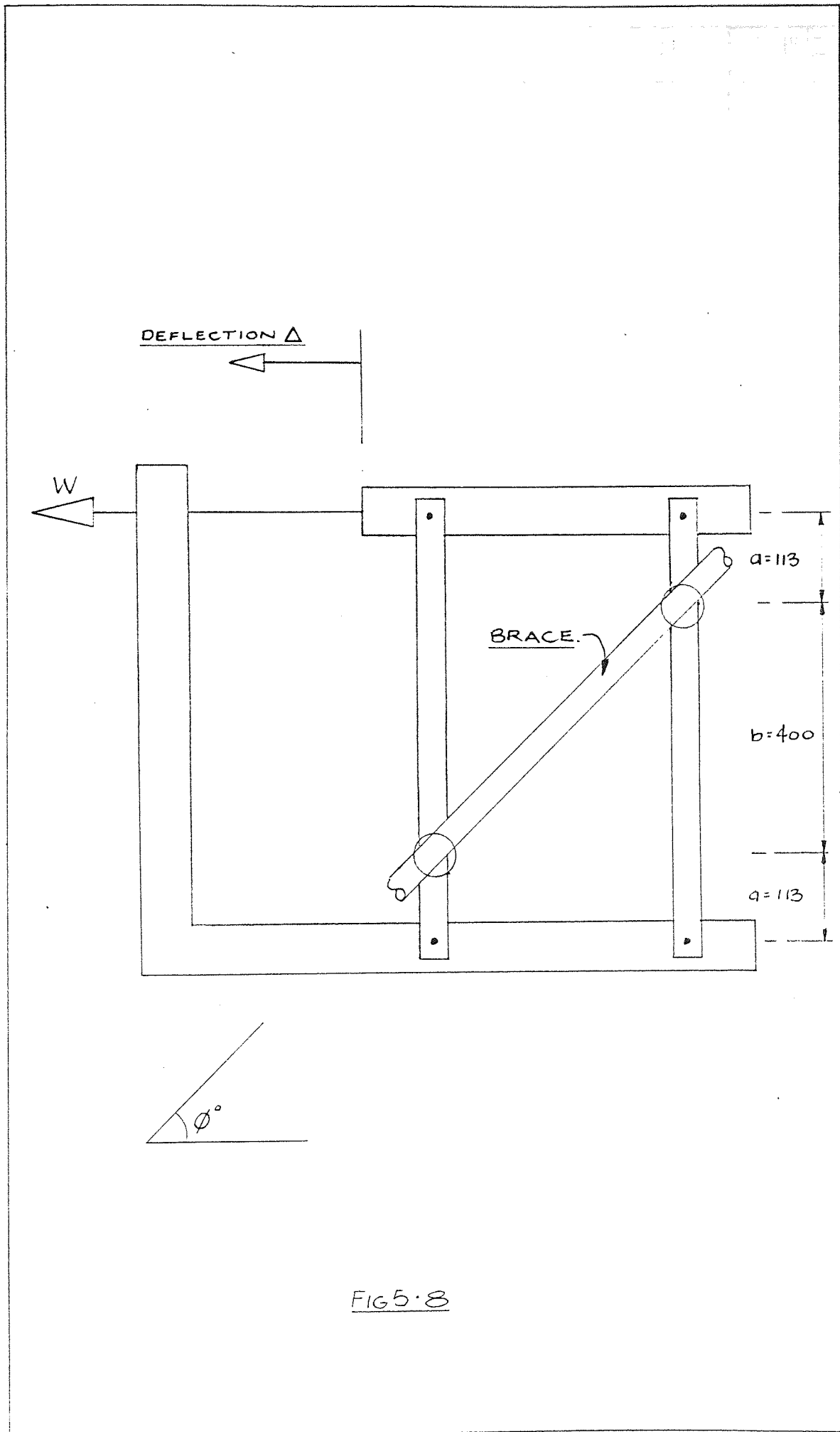
$$\therefore \text{ at } W = 5 \text{ KN} \quad \Delta_{AX} = 0.19 \text{ mm}$$

Secondly and conversely bending of members becomes important because of the short slenderness ratios of members and the fact that bending moments are induced since the coupler position is not coincident with the pins at A and B (Fig. 5.8).

$$\Delta_B = 4.34 \text{ mm} \quad \text{at } W = 5 \text{ KN}$$

$$\begin{aligned} \therefore \Delta &= \Delta_R + \Delta_{AX} + \Delta_B \\ &= 15.44 \text{ mm} \quad \text{at } W = 5 \text{ KN} \end{aligned}$$

The comparison between this theoretical figure and the experimental results from the coupler rig is given in Fig. 5.9. This shows that the model gives as good a prediction as can be expected given the variability of couplers. This is provided the coupler has not entered the zone where slipping of the brace through the coupler begins. It is interesting to note, however, that for the experiments on full scale assemblies, the model was valid over a much greater range and gave accurate predictions even after slipping of the brace was plainly visible (Fig. 5.10).



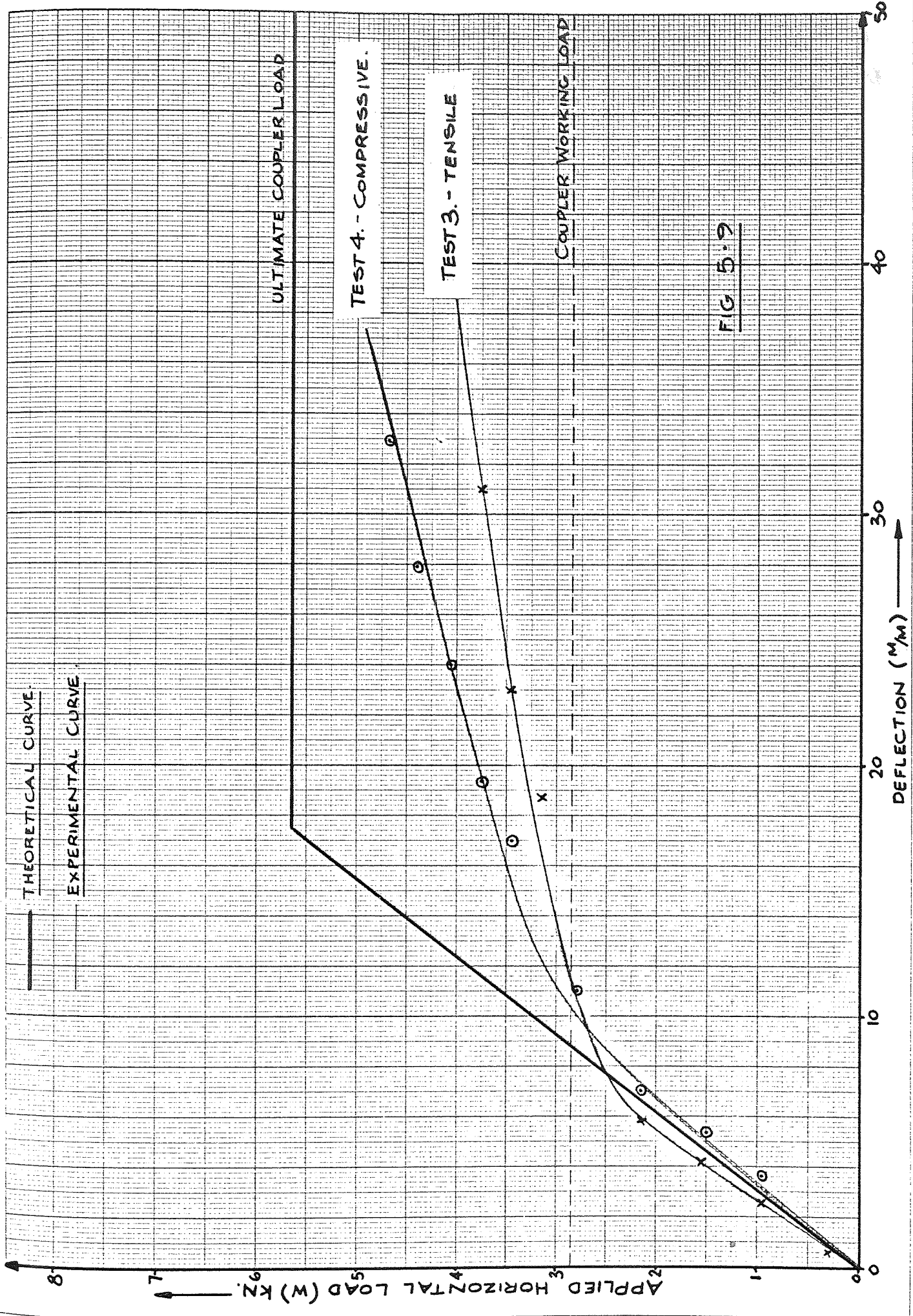
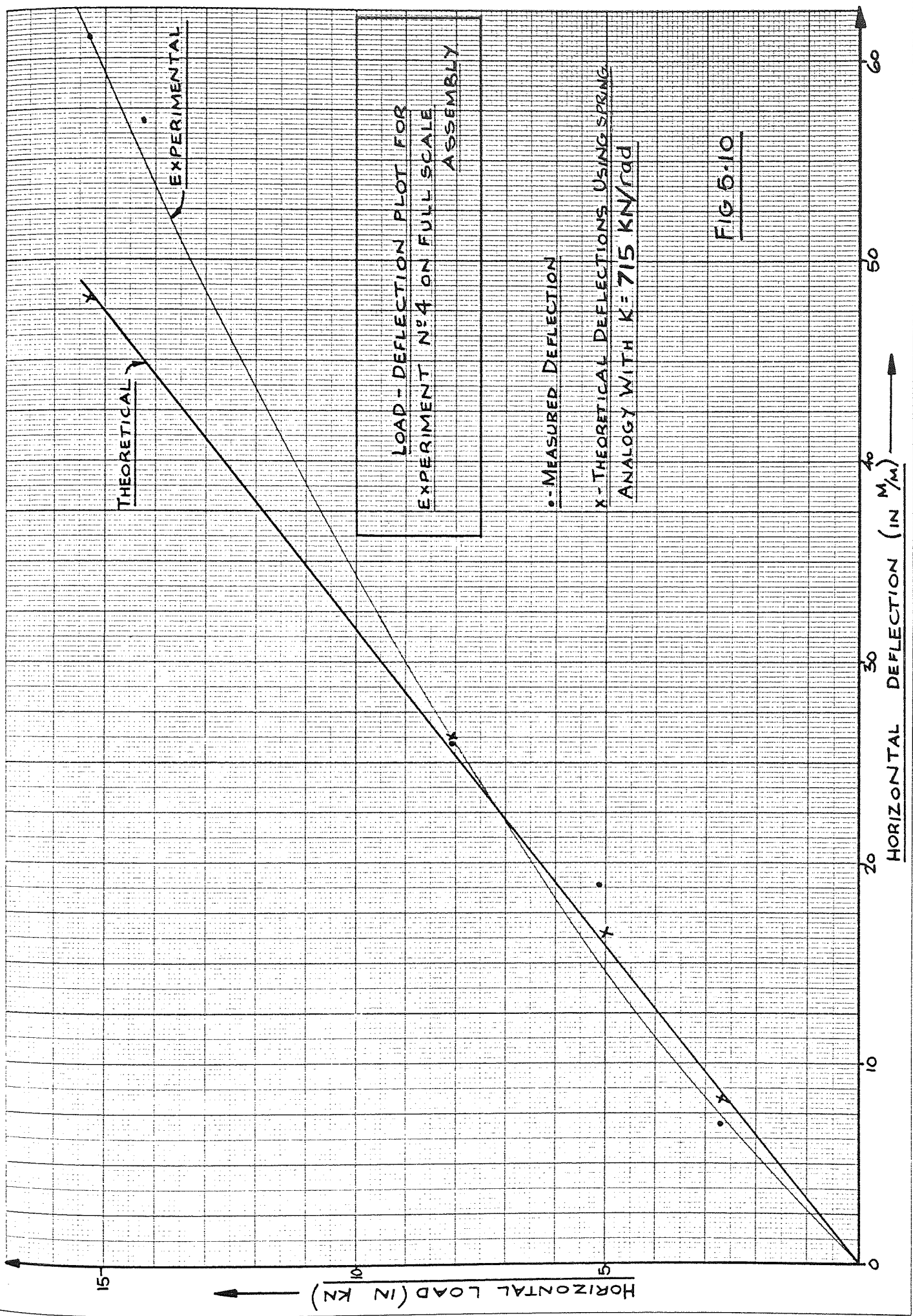


FIG 5.9



# 6

## THE LOAD CARRYING CAPACITY OF A BRACED FRAME

Having dealt with the prediction of deflections it is now appropriate to discuss the ultimate load-carrying capacity of a braced frame and the factors which effect it. For although in most cases horizontal loading will be limited by deflection considerations, it is normal to use a lower safety factor on these deflections than on ultimate load and thus both cases must be considered.

It may seem unusual to have discussed the deflection of the braced bay before its ultimate loading. The reasons for this will become apparent when discussing the sources of horizontal load and the effect of deflections on member forces.

## 6.1 EXTERNALLY AND INTERNALLY GENERATED HORIZONTAL LOADS

In the Final Report of the Advisory Committee on Falsework (the so-called Bragg report - Reference 24), one of the principal recommendations concerned the ability of falsework structures to resist horizontal loads. It suggested that :

"All falsework structures should be designed to accommodate all identifiable horizontal loads plus an additional allowance of 1% of the vertical load in any direction to allow for unknowns. But in no case should the allowance for the horizontal load in any direction be less than 3% of the vertical."

The identifiable horizontal loads include unbalanced concrete pressures, wind forces and plant loading. Many designers have their own ideas about how to allow for these and the subject is comprehensively covered by Grant (Reference 25). However, the additional 1% does not, at first glance, make much sense and it seems that Bragg is being unjustifiably conservative. After all, what other horizontal forces are there?

The answer is that two sources of internally generated horizontal loading have been identified during this project and whilst not applicable to all falsework structures they are at least valid for proprietary systems. These sources are eccentricity of loading and deviation from verticality and they are discussed below.

### 6.1.1 Horizontal forces caused by eccentricity of loading

If the spigot joint can be treated as a pin (see paragraph 4.2(5) ) then standard number 1 in Fig. 6.1a can be represented by the structure in Fig. 6.1b. Since the base of this structure is a pin

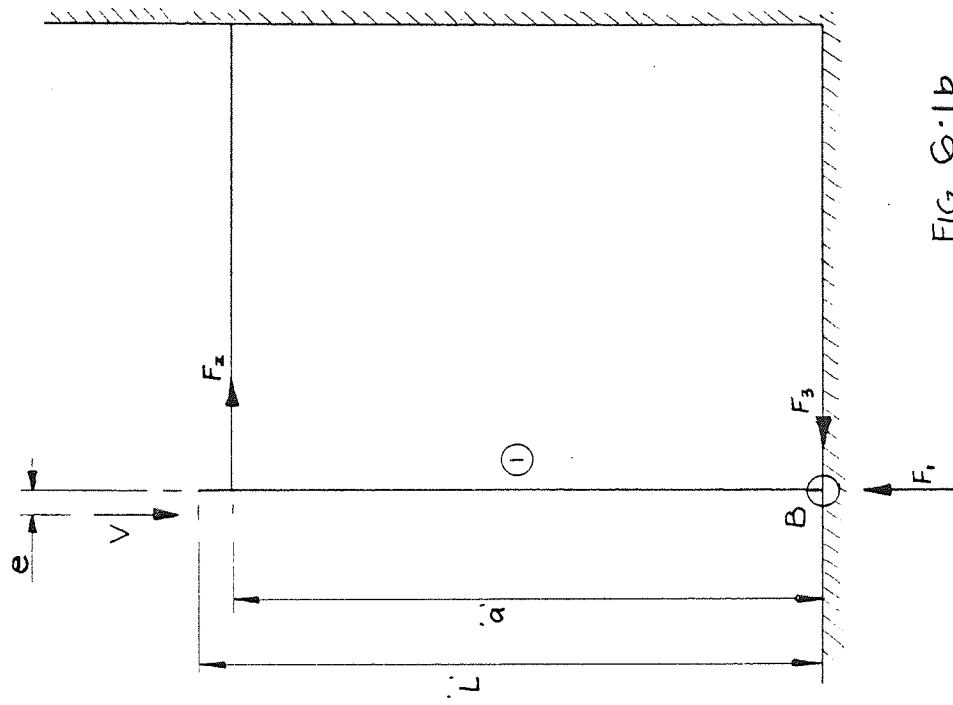


FIG G-1b

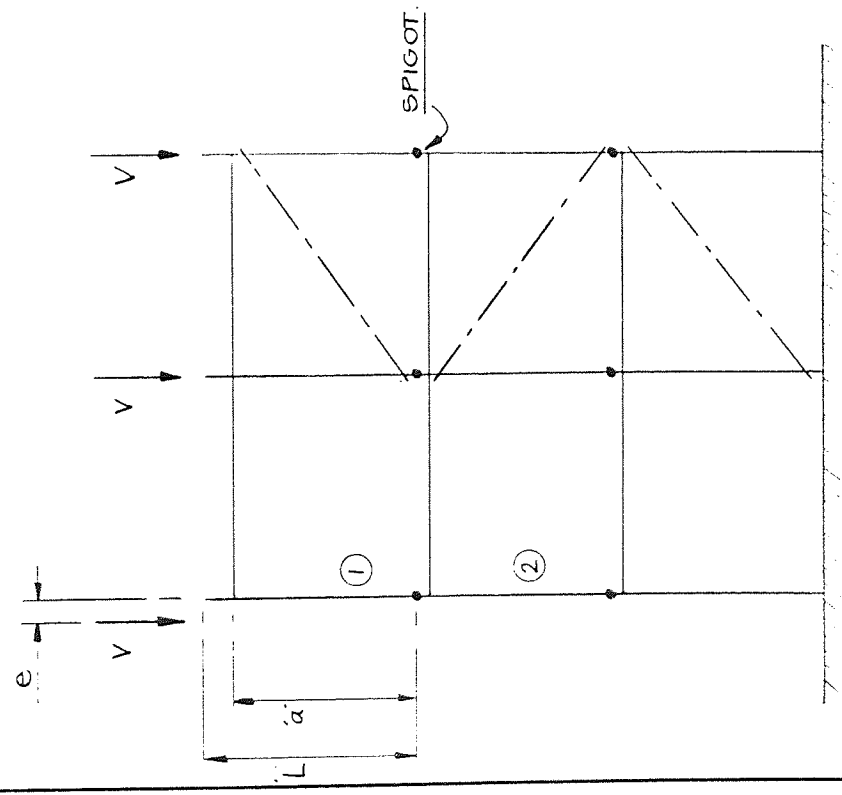


FIG G-1a



then the reaction  $F_1$  must be concentric. Thus :

$$\text{Resolving vertically} \quad F_1 = V$$

$$\text{Taking moments about B} \quad F_2 = V \cdot \frac{e}{a}$$

$$\text{Resolving horizontally} \quad F_3 = F_2 = V \cdot \frac{e}{a}$$

The eccentric load has an effect on the buckling load of the standard and this is discussed further in Chapter 7. More pertinent at this stage is that the axial load  $F_2$  must be resisted by the braced bay. Substituting typical values for  $e, a$  will give some idea of the magnitude of the horizontal load to be resisted :

$$e = 25 \text{ mm (1")}$$

$$a = 1870 \text{ mm (6' 1}\frac{1}{2}\text{")}$$

$$L = 1981 \text{ mm (6' 6")}$$

$$\therefore F_2 = \frac{25}{1870} \cdot V = 1.36\% \text{ of } V$$

This is obviously higher than the 1% suggested by Bragg but then 25 mm is a very large eccentricity.

Remember also that it is normal practice to brace every sixth bay so that the horizontal load to be resisted by the braced bay may be up to 8.16% of the load on a single standard if every standard is loaded eccentrically.

The reaction  $F_3$  is transferred by the spigot to standard number 2 immediately below and from there down through subsequent standards until it is resisted by friction between the base and the ground.

At each level a horizontal load is transferred to the braced bay by the ledger as shown in Fig. 6.2.

$$\text{Resolving vertically} \quad F_D = V$$

$$\text{Moments about C} \quad F_B = F_A \cdot \frac{L}{a}$$

$$\text{Resolving horizontally} \quad F_C = F_B - F_A$$

Using these general equations for the equilibrium of lower standards the shear forces in the spigot and load transferred to the braced bay can be determined for each lift. This is shown in Fig. 6.3 where the assumption is made for ease of demonstration that each lift is identical.

It can be seen that both the shear across the spigots and the loads transmitted to the braced bay take the form of a geometric progression with a multiplying factor of  $-\frac{b}{a}$ . Thus if this ratio is greater than 1.0, in other words if the ledger is below half way down the standard, then these forces will be magnified as they are transferred down the standard. So to keep them within reasonable limits and thus to reduce the bending in the standard, it is best to position the ledger near to the top of the standard. Then only the loads transmitted to the braced bay by the top two ledgers are significant.

Alternatively, if there are two ledgers on the top standard then the situation is changed. In this case, in view of the play between the spigot and parent tube, it is unlikely that there will be sufficient deflection at this point for any shear to be transferred.

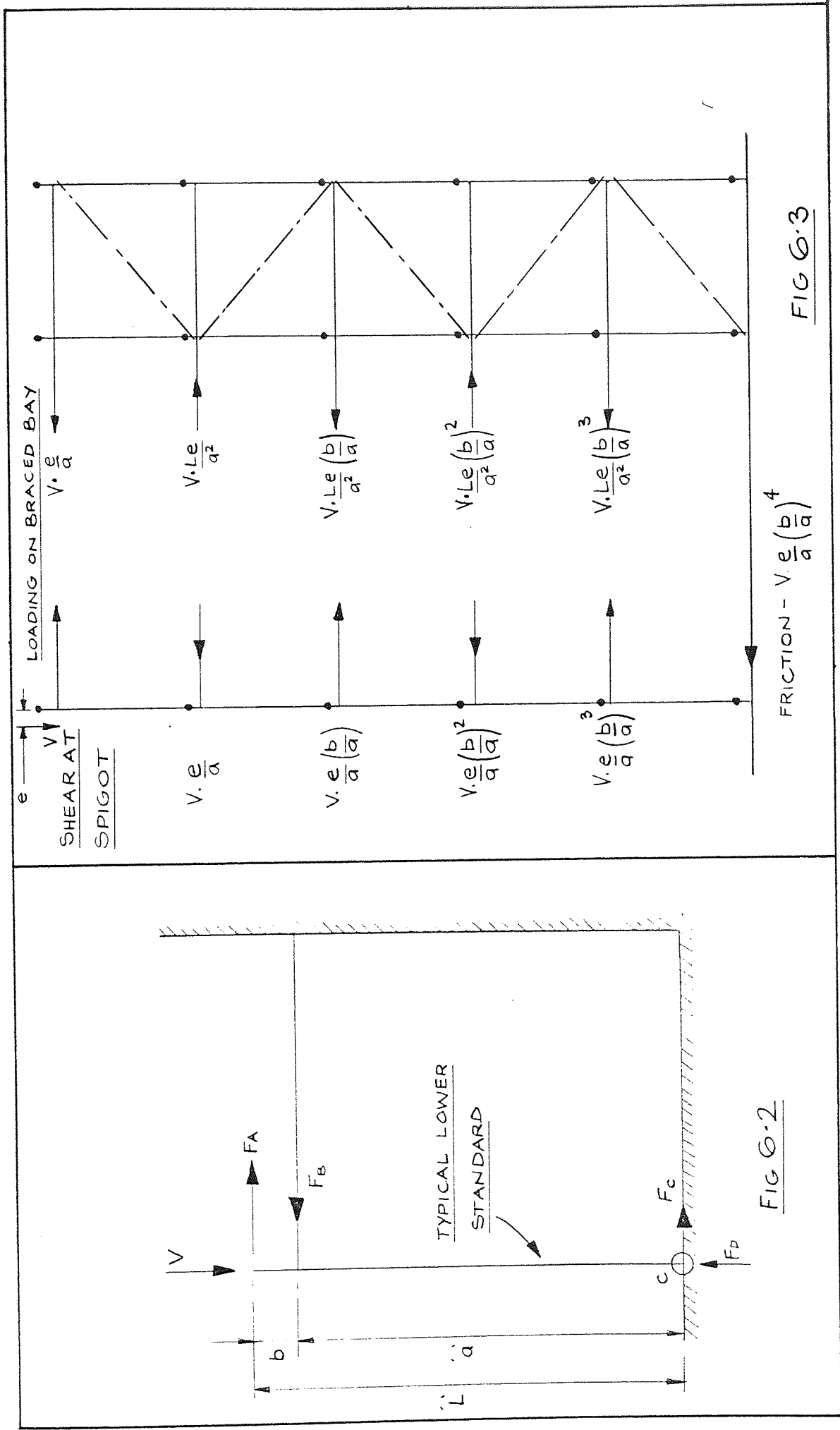


FIG 6-2

FIG 6.3

Thus the situation in Fig. 6.4 arises.

$$\text{Resolving vertically} \quad F_1 = V$$

$$\text{Taking moments about D} \quad F_2 = V \cdot \frac{e}{a_1 - a_2}$$

$$\text{Resolving horizontally} \quad F_3 = V \cdot \frac{e}{a_1 - a_2}$$

Obviously then the standards below will be required to take axial load only and the braced bay resist ledger loads  $F_2$  and  $F_3$ .

### 6.1.2 Horizontal forces caused by deviation from verticality

Scaffolding may be out of plumb either through bad erection or due to deflection under horizontal load. Assuming as before that the spigot acts as a pin, standard number 1, in Fig. 6.5a, can be represented by the structure in Fig. 6.5b.

$$\text{Resolving vertically} \quad F_1 = V$$

$$\text{Taking moments about E} \quad F_2 = V \cdot \frac{L \tan \alpha}{a}$$

$$\text{Resolving horizontally} \quad F_3 = F_2 = V \cdot \frac{L \tan \alpha}{a}$$

Putting in typical figures as before :

$$\alpha = 0.01 \text{ rads. } (0.57^\circ)$$

$$L = 1981 \text{ mm } (6' 6")$$

$$a = 1870 \text{ mm } (6' 1\frac{1}{2}')$$

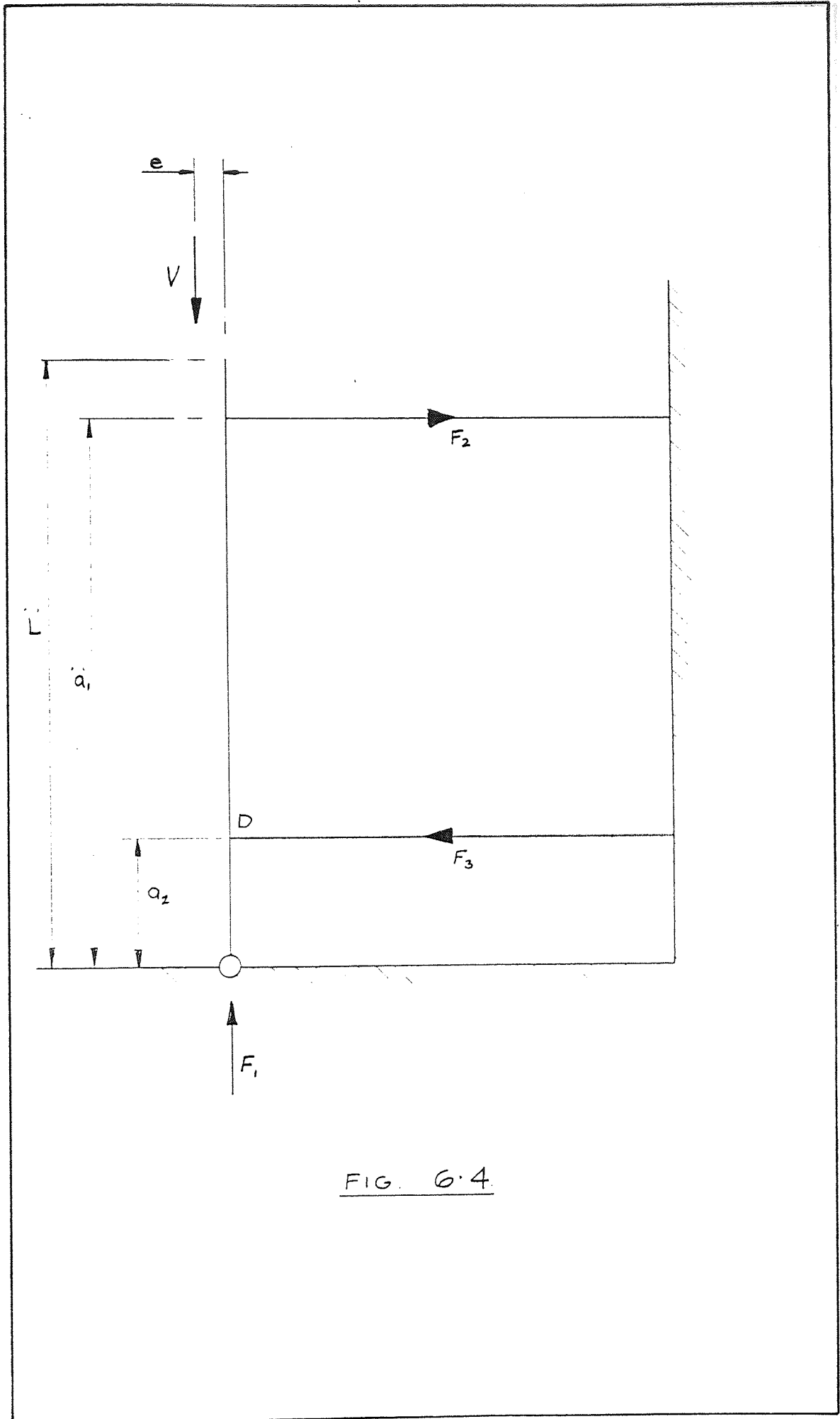


FIG. 6.4

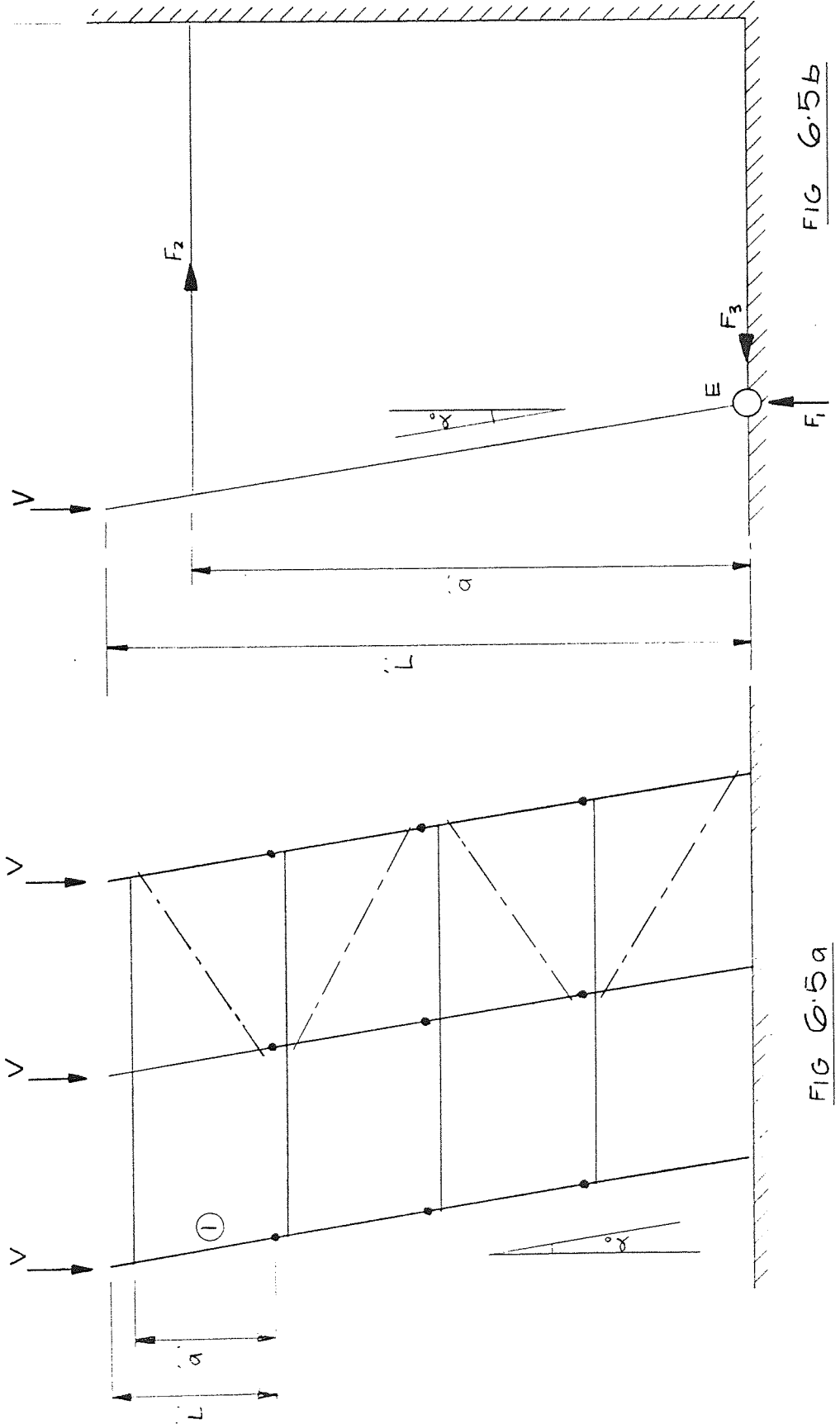


FIG 6.5b

FIG 6.5a

$$\begin{aligned} \therefore F_2 &= V \cdot \frac{1981}{1870} \times 0.01 \\ &= 1.06\% \text{ of } V \end{aligned}$$

This figure is again of the same order of the 1% suggested by Bragg.

The difference between this figure and that of 1.36% horizontal load due to eccentricity is that in this case if one standard is out of plumb then all standards will be out of plumb by the same amount. Thus for a braced bay every sixth bay, the horizontal load to be resisted is 6.36% of the vertical load on a single standard. When dealing with eccentricity of loading there may be no standards eccentrically loaded or there may be up to six standards eccentrically loaded and thus the situation is less clear.

It is also necessary to look at the lower standards and this is shown in Fig. 6.6.

$$\text{Taking moments about G} \quad F_B = \frac{L}{a} (V \tan \alpha - F_A)$$

$$\text{Resolving horizontally} \quad F_C = F_A \left(1 - \frac{L}{a}\right) + V \cdot \frac{L}{a} \tan \alpha$$

Using these general equations it is possible to find both the shear across the spigot and load transferred to the braced bay at all levels down the standard. This is shown in Fig. 6.7.

The change of ledger load and shear in the spigot is not a straightforward progression as for eccentricity of load and is best looked at by substituting for various values of  $\frac{b}{a}$ . This is done in Fig. 6.8.

Again it can be seen that it is better to keep the value of  $\frac{b}{a}$  small and certainly less than unity. Otherwise there is a magnification



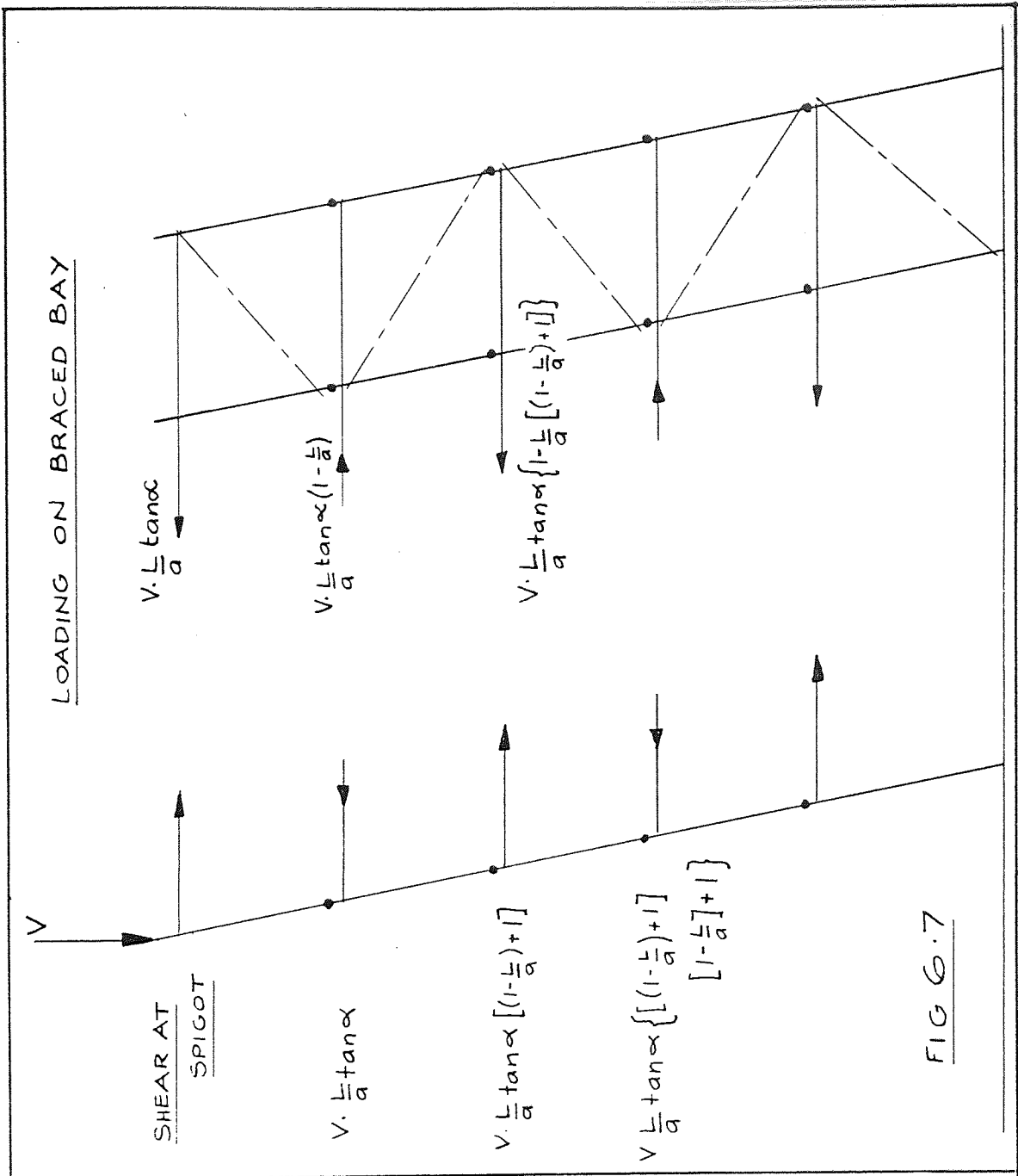


FIG 6.7

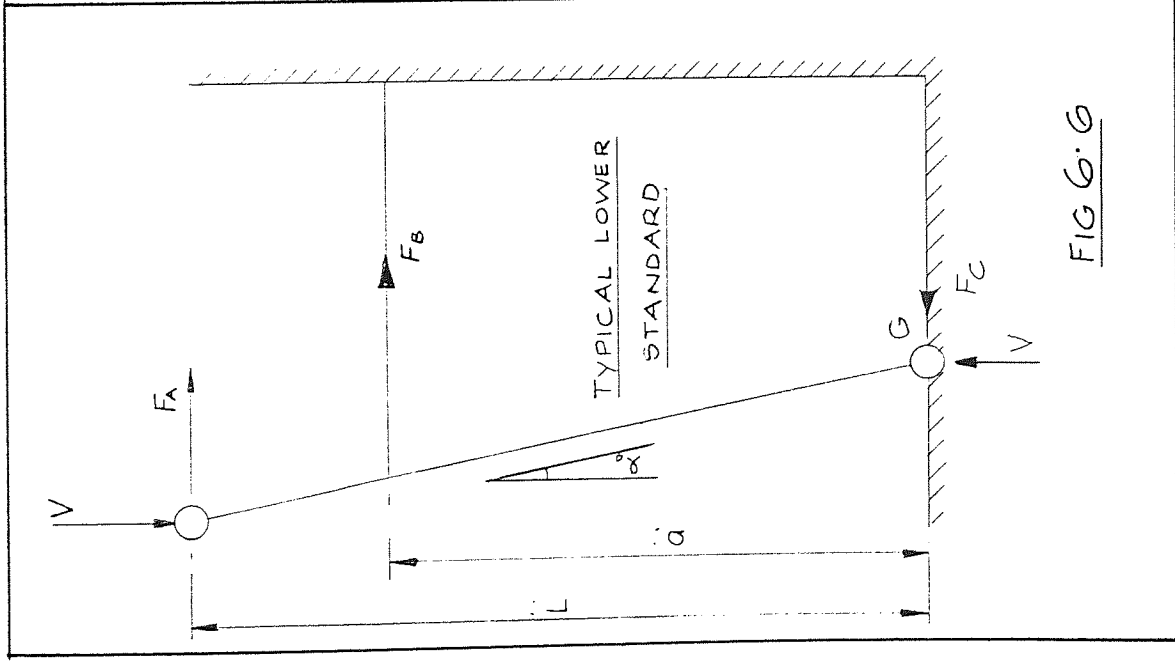


FIG 6.6



POSITION OF LEDGER OR SPIGOT - COUNTED FROM TOP	$\frac{b}{a} = 0.1$		$\frac{L}{a} = 1.1$		$\frac{b}{a} = 1$		$\frac{L}{a} = 2$		$\frac{b}{a} = 10$		$\frac{L}{a} = 11$	
	COEFFICIENT FOR SHEAR AT SPIGOT	COEFFICIENT FOR LOAD IN LEDGER	COEFFICIENT FOR SHEAR AT SPIGOT	COEFFICIENT FOR LOAD IN LEDGER	COEFFICIENT FOR SHEAR AT SPIGOT	COEFFICIENT FOR LOAD IN LEDGER	COEFFICIENT FOR SHEAR AT SPIGOT	COEFFICIENT FOR LOAD IN LEDGER	COEFFICIENT FOR SHEAR AT SPIGOT	COEFFICIENT FOR LOAD IN LEDGER	COEFFICIENT FOR SHEAR AT SPIGOT	COEFFICIENT FOR LOAD IN LEDGER
TOP	1	1	1	1	1	1	1	1	1	1	1	1
2 <sup>ND</sup>	0.9	-0.1	0	-1	0	-1	-9	-10	-9	-10	-9	-10
3 <sup>RD</sup>	0.91	0.01	1	1	1	1	91	100	91	100	91	100
4 <sup>TH</sup>	0.909	-0.001	0	-1	0	-1	-909	-1000	-909	-1000	-909	-1000
5 <sup>TH</sup>	0.9091	0.0001	1	1	1	1	9091	10000	9091	10000	9091	10000

SHEAR FORCE IN SPIGOT = COEFFICIENT  $\times V \cdot \frac{L}{a} \cdot \tan \alpha$

AXIAL FORCE IN LEDGER = COEFFICIENT  $\times V \cdot \frac{L}{a} \cdot \tan \alpha$

FIG 6.8

of bending and shear in the standard and of horizontal load on the braced bay.

### 6.1.3 Correlation between theory and experiment on internally generated horizontal loads

How is it possible to check whether the effects described in the above sections actually take place in a real scaffold? One obvious way is to measure the loads in the ledgers remote from a braced bay. However, the stresses involved would be very low and thus open to error.

Another way is to carry out a test with eccentric loads and measure the load deflection characteristics. Then by adding the internally generated loads to the externally applied loads it is possible, using the method described in Chapter 5, to determine the theoretical load-deflection curve. These can then be compared.

This is done in Fig. 6.9 and it can be seen that the theory and experiment differ greatly. This is because there were very high loads in the bracing caused by the eccentricity of loading. Thus sliding of the braces through the couplers took place very early in the experiment so that the theory of the previous chapter was no longer valid. This is further illustrated by the fact that when failure took place by slipping of bracing, the externally applied load was only 1.6 KN per frame.

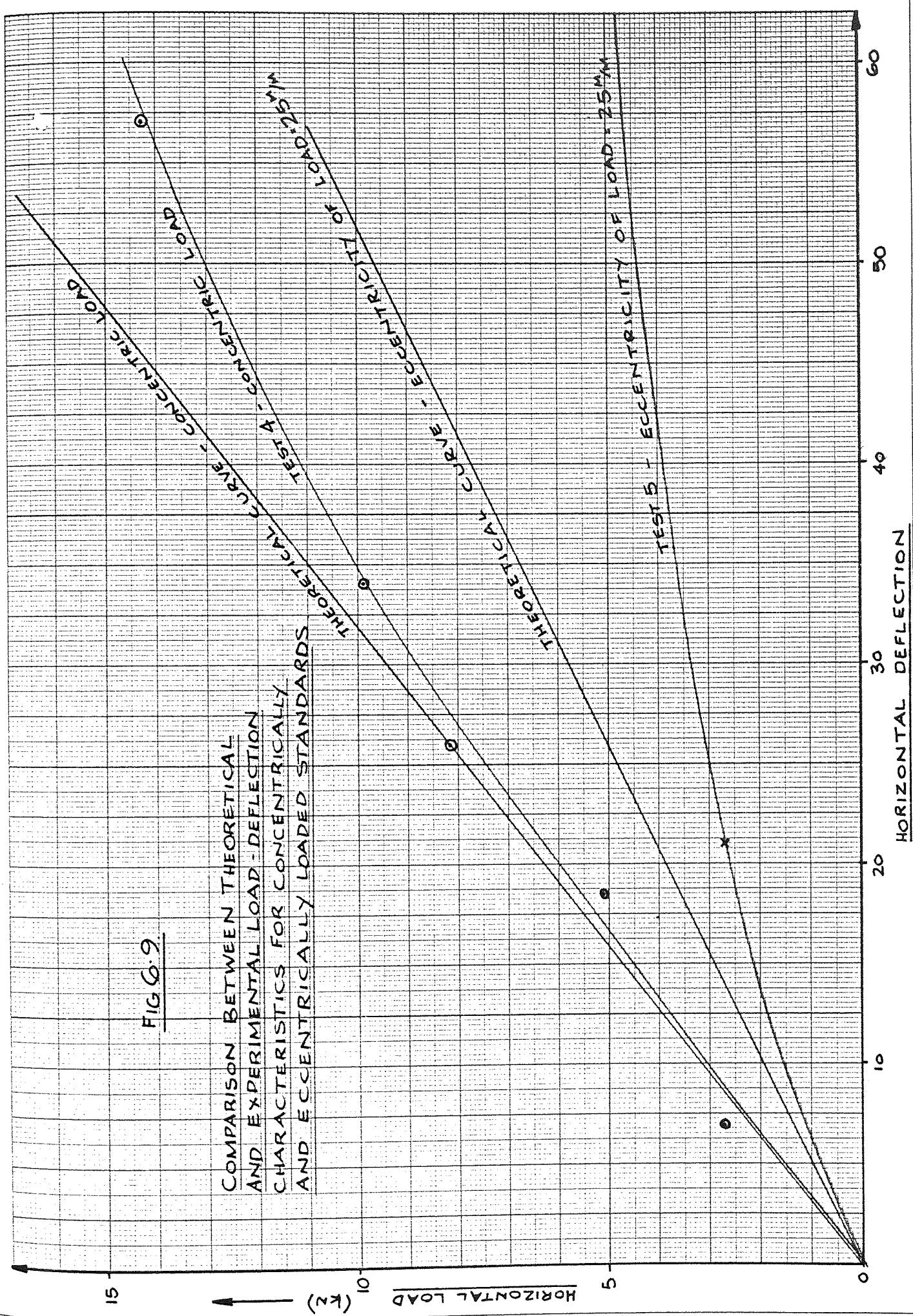


FIG 6.9.

COMPARISON BETWEEN THEORETICAL AND EXPERIMENTAL LOAD-DEFLECTION CHARACTERISTICS FOR CONCENTRICALLY AND ECCENTRICALLY LOADED STANDARDS

## 6.2 THE ULTIMATE LOAD CARRYING CAPACITY OF A BRACED BAY

As explained in the introduction to this chapter, it is important to examine the ultimate load carrying capacity of a braced bay and the factors which effect it. In the experiments on full scale assemblies two failure modes were observed, namely, buckling of the standard on the compression side of the braced bay and sliding of the brace through the coupler.

The former can be treated in the same manner as buckling of individual standards by making the assumption that the bracing has no stiffening effect. This is reasonable because a swivel coupler is obviously not a moment connection. However, it should be remembered, as explained below, that deflection of the frame can increase the loading on the standard on the compression side of the braced bay (e.g. Fig. 6.11a, member BA has an axial load of 120.97 KN and in Fig. 6.11b an axial load of 125.24 KN - an increase of 4%).

Sliding of the brace through the coupler was the other mode of failure. Now the coupler has a relatively low working load (6.25 KN). It is, therefore, essential to be able to predict the load in a brace accurately and so all relevant factors should be considered. In doing so remember that the bending stresses can be neglected and thus the axial forces are found by treating the structure as a pin-jointed frame.

### 6.2.1 The effect of deflection on the analysis of a braced frame

In conventional structures, building frames for example, deflections are generally so small that analysis of the underformed frame is

Fig 6.10

sufficiently accurate. However, as discussed in Chapter 5, large deflections can take place in scaffolds under relatively small horizontal loads and thus redistributes member forces. Consider the frame shown in Fig. 6.10. This is in fact the braced bay from the full scale assembly experiments. The axial forces can be found by treating it as a pin-jointed frame. This is done in Fig. 6.11a. The same procedure can be carried out for the deformed shape (Fig. 6.11b).

Now the difference between the brace loads in the underformed and deformed state can be compared. On the experiments on full scale assemblies the following conditions were recorded :

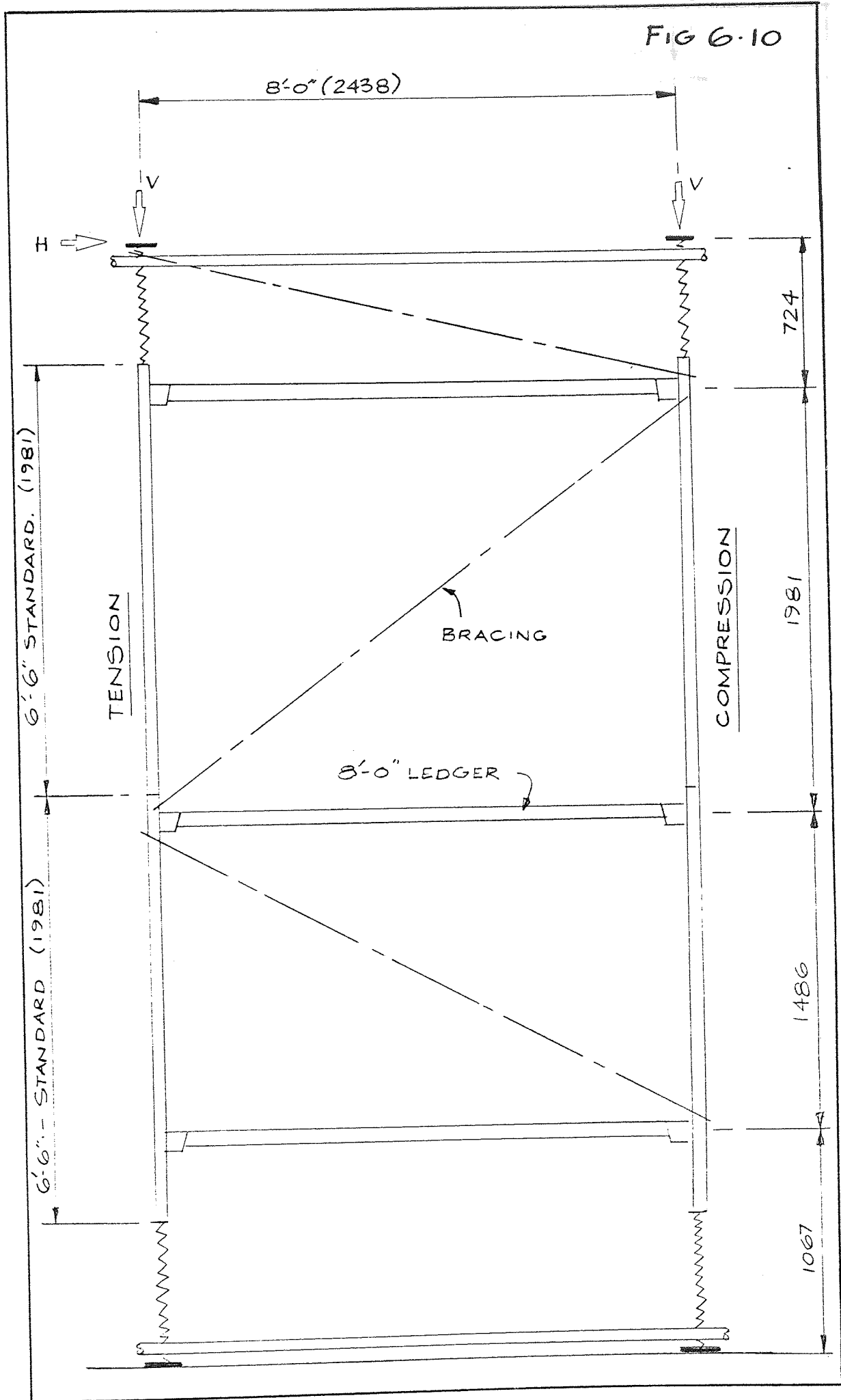
$$\begin{aligned} V &= 88 \text{ KN} \\ H &= 15.25 \text{ KN} \\ \Delta &= 61 \text{ mm at header beam level} \end{aligned}$$

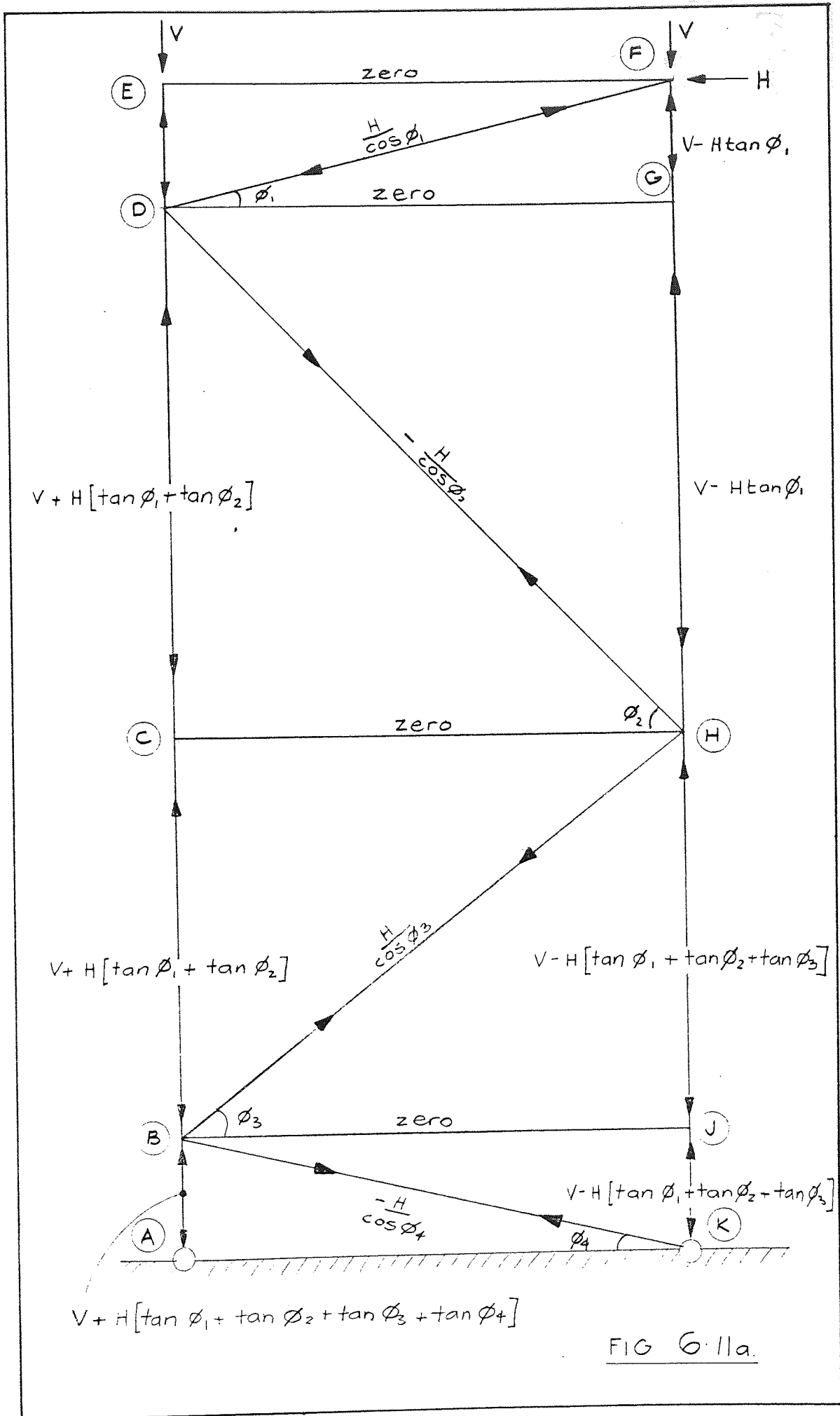
$$\begin{aligned} \phi_1 &= 17.87^\circ \\ \phi_2 &= 39.09^\circ \\ \phi_3 &= 31.36^\circ \\ \phi_4 &= 22.67^\circ \end{aligned}$$

$$\text{Total height of structure} = 5238$$

$$\therefore \alpha = \frac{61}{5238} = 0.667^\circ \text{ (0.0117 rads)}$$

FIG 6-10





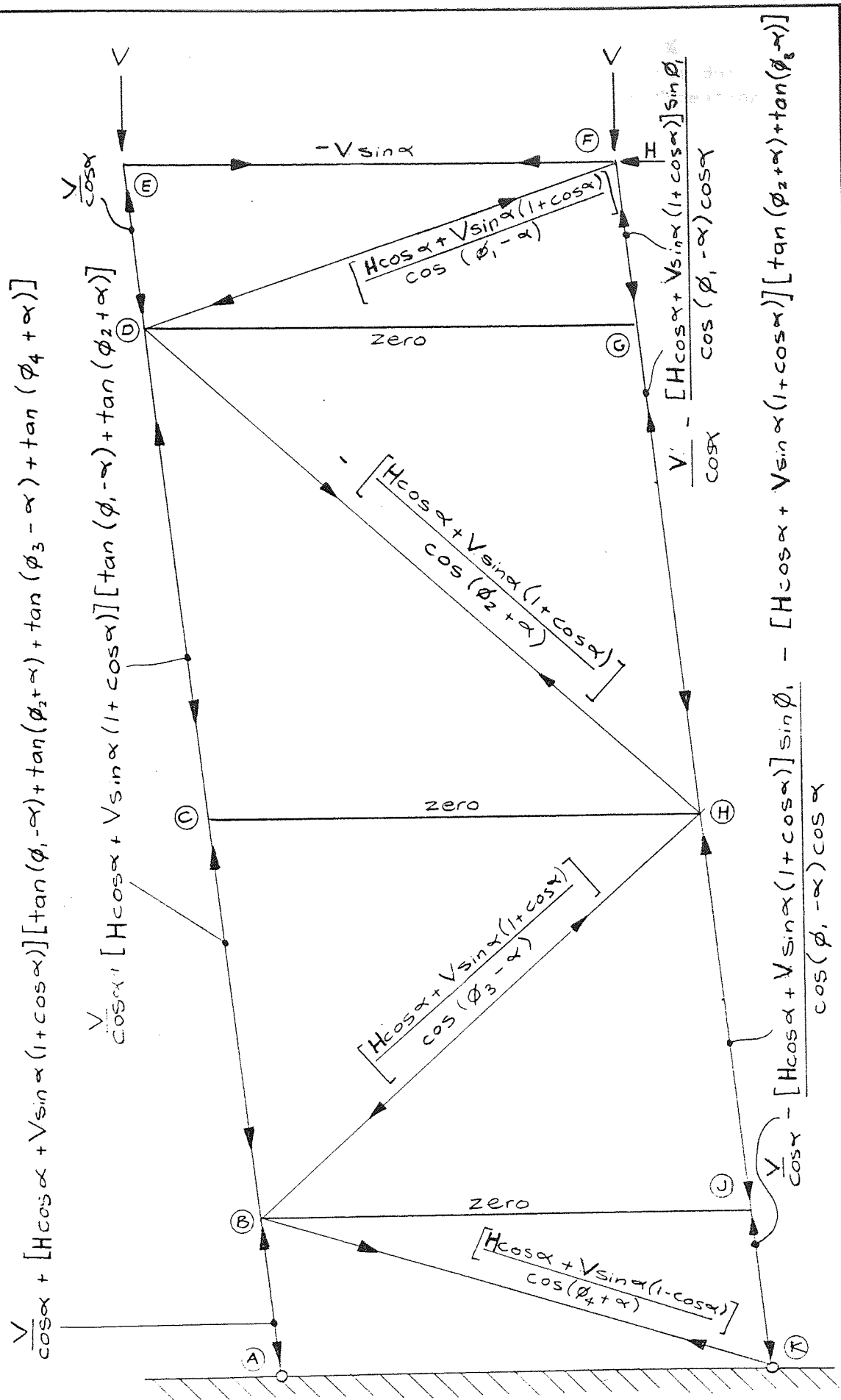


FIG 6.11b



Member	Member Load in underformed state (KN)	Member Load in deformed state (KN)	% increase due to deformation
DF	16.02	18.11	+ 13%
DH	- 19.64	- 22.50	+ 15%
HB	17.86	20.12	+ 13%
BK	- 16.45	- 18.75	+ 14%

This variation is important since an increase of 15% in load in a brace reduces the load factor from 2.0 to only 1.74. It may, therefore, be appropriate on some structures to allow a load factor on bracing members greater than 2.0 to cater for this effect.

#### 6.2.2 The effect of surface condition of tube on the slip load of a brace

As discussed in Chapter 5, the two factors which affect deflection characteristics of a scaffold are the eccentricity between the bracing tube, the frictional properties of coupler and brace and the slope of the brace  $\phi$ . Of these perhaps the most important so far as ultimate horizontal loading of the structure is concerned is the frictional properties of the coupler and tube.

For in the experiments on full scale assemblies a variety of bracing tubes were used, both new and old, galvanised, painted and black. Yet when slipping took place it was most frequently and most extensively observed to have occurred on galvanised tube. This is very much in agreement with the findings of research into the slipping of joints incorporating friction grip bolts. In Reference 26, for example, the average coefficient of friction for joints with galvanised parts was

0.23 compared with 0.29 for joints with untreated parts. Similarly old rusty tube tended to slip more than new or painted tube and thus again conforms to the findings of Reference 27.

During these experiments there was recorded one isolated case of a coupler sliding along a standard. This took place in a fairly steep brace ( $\phi = 50^\circ$ ) and serves as a reminder that such a failure is possible when bracing is used at steep angles ( $55^\circ$  and above) such that  $\tan \phi$  has a value greater than  $\frac{e}{D}$ .

### 6.3 CORRELATION BETWEEN THEORETICAL AND RECORDED SLIP LOAD OF A COUPLER

During the full scale assembly experiments the load at which slipping of a coupler first took place was recorded. This was possible because when slip occurred it was accompanied by a distinctive noise and a reduction of the applied load measured by the load cells. It was also possible to identify which brace had slipped since their original positions had been marked with white gloss paint. Fig. 6.12 shows the results of these measurements.

After one or even multiple slips it is often still possible to increase the applied horizontal loads (see Fig. 5.9). The reasons for this are twofold. Firstly, the load required to push a tube through a coupler does not remain constant, but increases as slipping proceeds. This is due to the coupler scoring the surface of the tube and thus increasing the coefficient of friction between tube and coupler (see section 5.3).

Secondly, it is possible for certain scaffolds to redistribute the

applied horizontal load between frames. Since this relies on a certain amount of plan stiffness it is unlikely to occur in U.P. scaffolding under site conditions. However, this may have happened in the experimental scaffold used, as a result of the method of loading.

Test Number	Load in brace at first slip of that brace (KN)	Load in that brace at ultimate load assuming no redistribution (KN)	Comments
2	-	3.75	No slipping, failure by buckling
4	6.08	22.50	Failure by sliding of bracing
5	8.96 11.00	12.91 15.85	Galvanised tube 'Black' tube  Slipping occurred in these tubes simultaneously. Allowance has been made for eccentricity of load.

Fig. 6.12

B.S. 1139 (Ref. 23) states : A coupler connecting two tubes shall be capable of sustaining a load of 2,800 lb.f. (12.5 KN).

Thus it can be seen that :

- a) Slip can take place below the specified ultimate load of the coupler.
- b) This does not mean, however, that the structure is unsafe since the coupler will eventually reach the required strength.

# 7

## THE BUCKLING OF STANDARDS

The previous chapter discussed the failure of a properly braced scaffolding under horizontal load. Such a scaffold can also fail under vertical load by buckling of a standard. Now the load at which a strut will buckle is dependent on many factors. Positional and rotational restraint, the initial straightness, the yield stress and locked-in stresses each have their effect. All of this is dealt with in chapter seven where analysis of the buckling phenomena is a two stage process. The first stage is to determine the effective length of the standard which is dependent on positional and rotational restraint. The second stage is the determination of the buckling

load using this effective length and taking into account the other factors mentioned above. The correlation between this type of analysis and experimental results is also discussed.

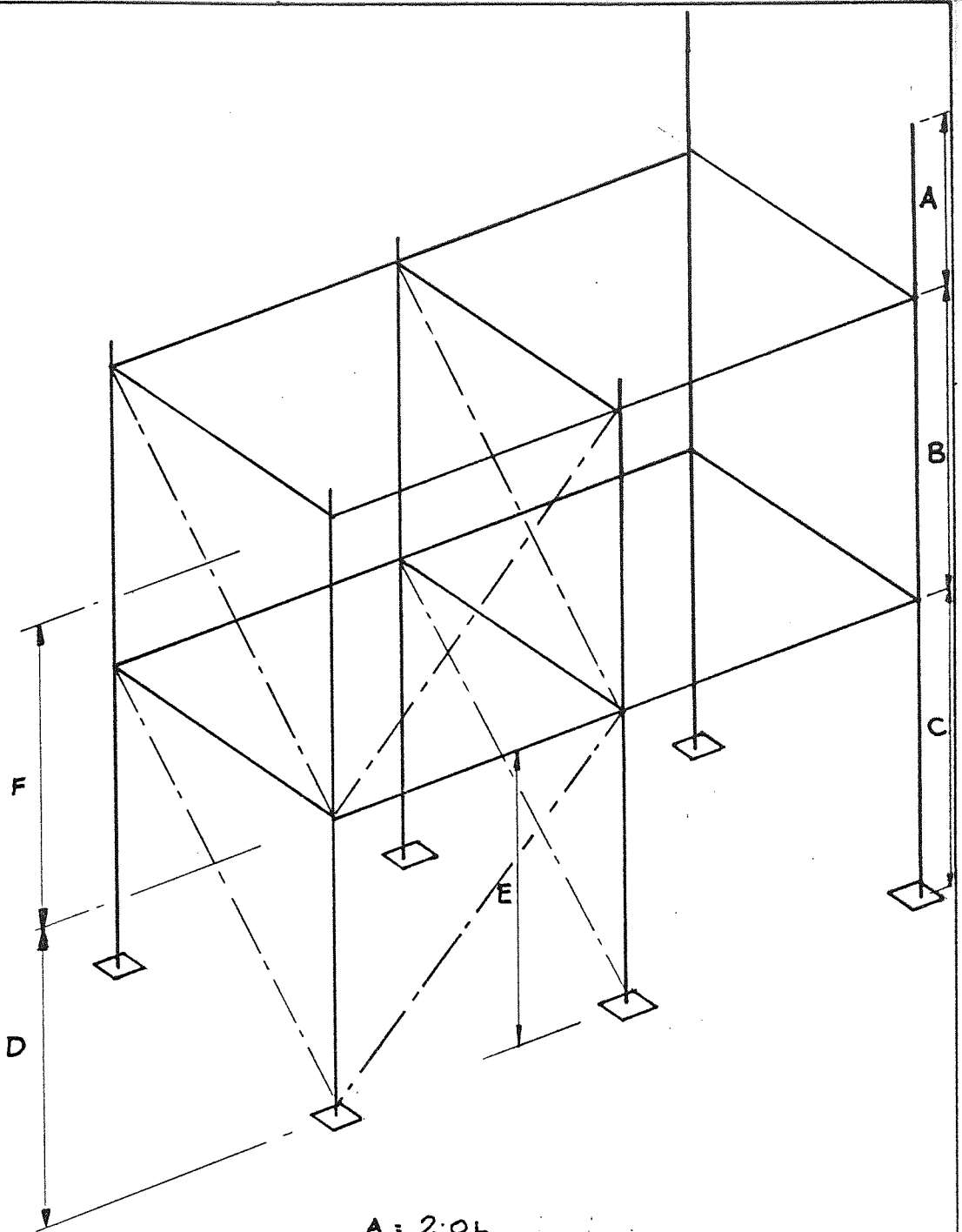
## 7.1 THE DETERMINATION OF EFFECTIVE LENGTH

When steel tube first replaced timber for use in scaffolding, engineers turned to the only guide available to design their scaffold. This was B.S. 449 which stated that when considering the buckling of a strut, to determine the effective length of a strut in a frame, one should take the distance between horizontal members and multiply it by a factor whose value depended on the stiffness and positional fixity of these members. This method of determining  $L_e$  is shown in Fig. 7.1. When systems scaffolds were introduced exactly the same design procedure was adopted.

One of the major outcomes of this project is to show that this approach might well be unsafe. This is because the traditional approach ignores the fact that there are discontinuities of bending moment at the spigot (see paragraph 4.2 - 5). So to determine the effective length of a strut in a proprietary scaffold the length between spigots should be considered. This is done for four cases below, namely, a standard at mid-height in a scaffold with ledgers attached at one or two positions and a top or base standard with one or two ledgers attached. Using these four modules virtually any scaffold can be constructed.

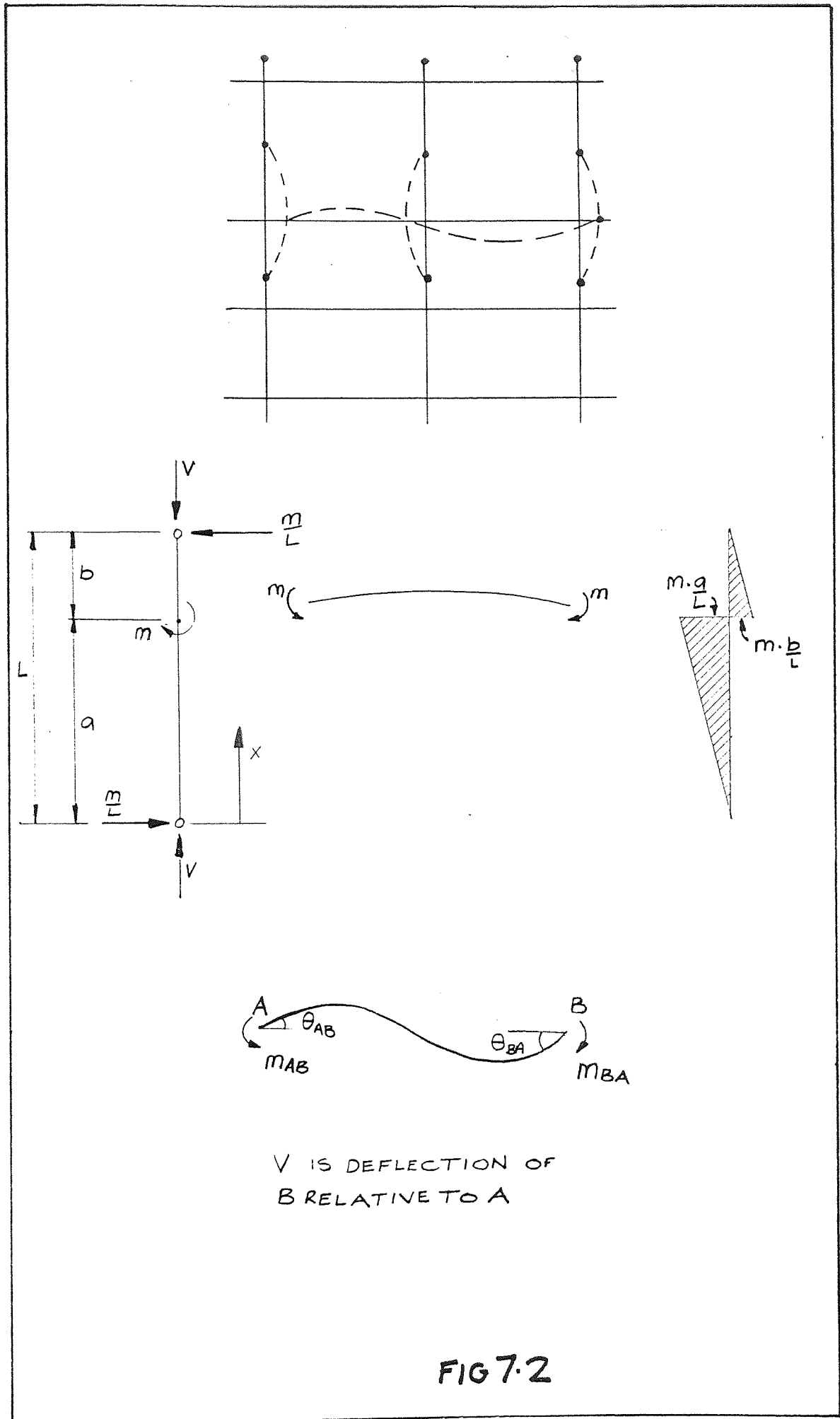
### 7.1.1 Standard with ledgers attached at one lug cluster only

Consider the simple case of a standard in one plane with ledgers attached at one lug cluster only (see Fig. 7.2). The equilibrium equation for this strut is :



- A = 2.0L
- B = 0.85L to 1.8L
- C = 1.5L to 2.0L
- D = 0.85L to 1.3L
- E = 1.0L to 1.5L
- F = 0.7L to 1.0L

FIG 7.1





$$- EI \frac{d^2 y}{dx^2} - Vy + \left\{ M \cdot \frac{x}{L} - M \cdot h(x-a) \right\} = 0$$

$$\text{where } h(x-a) = 0 \text{ for } x \leq a$$

$$h(x-a) = 1 \text{ for } x > a$$

Using the D operator gives :

$$(D^2 + k^2)y = \frac{1}{EI} \left\{ M \cdot \frac{x}{L} - M \cdot h(x-a) \right\}$$

$$\text{where } k^2 = \frac{V}{EI}$$

The differential equation can be solved using Laplace transforms :

$$D^2 y = s^2 \bar{y} - s \cdot y(0) - y'(0)$$

$$\text{if } y = 0 \text{ at } x = 0$$

$$\therefore D^2 y = s^2 \bar{y} - y'(0)$$

$$= s^2 \bar{y} - A$$

$$\therefore \bar{y} (s^2 + k^2) = A - \frac{1}{EI} \left\{ \frac{M}{L} \cdot \frac{1}{s^2} - M \cdot \frac{e^{-as}}{s} \right\}$$

$$\therefore \bar{y} = \frac{A}{s^2 + k^2} - \frac{1}{EI(s^2 + k^2)} \cdot \left\{ \frac{M}{L} \cdot \frac{1}{s^2} - M \cdot \frac{e^{-as}}{s} \right\}$$

by using partial fractions and transforming the complete solution is

$$y = \frac{A \sin(kx)}{k} - \frac{M}{EI} \cdot \frac{1}{Lk^2} \left\{ x - \frac{\sin(kx)}{k} \right\} \\ - \frac{M}{EI} \cdot \frac{1}{k^2} \left\{ 1 - \cos k(x-a) \right\} \cdot h(x-a)$$

solving for the constant A using  $y = 0$  at  $x = L$  yields :

$$y = \frac{M}{V} \left\{ \frac{\cos kb \sin kx}{\sin kL} - \frac{x}{L} \right\} + \frac{M}{V} \left\{ 1 - \cos k(x-a) \right\} \cdot h(x-a)$$

using this equation the slope of the standard may be found at any part.

$$\frac{dy}{dx} = \frac{M}{V} \left\{ k \frac{\cos kb \cos kx}{\sin kL} - \frac{1}{L} \right\} + \frac{M}{V} \left\{ k \sin k(x-a) \right\} \cdot h(x-a)$$

thus at the lug cluster :

$$\frac{dy}{dx}_{x=a} = \frac{M}{kEI} \left\{ \frac{\cos ka \cos kb}{\sin kL} - \frac{1}{kL} \right\} \quad \dots 7.1$$

now the slope deflection equation for the ledger (see Fig. 7.2)

is :

$$M = - \frac{6 EI' V}{(L')^2} + \frac{4 EI'}{L'} \theta_{AB} + \frac{2 EI'}{L'} \theta_{EA}$$

for the buckling mode shown :

$$\theta_{AB} = - \theta_{EA} \quad \text{and} \quad V = 0$$

$$\therefore M = \frac{2 EI'}{L'} \theta$$

$$\therefore \theta = \frac{ML'}{2EI'}$$

assuming the lug-clevis joint to be rigid (see paragraph 4.2 - 6)

$$- \left\{ \frac{dy}{dx} \right\}_{x=a} = \theta$$

$$\therefore \frac{ML'}{2EI'} = \frac{M}{kEI} \left\{ \frac{\cos kb \cos ka}{\sin kL} - \frac{1}{kL} \right\}$$

Solving this equation for  $kL$  gives the Euler buckling load for the strut from which can be found the effective length.

Putting this equation in a more general form :

$$T = \frac{1}{kL} \left\{ \frac{\cos ka \cos kb}{\sin kL} - \frac{1}{kL} \right\} \quad \dots 7.2$$

where

$$T = t \cdot \frac{I}{I'} \cdot \frac{L'}{L}$$

and  $I, L$  refer to the properties of the standard.

$I', L'$  refer to the properties of the ledger.

$t$  is a constant which varies depending on the number of ledgers attached at the lug cluster and the mode of failure (see Fig. 7.3).

Equation 7.2 can be solved for  $kL$  for any given value of  $T$  and known ratio of  $\frac{a}{L}$ .

For example, consider the standard shown in Fig. 7.3a.

$$\text{if } L = 1981 \text{ mm (6'6")}$$

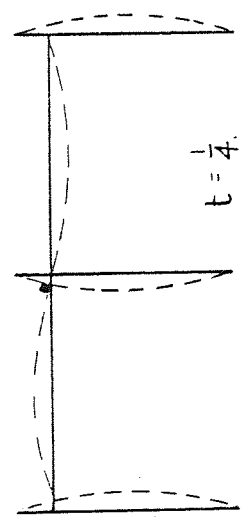
$$L' = 2440 \text{ mm (8' 0")}$$

$$a = 496 \text{ mm (1' 7}\frac{1}{2}\text{")}$$

$$I = 140,300 \text{ mm}^4$$

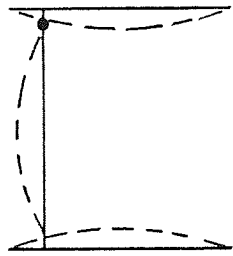
$$I' = 216,000 \text{ mm}^4$$

$$\therefore T = \frac{1}{4} \cdot \frac{2440}{1981} \cdot \frac{140,300}{216,000} = 0.2$$



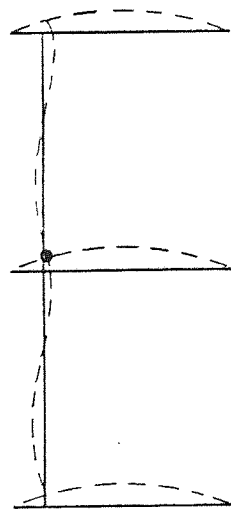
$$t = \frac{1}{4}$$

FIG 7.3a



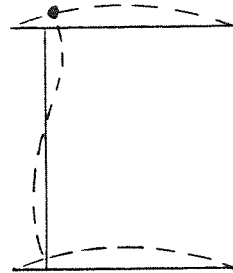
$$t = \frac{1}{2}$$

FIG 7.3b



$$t = \frac{1}{12}$$

FIG 7.3c



$$t = \frac{1}{6}$$

FIG 7.3d

solution is  $kL = 3.72$

$$\therefore L \sqrt{\frac{V_E}{EI}} = 3.72$$

$$\begin{aligned} \therefore \text{Euler Buckling Load, } P_E &= \frac{13.84 EI}{L^2} \\ &= \frac{\pi^2 EI}{(0.844 L)^2} \end{aligned}$$

$$\therefore L_e = 0.844 L$$

Plotting equation 7.2 in various ways brings out several points. For example for a given buckling mode and relative stiffness ratio  $(\frac{I}{I'}, \frac{L'}{L})$  a curve can be drawn plotting Euler buckling load or effective length ratio against the position of the ledger. This is done in Fig. 7.4 using the value  $T = 0.2$  as above. This shows that the effective length is shortest and thus the buckling load is highest when the ledgers are positioned near to the ends of the standard. Also that the buckling load decreases as the ledgers are moved away from the ends and when they are at mid-height they have no effect whatsoever.

Alternatively, if equation 7.2 is plotted for given lengths of  $L$  and constant ratio of  $\frac{a}{L}$  it is possible to examine how the effective length ratio varies from mode to mode and for different ledger stiffnesses. This is done in Fig. 7.5. Using this graph it can be shown quite clearly that the failure modes shown in Figs. 7.3c and 7.3d should never occur. This is because these modes always have a lower value of  $t$  and thus give a shorter effective length and correspondingly higher failure load than those modes of Figs. 7.3a and 7.3b.

Fig 7.4

EFFECTIVE LENGTH RATIO & BUCKLING LOAD: VARIATION WITH POSITION OF LEDGER

PLOTTED FOR  $T = 0.2$

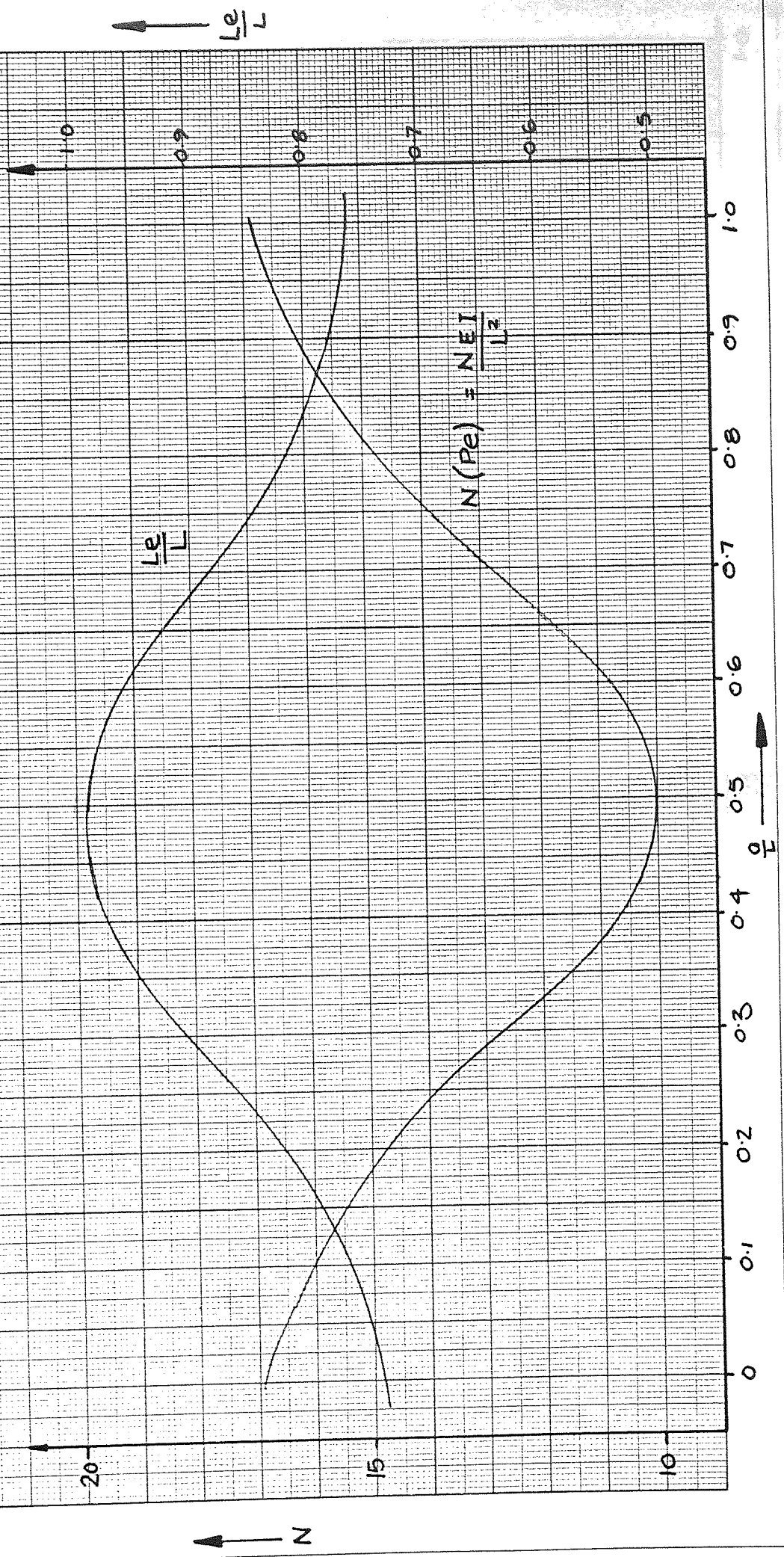
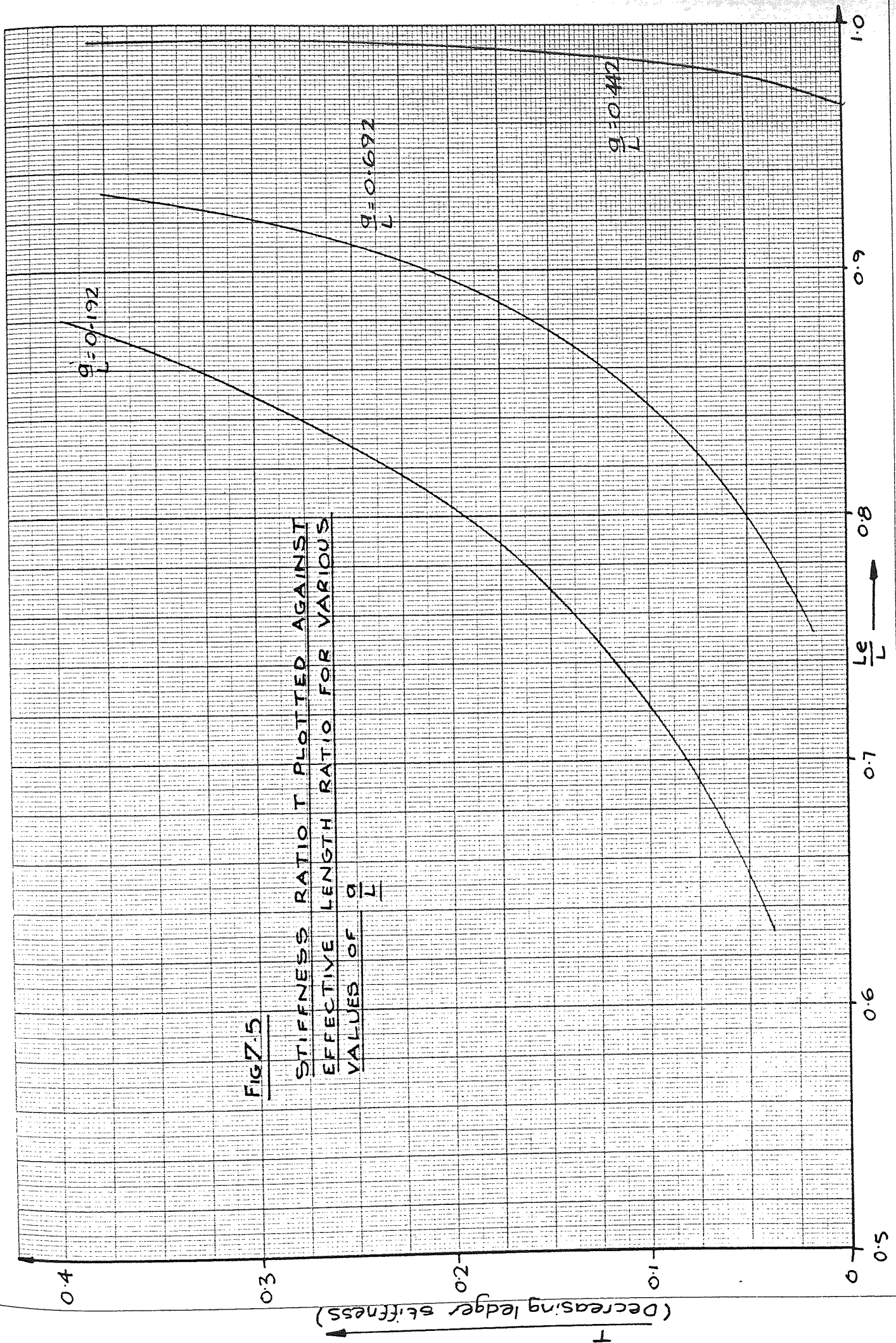


Fig 7.5

STIFFNESS RATIO  $T$  PLOTTED AGAINST  
EFFECTIVE LENGTH RATIO FOR VARIOUS  
VALUES OF  $\frac{a}{L}$



### 7.1.2 Standard with ledgers at two lug clusters

The above analysis is of course a very simple example. More complex analyses are required when ledgers join the standard at more than one point. For instance, if ledgers join the standard at two points then the situation in Fig. 7.6 arises.

$$- EI \frac{d^2 y}{dx^2} - Vy + \left\{ (M_1 + M_2) \frac{x}{L} - M_2 \cdot h(x-a_2) - M_1 \cdot h(x-a_1) \right\} = 0$$

if  $k^2 = \frac{V}{EI}$  and  $D = \frac{d}{dx}$

$$(D^2 + k^2)y = \frac{1}{EI} \left\{ (M_1 + M_2) \frac{x}{L} - M_2 \cdot h(x-a_2) - M_1 \cdot h(x-a_1) \right\}$$

Transforming by Laplace and using  $y = 0$  at  $x = 0$

$$(s^2 + k^2)\bar{y} + A = \frac{1}{EI} \left\{ (M_1 + M_2) \cdot \frac{1}{s^2 L} - \frac{M_2 e^{-a_2 s}}{s} - \frac{M_1 e^{-a_1 s}}{s} \right\}$$

$$\therefore EI\bar{y} = A \frac{EI}{s^2 + k^2} + \frac{(M_1 + M_2)}{L} \cdot \frac{1}{s^2 (s^2 + k^2)} - \frac{M_2 e^{-a_2 s}}{s (s^2 + k^2)} - \frac{M_1 e^{-a_1 s}}{s (s^2 + k^2)}$$

using partial fractions and transforming yields :

$$\begin{aligned} y \cdot EI &= A \cdot EI \frac{\sin kx}{k} + \frac{(M_1 + M_2)}{Lk^2} \left( x - \frac{\sin kx}{k} \right) \\ &\quad - \frac{M_2}{k^2} (1 - \cos k(x-a_2)) \cdot h(x-a_2) \\ &\quad - \frac{M_1}{k^2} (1 - \cos k(x-a_1)) \cdot h(x-a_1) \end{aligned}$$

solving for A using  $y = 0$  at  $x = L$  yields :



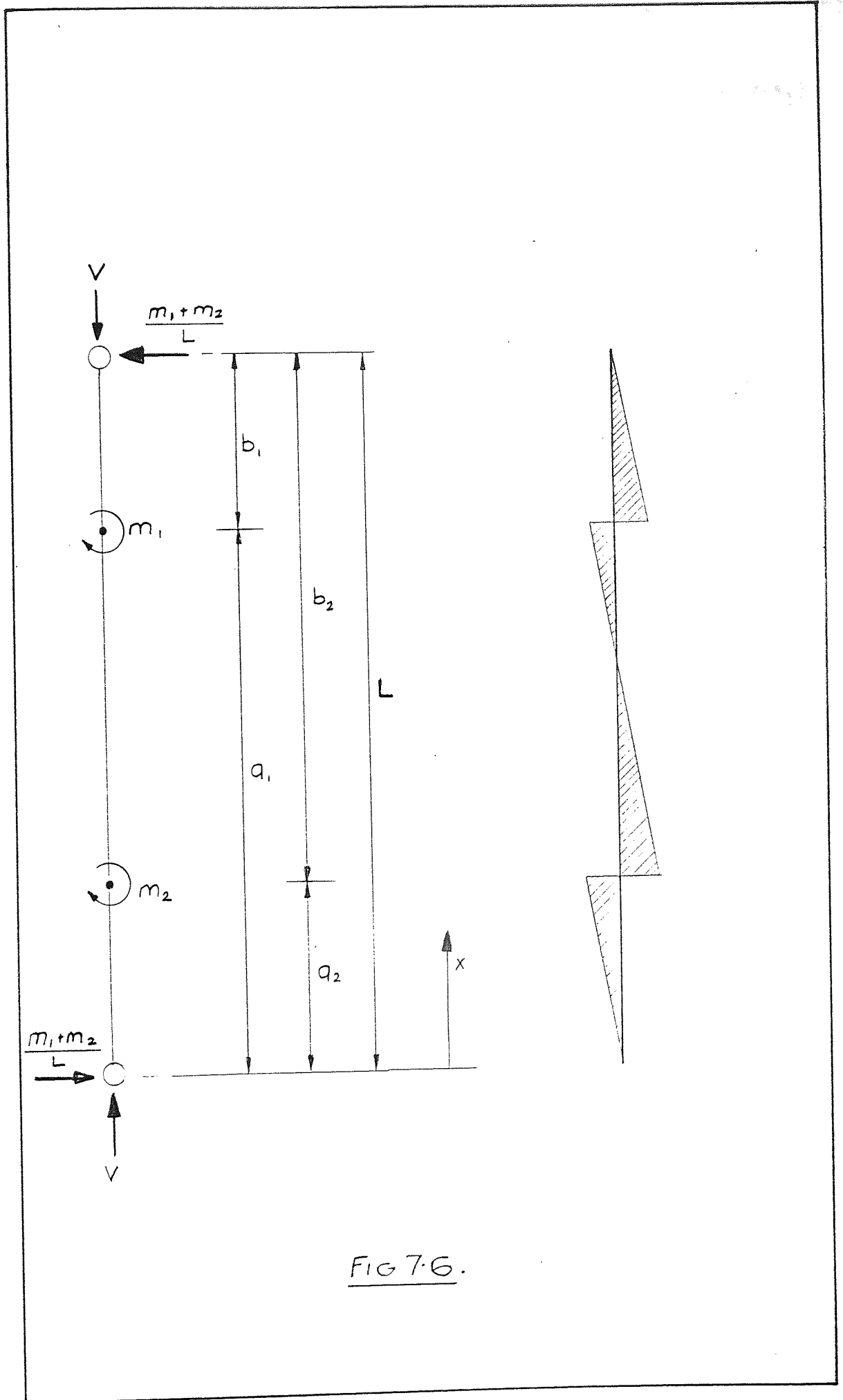


FIG 7.6.

$$y = \frac{M_1+M_2}{V} \cdot \frac{x}{L} - \frac{M_1}{V} \frac{\cos kb_1 \sin kx}{\sin kL} - \frac{M_1}{V} (1-\cos k(x-a_1)) \cdot h(x-a_1) \\ - \frac{M_2}{V} \frac{\cos kb_2 \sin kx}{\sin kL} - \frac{M_2}{V} (1-\cos k(x-a_2)) \cdot h(x-a_2)$$

As before the slope of the standard can be found at any point :

$$\frac{dy}{dx} = \frac{M_1+M_2}{VL} - \frac{M_1}{V} \frac{\cos kb_1}{\sin kL} \cdot k \cos kx - \frac{M_1}{V} \cdot k \sin k(x-a_1) \cdot h(x-a_1) \\ - \frac{M_2}{V} \cdot \frac{\cos kb_2}{\sin kL} \cdot k \cos kx - \frac{M_2}{V} \cdot k \sin k(x-a_2) \cdot h(x-a_2)$$

This applies provided  $a_1 > a_2$

∴ at  $x = a_1$

$$\left(\frac{dy}{dx}\right)_{a_1} = \frac{M_1+M_2}{VL} - \frac{M_1}{V} \cdot k \frac{\cos kb_1 \cos ka_1}{\sin kL} \\ - \frac{M_2}{V} \cdot k \frac{\cos kb_2 \cos ka_1}{\sin kL} - \frac{M_2}{V} k \sin k(a_1-a_2) \quad \dots 7.3$$

and at  $x = a_2$

$$\left(\frac{dy}{dx}\right)_{a_2} = \frac{M_1+M_2}{VL} - \frac{M_1}{V} k \frac{\cos kb_1 \cos ka_2}{\sin kL} - \frac{M_2}{V} k \frac{\cos kb_2 \cos ka_2}{\sin kL} \quad \dots 7.4$$

Using slope deflection equations it is possible to find the slope at the end of the ledgers. Assuming the joints to be perfectly rigid:

$$\left(\frac{dy}{dx}\right)_{a_1} = \theta_1 = - \frac{M_1 L'}{4EI'}$$

$$\left(\frac{dy}{dx}\right)_{a_2} = \theta_2 = \frac{M_2 L'}{4EI'}$$

substituting these into equations 7.3 and 7.4 respectively yields :

$$\begin{aligned} & \frac{M_1}{V} \left( \frac{1}{L} - k \frac{\cos kb_1 \cos ka_1}{\sin kL} + \frac{L'k^2 I}{4I'} \right) \\ & + \frac{M_2}{V} \left( \frac{1}{L} - k \frac{\cos kb_2 \cos ka_1}{\sin kL} - k \sin k(a_1 - a_2) \right) = 0 \end{aligned}$$

and

$$\begin{aligned} & \frac{M_1}{V} \left( \frac{1}{L} - k \frac{\cos kb_1 \cos ka_2}{\sin kL} \right) \\ & + \frac{M_2}{V} \left( \frac{1}{L} - k \frac{\cos kb_2 \cos ka_2}{\sin kL} + \frac{L'k^2 I}{4I'} \right) = 0 \end{aligned}$$

These are two simultaneous equations in  $M_1$  and  $M_2$ . Substituting for

$T = t \cdot \frac{L'}{L} \cdot \frac{I}{I'}$ , and solving gives :

$$\begin{aligned} & \left( \frac{1}{kL} - \frac{\cos kb_1 \cos ka_1}{\sin kL} + kL.T \right) \left( \frac{1}{kL} - \frac{\cos kb_2 \cos ka_2}{\sin kL} + kL.T \right) \\ & - \left( \frac{1}{kL} - \frac{\cos kb_2 \cos ka_1}{\sin kL} - \sin k(a_1 - a_2) \right) \left( \frac{1}{kL} - \frac{\cos kb_1 \cos ka_2}{\sin kL} \right) = 0 \end{aligned}$$

.... 7.5

for known ratios of  $\frac{a_1}{L}$ ,  $\frac{a_2}{L}$ ,  $\frac{b_1}{L}$  and  $\frac{b_2}{L}$  and a known value of  $T$  equation 7.5 can be solved for  $kL$ . Alternatively a curve can be plotted showing the variation of effective length with relative stiffness  $T$ . This is done in Fig. 7.7.

(Decreasing Ledger Stiffness)

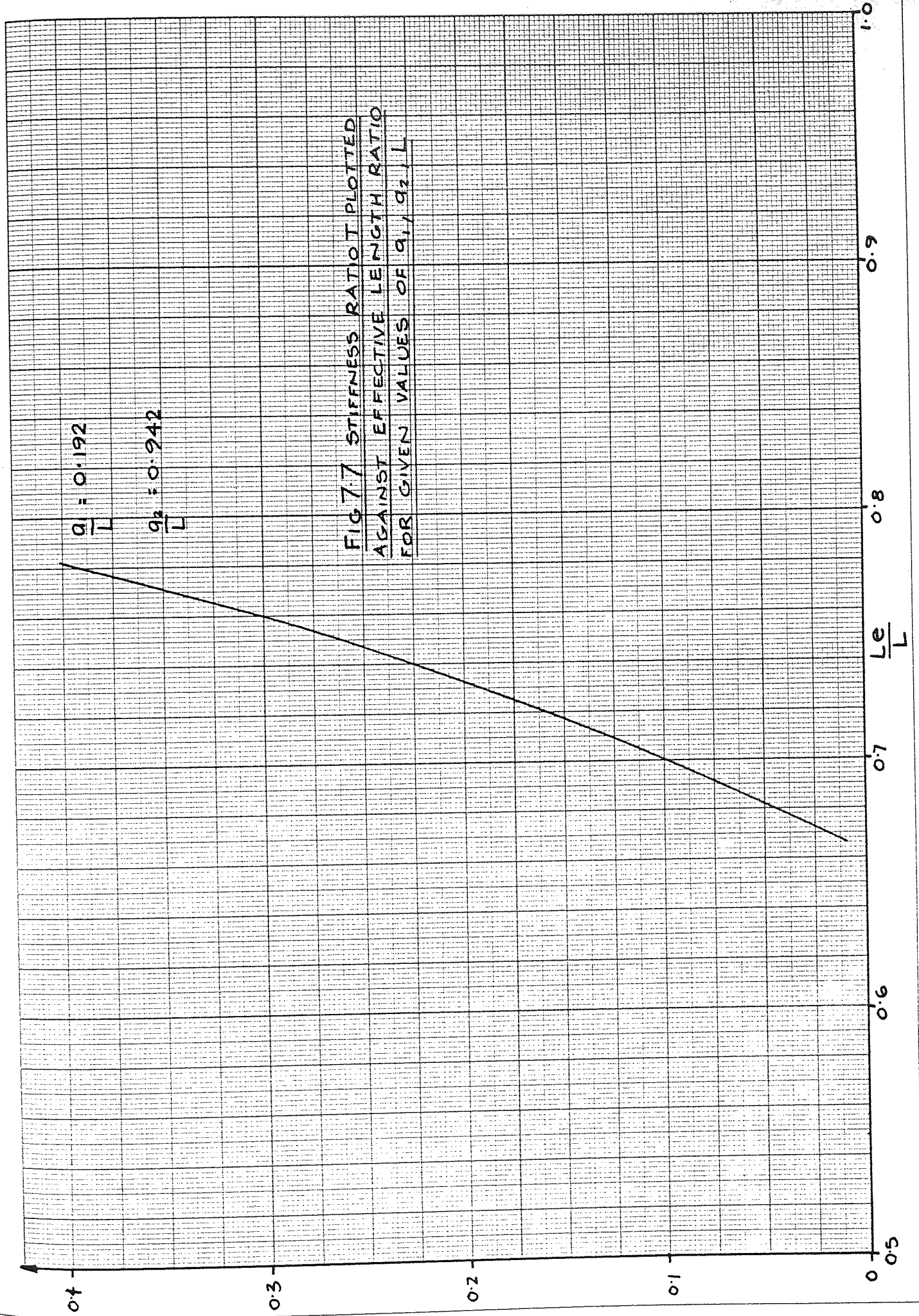


FIG 7.7 STIFFNESS RATIO PLOTTED AGAINST EFFECTIVE LENGTH RATIO FOR GIVEN VALUES OF  $q_1, q_2, L$

$\frac{q_1}{L} = 0.192$

$\frac{q_2}{L} = 0.242$

Thus for :

$$L = 1981 \text{ mm (6' 6")}$$

$$a_1 = 381 \text{ mm (1' 3")}$$

$$a_2 = 1867 \text{ mm (6' 1\frac{1}{2}")}$$

$$L' = 2440 \text{ mm (8' 0")}$$

$$I = 140,300$$

$$I' = 216,000$$

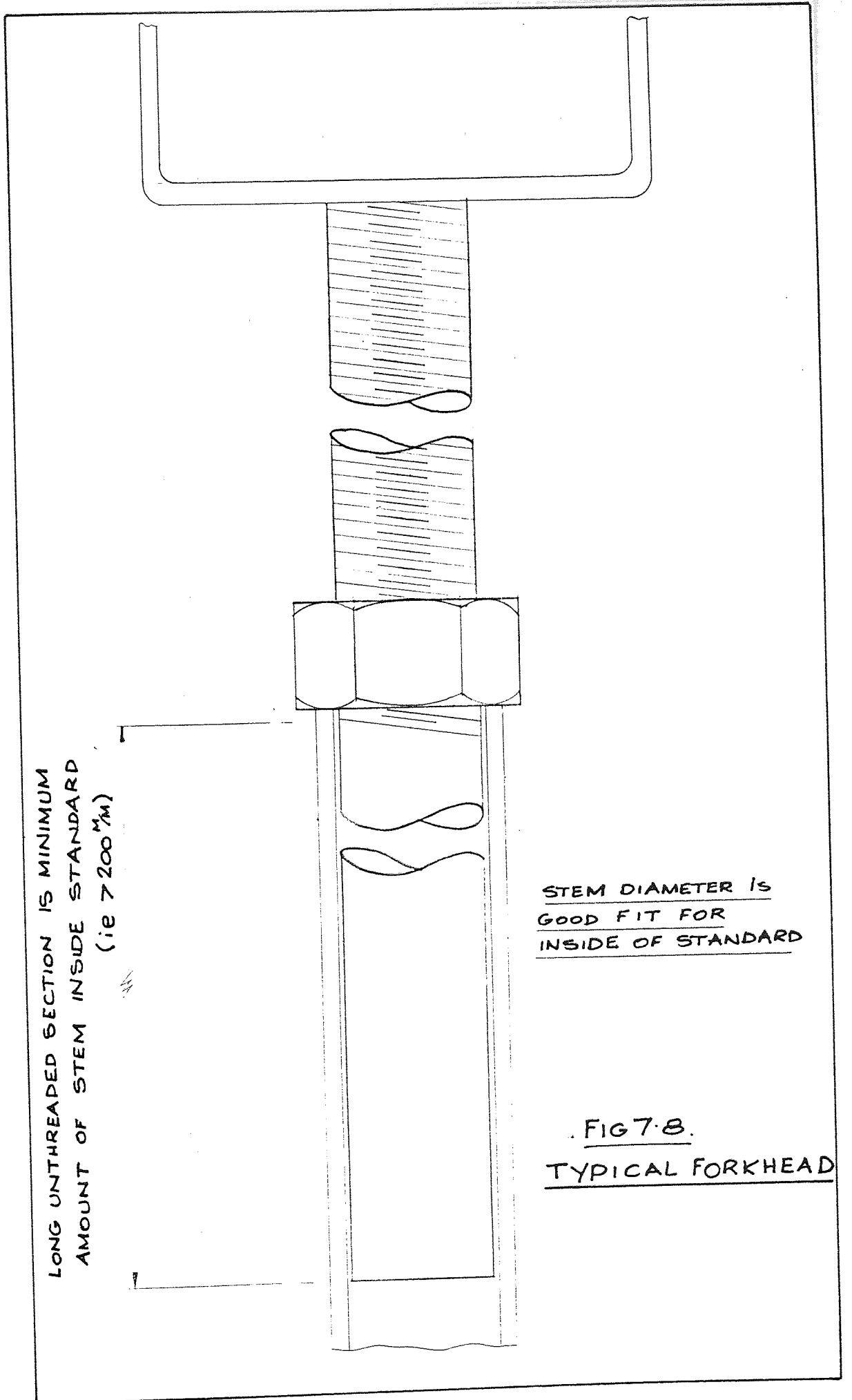
$$\therefore T = 0.2$$

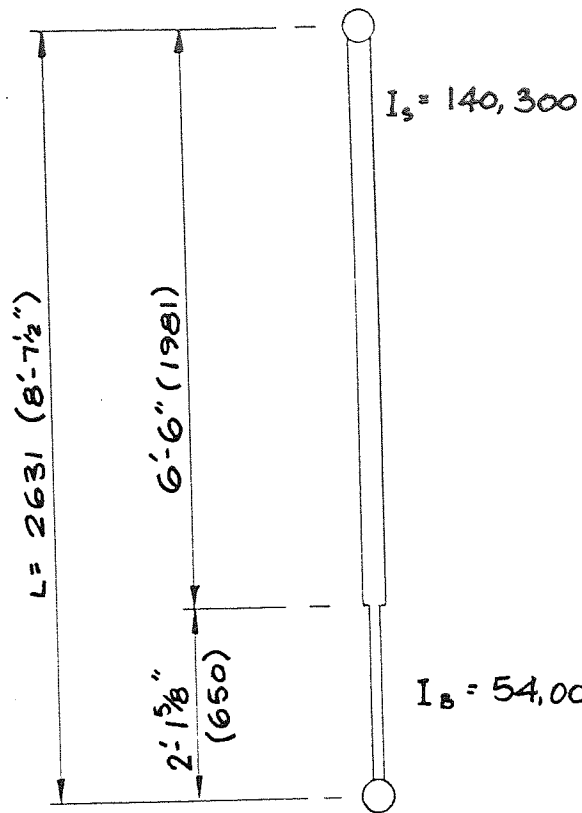
$$L_e = 0.728 L$$

### 7.1.3 Top or base standards with ledgers attached at one lug cluster

When dealing with real falsework scaffolding there will almost always be either an adjustable base at the bottom, an adjustable forkhead at the top or possibly both. Both bases and forkheads fit inside the tube in such a way that they can be considered to be structurally an extension of the standard (see Fig. 7.8). Whilst the strength of the forkhead or base must be considered separately, the effect of their smaller inertias is to increase the effective length of the standard. This can be demonstrated by a simple analysis of the standard/base arrangement shown in Fig. 7.9. Although both ends of the standard are pin jointed and held in position, the effective length is still greater than the total length of the strut, ( $L_e = 1.08L$ ). This lowers the buckling load significantly and must be considered.

The analysis of the strut shown in Fig. 7.10 where ledgers are joined to the standard at only one lug cluster is carried out by considering the two sections separately.





$L_e = 1.08L$

FIG 7.9

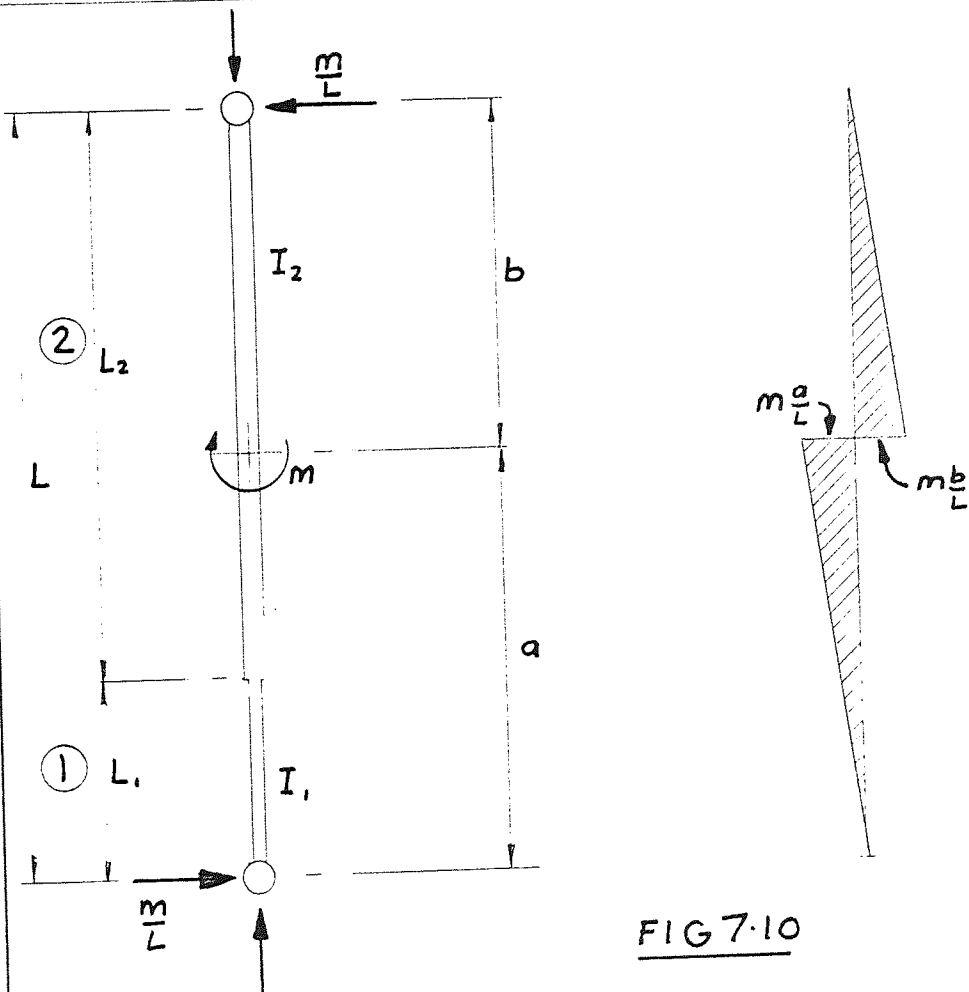


FIG 7.10

For section 1 :

$$- EI_1 \frac{d^2 y_1}{dx^2} - V \cdot y_1 + \frac{M \cdot x}{L} = 0 \quad \dots 7.6$$

For section 2 :

$$- EI_2 \frac{d^2 y_2}{dx^2} - V \cdot y_2 + \frac{M \cdot x}{L} - M \cdot h(x-a) = 0 \quad \dots 7.7$$

The critical load and hence effective length can be determined from the solution of these two differential equations :

Using  $y_1 = 0$  at  $x = 0$  equation 7.6 gives :

$$y_1 = A \sin kx + \frac{M}{V} \cdot \frac{x}{L}$$

Equation 7.7 gives :

$$y_2 = B \cos k_2 x + C \frac{\sin k_2 x}{k_2} + \frac{M}{EI_2} \cdot \frac{1}{Lk_2^2} \left( x - \frac{\sin k_2 x}{k_2} \right) - \frac{M}{EI_2} \cdot \frac{1}{k_2^2} (1 - \cos k_2(x-a)) \cdot h(x-a) \quad \dots 7.8$$

the constants of integration (A, B and C) are found from :

$$y_2 = 0 \text{ at } x = L$$

$$y_1 = y_2 \text{ at } x = L_1$$

$$\frac{dy_1}{dx} = \frac{dy_2}{dx} \text{ at } x = L_1$$

These yield :



$$C = \frac{Mk_2}{V} \left\{ \frac{\cos k_2 L \sin k_1 L_1}{k_1 L} - \frac{\cos k_1 L \sin k_2 L_1}{k_2 L} + \left( \cos k_2 b - \frac{\sin k_2 L}{k_2 L} \right) \frac{\left( \cos k_2 L_1 \cos k_1 L_1 + \frac{k_2}{k_1} \sin k_2 L_1 \sin k_1 L_1 \right)}{\cos k_2 L} \right\} \\ \left\{ \left( \sin k_2 L_1 \cos k_1 L_1 - \frac{k_2}{k_1} \cos k_2 L_1 \sin k_1 L_1 \right) - \frac{\sin k_2 L}{\cos k_2 L} \left( \cos k_2 L_1 \cos k_1 L_1 + \frac{k_2}{k_1} \sin k_2 L_1 \sin k_1 L_1 \right) \right\}$$

$$B = \frac{\frac{M}{P} \left( \frac{\sin k_2 L}{k_2 L} - \cos k_2 b \right) - C \frac{\sin k_2 L}{k_2}}{\cos k_2 L}$$

Putting these constants into equation 7.8 the next stage is to find the gradient at the point where the ledgers join ( $x = a$ ). Equating this gradient to that at the end of the ledger as before gives :

$$T = -B' \frac{\sin k_2 a}{k_2 L} + C' \frac{\cos k_2 a}{k_2 L} + \left( \frac{1}{k_2 L} \right)^2 (1 - \cos k_2 a) \quad \dots 7.9$$

Where  $T$  is the relative stiffness as before

$$C' = \frac{\left\{ \left( \frac{\cos k_2 L_1 \sin k_1 L_1}{k_1 L} - \frac{\sin k_2 L_1 \cos k_1 L_1}{k_2 L} \right) - \left( \cos k_2 b - \frac{\sin k_2 L}{k_2 L} \right) \frac{\left( \cos k_2 L_1 \cos k_1 L_1 + \frac{k_2}{k_1} \sin k_2 L_1 \sin k_1 L_1 \right)}{\cos k_2 L} \right\}}{\left\{ \left( \sin k_2 L_1 \cos k_1 L_1 - \frac{k_2}{k_1} \cos k_2 L_1 \sin k_1 L_1 \right) - \frac{\sin k_2 L}{\cos k_2 L} \left( \cos k_2 L_1 \cos k_1 L_1 + \frac{k_2}{k_1} \sin k_2 L_1 \sin k_1 L_1 \right) \right\}}$$

$$B' = \frac{1}{\cos k_2 L} \left( \frac{\sin k_2 L}{k_2 L} - \cos k_2 b - C' \sin k_2 L \right)$$

As before, equation 7.9 can be solved for  $kL$  from which the Euler buckling load, and hence effective length, can be found.

7.1.4 Top or base standard with ledgers attached at two lug clusters

The final case to be considered is that of a standard which has a base or forkhead attached and ledgers connected at two points. This is shown in Fig. 7.11. The solution is found from consideration of the equilibrium equation of each section as above :

For section 1 :

$$- EI_1 \frac{d^2 y_1}{dx^2} - Vy_1 + (M_1 + M_2) \cdot \frac{x}{L} = 0$$

For section 2 :

$$- EI_2 \frac{d^2 y_2}{dx^2} - Vy_2 + (M_1 + M_2) \cdot \frac{x}{L} - M_1 \cdot h(x-a_1) - M_2 \cdot h(x-a_2)$$

The solution to these equations can be found using Laplace transforms as before and assuming  $y = 0$  at  $x = 0$

$$y_1 = A \sin k_1 x + \frac{(M_1 + M_2)}{V} \cdot \frac{x}{L} \quad \dots 7.10$$

$$y_2 = B \cos k_2 x + C \frac{\sin k_2 x}{k_2} + \frac{(M_1 + M_2)}{VL} x - \frac{\sin k_2 x}{k_2}$$

$$- \frac{M_1}{V} [1 - \cos k_2(x-a_1)] \cdot h(x-a_1) - \frac{M_2}{V} [1 - \cos k_2(x-a_2)] \cdot h(x-a_2)$$

.... 7.11

as before the constants A, B, C are evaluated from :

$$y_2 = 0 \quad \text{at} \quad x = L$$

$$y_1 = y_2 \quad \text{at} \quad x = L_1$$

$$y_1' = y_2' \quad \text{at} \quad x = L_1$$

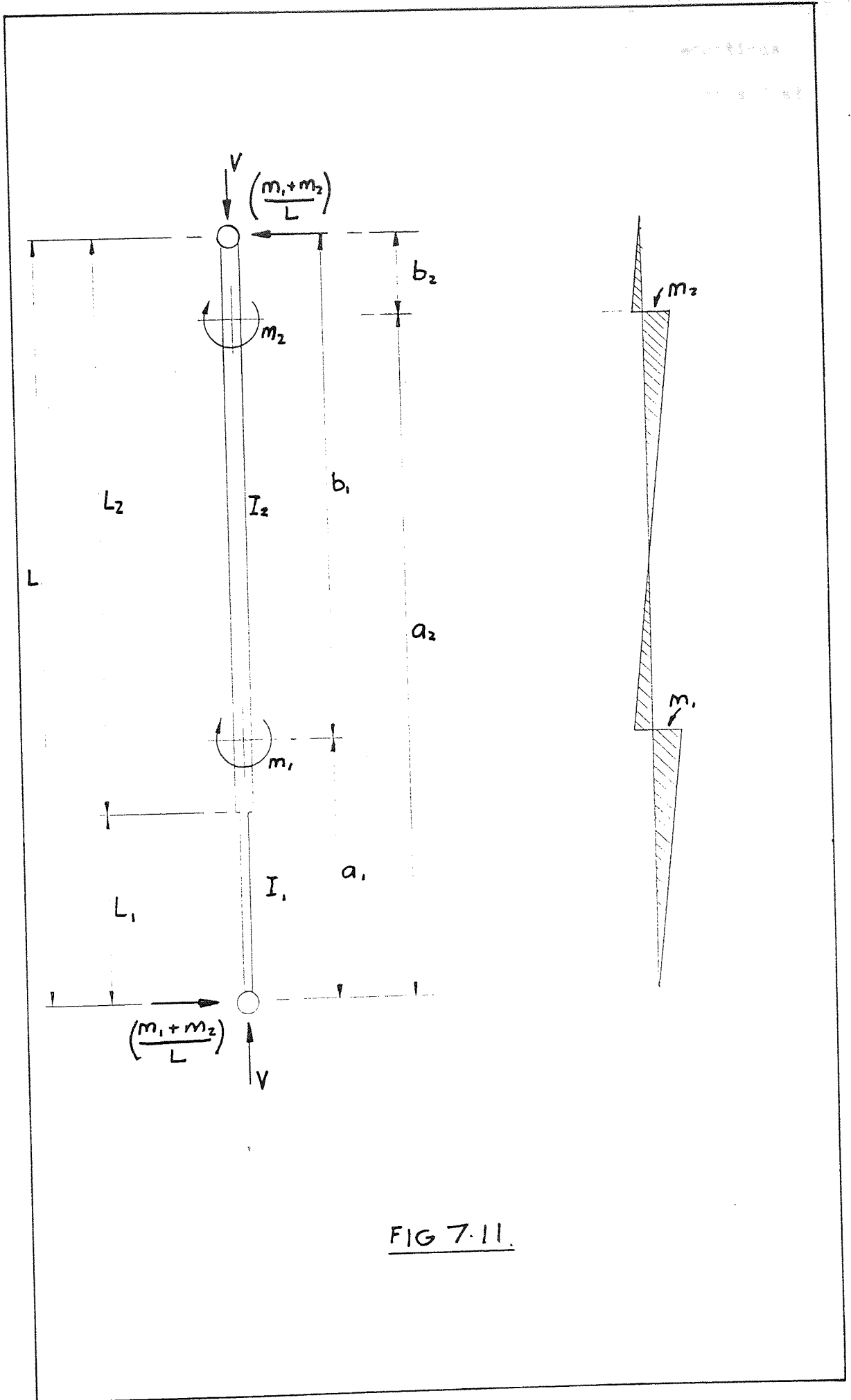


FIG 7.11.

Proceeding as before by substituting the constants into equations 7.10 and 7.11, differentiating to find the slope of the standard at  $x = a_1, a_2$  and equating this to the slope of the ledger gives :

$$\left\{ T + \frac{\cos k_2 b_1 (Z \cos k_2 a_1 - \sin k_2 a_1)}{\sin k_2 L (Z - \cot k_2 L) k_2 L} + \frac{1}{(k_2 L)^2} \right\} \times$$

$$\left\{ T + \frac{\cos k_2 b_2 (Z \cos k_2 a_2 - \sin k_2 a_2)}{\sin k_2 L (Z - \cot k_2 L) k_2 L} + \frac{1}{(k_2 L)^2} \right\}$$

$$- \left\{ \frac{\cos k_2 b_2 (Z \cos k_2 a_1 + \sin k_2 a_1)}{\sin k_2 L (Z - \cot k_2 L) k_2 L} + \frac{1}{(k_2 L)^2} \right\} \times$$

$$\left\{ \frac{\cos k_2 b_1 (Z \cos k_2 a_2 - \sin k_2 a_2)}{\sin k_2 L (Z - \cot k_2 L) k_2 L} + \frac{1}{(k_2 L)^2} - \frac{\sin k_2 (a_2 - a_1)}{k_2 L} \right\} = 0$$

where  $Z = \frac{\left\{ \frac{k_2}{k_1} \sin k_2 L_1 \sin k_1 L_1 + \cos k_2 L_1 \cos k_1 L_1 \right\}}{\left\{ \frac{k_2}{k_1} \cos k_2 L_1 \sin k_1 L_1 - \sin k_2 L_1 \cos k_1 L_1 \right\}}$

again this can be solved for  $k_2 L$  and hence :

$$\frac{L_e}{L} = \frac{\pi}{k_2 L}$$

#### 7.1.5 Discussion of the validity of end conditions used

The four analyses listed in sections 7.1.1 - 7.1.4 are all, of course, approximations to the real behaviour of the scaffold. As such their

validity is dependant to a great extent on the boundary conditions used in the model and which appear as constants of integration. In all the above analyses the conditions  $y = 0$  at  $x = 0, L$  are used. These may not be valid for every conceivable case but err if anything on the conservative side.

Consider for example the situation shown in Fig. 7.12a where the braced bay is assumed to be very rigid. Now treating the spigots as pins implies that each standard in a vertical acts independantly and that the weakest will fail, rather like a chain. Using the arguments of section 7.1.1 then standard number 2 will fail since it has only one ledger attached. So consider this standard in isolation assuming that standards 1 and 3 are much stronger. Now if the ledger attached to standard 2 is positioned near to the end (Fig. 7.12b) then the theory of section 7.1.1 is reasonable in that the assumption of no positional restraint at ledger level involves only a small error. If, however, the ledger is positioned near to the centre of the standard then ignoring the positional fixity at this level results in the strength of the strut being underestimated. Similar arguments apply when considering the top or base standard or an intermediate standard with two ledgers attached, but in all cases the effective length is overestimated.

So having determined a lower bound value of effective length with a certain degree of confidence, it is now possible to calculate the buckling load.

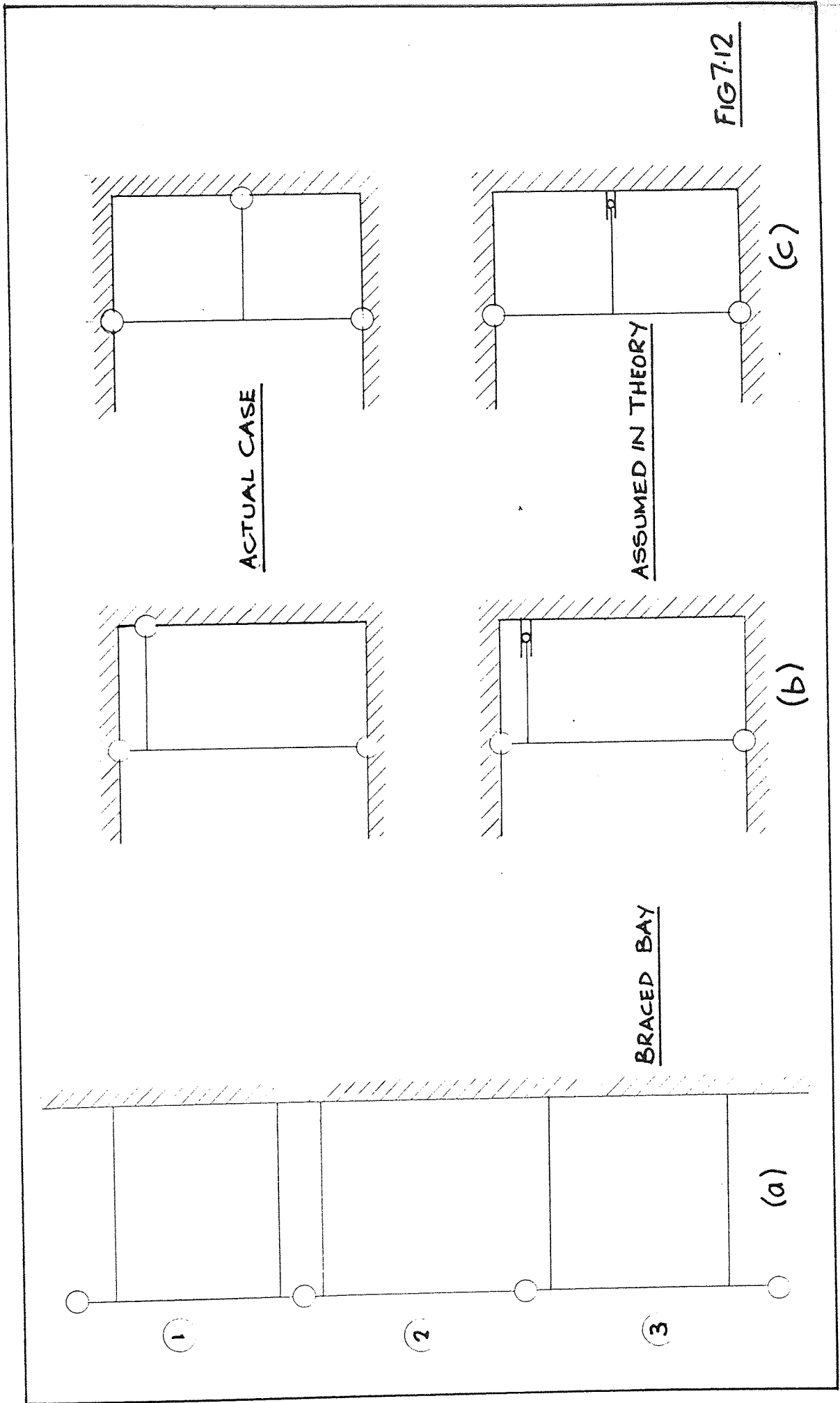


FIG. 7.12

## 7.2 THE DETERMINATION OF BUCKLING LOAD

### 7.2.1 Concentric Loading

Having determined the effective length of a standard it is now possible to determine its buckling load. It is, of course, possible to use the theory of section 7.1 directly to determine the Euler buckling load directly but allowance must be made for the yield stress of the steel. The most obvious way of doing this is to use the Perry-Robertson formula. This has the advantage of being well known amongst practising engineers since it is used in B.S. 449. The equation is :

$$\sigma = \frac{\sigma_y + (\eta + 1) \sigma_E}{2} - \sqrt{\left\{ \frac{\sigma_y + (\eta + 1) \sigma_E}{2} \right\}^2 - \sigma_y \cdot \sigma_E} \quad \dots 7.12$$

where  $\sigma$  is the average stress at failure

$\sigma_y$  is the yield stress

$\sigma_E$  is the average stress at Euler buckling load

$\eta$  is a constant =  $0.3 \left(\frac{1}{100r}\right)^2$  for lower bound curve

=  $0.001 \left(\frac{1}{r}\right)^2$  for curve of average failure load

Although this formula has been used for many years and has been of great value as a design tool it does have several faults. These are :

- a. It assumes that failure takes place when the yield stress is first reached at extreme fibres. This is slightly pessimistic, the amount of error depending on the shape factor of the section.

- b. It ignores strain hardening and thus the curve starts to descend as soon as it leaves the stress axis. This gives pessimistic predictions at low slenderness ratios.
- c. The empirical choice of constant  $\eta$  implies that the initial out-of-straight of a member depends on its section. In practice the initial bow is independent of section geometry at least for rolled sections and symmetrically welded ones.
- d. The equation takes no account of locked in stresses which, when high, can reduce the buckling load of a member significantly.

For these reasons the European column curves have been derived which, although similar in form to the Perry-Robertson formula, does make allowance for the above points. The basic formula remains :

$$\sigma = \frac{\sigma_y + (1 + \eta)\sigma_E}{2} - \sqrt{\left\{ \frac{\sigma_y + (1 + \eta)\sigma_E}{2} \right\}^2 - \sigma_y \sigma_E}$$

but the constant  $\eta$  is changed :

$$\text{if } \frac{L}{r} \leq s_0 \quad \eta = 0$$

$$\text{if } \frac{L}{r} > s_0 \quad \eta = \alpha \left( \frac{L}{r} - s_0 \right)$$

$$\text{where } s_0 = 0.2\pi \sqrt{\frac{E}{\sigma_y}} \quad (= 19.7 \text{ for grade 13 steel})$$

and  $\alpha$  is one of three constants which define the curves according to the geometry of the cross section ( $\alpha = 0.0020$  for tubes).



The difference between the Perry-Robertson formula and the proposed European curve for scaffold tube is shown in Fig. 7.13. This shows that the new curve gives failure loads which are considerably higher than the original Perry-Robertson.

e.g.	for scaffold tube with effective length	=	2.0 m
	P-R failure load	=	48 KN
	Unified European code failure load	=	56.5 KN

This represents an increase of 18%.

Either of these equations can be used to determine buckling load although the latter is obviously preferable on economic grounds.

#### 7.2.2 Eccentricity of loading

The eccentric loading of standards by bad positioning of the header beam is a common fault in scaffold structures. The strength of such a standard is required in order to gauge the reduction in load factor attributable to such malpractice.

When Professor Robertson did his original research in the early 1920's (Ref. 28), he looked into the buckling of eccentrically loaded struts. He concluded that by using :

$$\eta^1 = \eta + \frac{\pi^2}{8} \cdot \frac{D}{2} \cdot \frac{e}{r^2}$$

by using equation 7.12 as before then a lower bound curve could be defined for a given eccentricity. His experiments showed that :

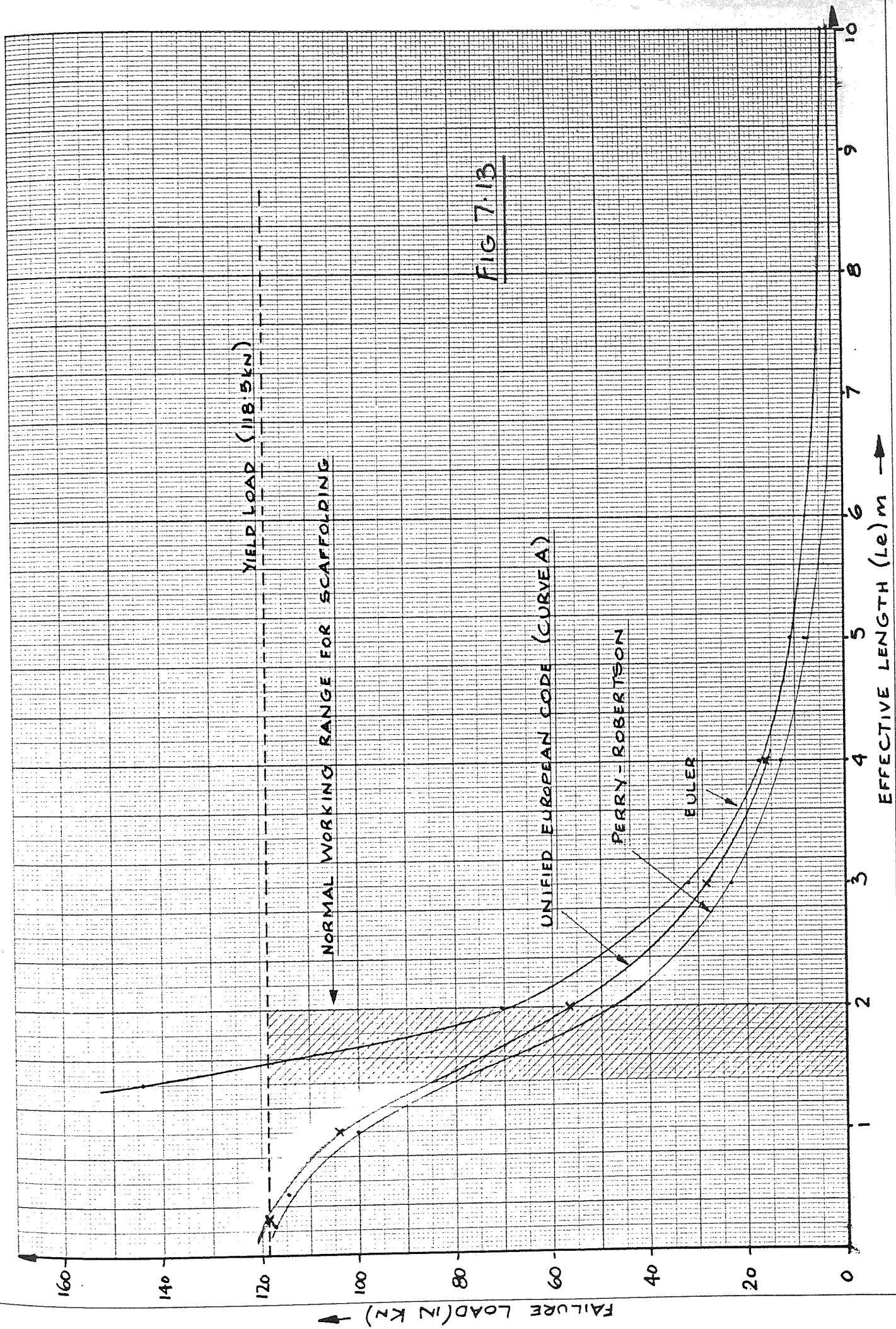
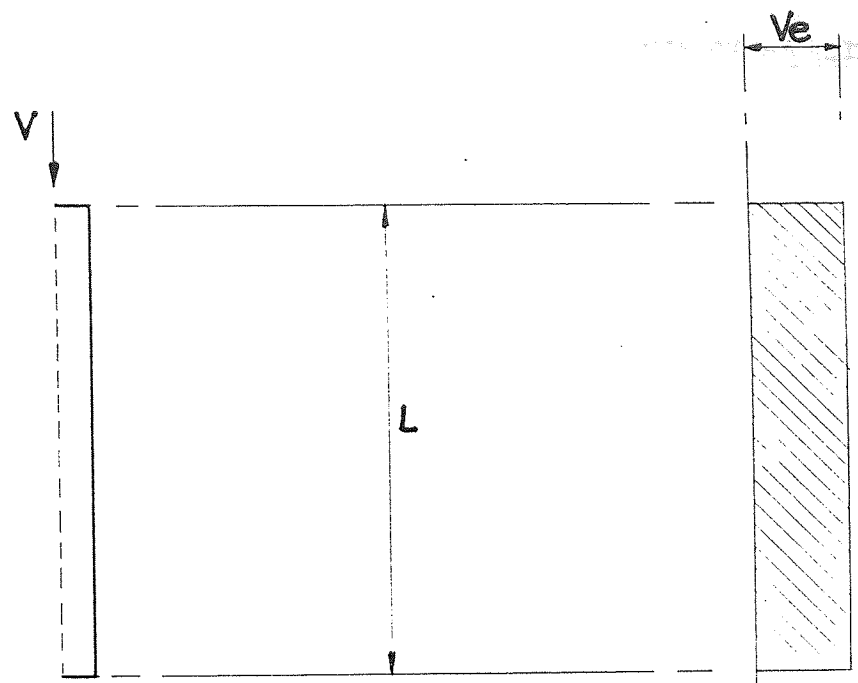


FIG 7.13

"For the struts with little eccentricity the collapsing load is very nearly that given by the formula. For struts having considerable eccentricity the value of the collapsing load is decidedly greater than that given by the formula and the difference increases as the eccentricity increases..... It is noteworthy too that for longer struts the divergence from the calculated failure load is small."

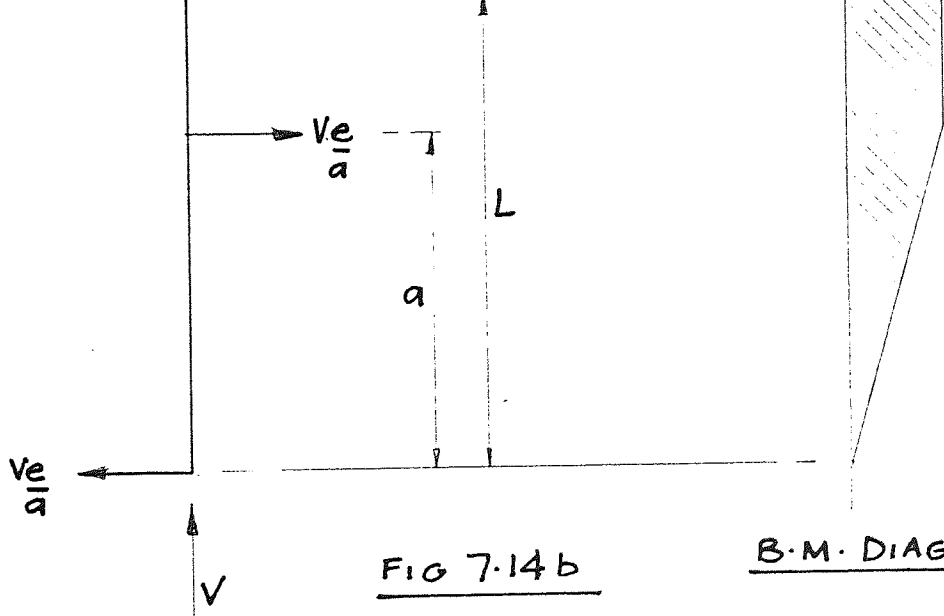
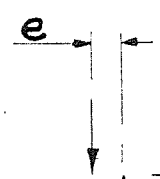
Using this approach is, strictly speaking, incorrect for when Robertson talks about eccentricity of load he is referring to the strut shown in Fig. 7.14a. Whereas the arguments contained in section 6 indicate that when dealing with scaffolding the arrangement shown in Fig. 7.14b applies. However, since failure is defined as the point where yield stress is first reached at mid-height, it is apparent by inspection of the bending moment diagrams that the former represents the worst case and thus applying Robertson's approach to scaffolding errs on the conservative side.

At present there is no such modification which can be used with the European curve to determine collapse load of an eccentrically loaded strut.



B·M· DIAGRAM

FIG 7.14a.



B·M· DIAGRAM.

FIG 7.14b

### 7.3 CORRELATION BETWEEN THEORY AND EXPERIMENTS ON BUCKLING OF STANDARDS

Two sets of experiments were completed during the course of this project to give data against which one would hope the validity of any theory can be checked. These were the experiments on individual standards and certain of the full scale assembly experiments. These were discussed in sections 3.2.1 and 3.2.2 respectively, and it is important to recall their original purpose.

Consider firstly the experiments on individual standards. They were completed before the theory outlined above was developed. Their primary purpose was to check the validity of the design method currently in use. But having discounted this method, the general arrangement of the experiment was unsuitable for verification of the theory in section 7.1.5. This is because failure generally occurred when the load in the horizontal transoms was sufficient to overcome the indeterminate amount of friction between the surrounding frame and the floor and thus move that frame. This was especially true of standards with transoms near mid-height where the positional fixity provided by the transoms resulted in the failure load being considerably higher than the theoretical value. The results of these experiments are shown in Fig. 7.15, and the corresponding arrangements in Fig. 7.16.

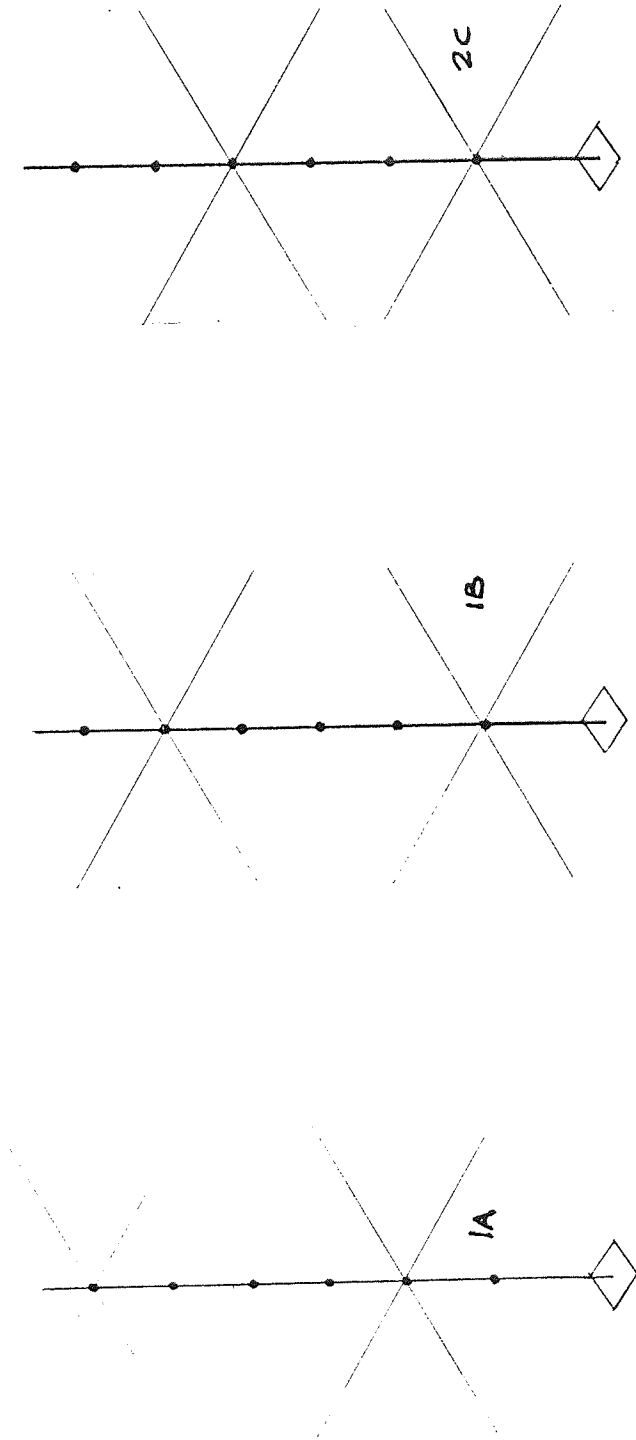
Now the full scale assembly experiments were carried out to observe failure modes in a real scaffold and as such represent a good check for the above theory. In one experiment buckling was observed to be the cause of primary failure. But even on the remainder the fact that buckling did not occur can be seen as verification. The results of these experiments are shown in Fig. 7.17, where it can be seen that

Test Number and Arrangement	MEASURED		PROPERTIES		Distance between Ledgers	Calculated effective length using 7.1	Actual measured failure load (kN)	Theoretical lower failure load using existing design method and ratio of this to actual failure load	Theoretical lower failure load using method outlined in Chap.7 and ratio of this to actual failure load
	Radius of Gyration	Yield Stress							
1 IA	15.74	288	1.981	2.000	106.2	53.65	1.98	52.72	2.01
2 IB	15.80	286	1.981	1.652	117.8	52.09	2.26	71.69	1.64
3 IB <sup>s</sup>	15.70	287	1.981	1.134	101.6	53.59	1.90	118.38	0.86
7 2C	15.72	321	1.486	2.057	147.8	91.37	1.62	52.15	2.83
8 2C	15.72	279	1.486	2.057	124.7	83.23	1.52	48.71	2.56(a)
12 2C	15.81	239	1.486	2.057	117.8	47.31	2.49	35.72	3.30 (b)
11 2C <sup>s</sup>	15.71	309	1.486	1.132	>150	90.68	>1.65	127.35	>1.18 (c)
13 IB <sup>s</sup>	15.73	270	1.981	1.134	>150	52.49	>2.86	12.71	>1.33 (d)

- (a) OUT OF PLUMB BY 1°
- (b) OUT OF STRAIGHT BY 12<sup>m</sup>/m
- (c) AS TEST 7 BUT WITH SPIGOT AT MID-HEIGHT
- (d) AS TEST 2 BUT WITH SPIGOT AT MID-HEIGHT

FIG 7.15

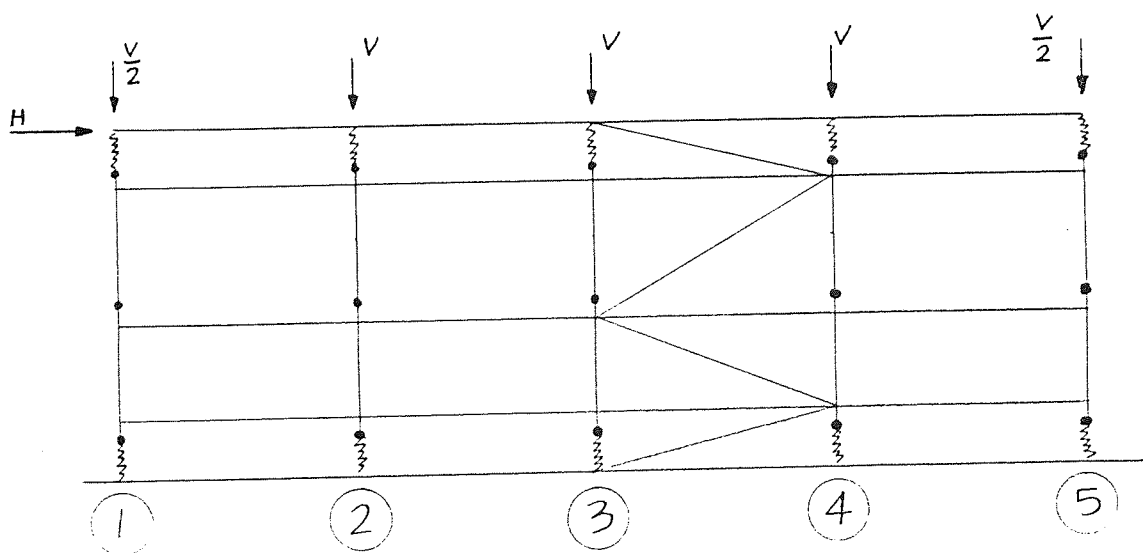
FIG 7-16



POSITION OF LEDGERS IN EXPERIMENTS ON INDIVIDUAL STANDARDS

TEST N <sup>o</sup>	STANDARD N <sup>o</sup>	HIGHEST VERTICAL LOAD OBSERVED IN TEST. (KN)	THEORETICAL FAILURE LOAD USING PERRY ROBERTSON FORMULA (KN)	RATIO: $\frac{\text{Highest obs load}}{\text{Theoretical failure load}}$	OBSERVATIONS
2 {	B4 B2, C2	117 114	104 100	1.12 1.14	Buckling was cause of primary failure
4 {	B4, C4 B2, C2	108 88	102 101	1.06 0.87	No buckling occurred.
5 {	B4, C4 B2, C2	95 88	38 38	2.50 2.32	Eccentricity of load (25). Coupler slip was primary cause of failure, followed by buckling of standards
7 {	B4, C4 B2, C2	94 88	101 101	0.93 0.87	No buckling occurred

STANDARDS ON GRID LINE 4. ARE ON COMPRESSION SIDE OF BRACED BAY AND ARE THEREFORE MORE HEAVILY LOADED. THOSE ON GRID LINE 2. REPRESENT A TYPICAL STANDARD REMOTE FROM THE BRACED BAY.



SCHMATIC ARRANGEMENT OF FULL SCALE ASSEMBLY EXPERIMENTS

FIG 7.17



the theory discussed earlier in this chapter appears to give a reasonably accurate prediction of the buckling load of a standard. However, it should be borne in mind that for these experiments the ledgers were in all cases near to the ends of the standards so none of the errors already mentioned arise.

The exception to this rule is the experiment with eccentrically loaded standards where the experimental loads far exceeded the theoretical failure load. The reason for this error is thought to be two-fold. Firstly, Robertson indicated (see paragraph 7.2.2) that his approach was unsuitable for struts with such a high eccentricity of loading. Secondly, the method in itself was known to be on the conservative side (see Fig. 7.14). However, the discrepancy in the eccentric loading experiment in no way invalidates the theory for use in the design of "perfect" scaffolds.

# 8

## CONCLUSIONS AND RECOMMENDATIONS

This concluding chapter falls into three sections. Firstly, recommendations are made for a design procedure which incorporates the theory outlined in earlier chapters. Secondly, it discusses the benefits of this approach and effects of the project in general. Finally there are recommendations for further work which would give additional information to a designer and thus improve the design procedure, hopefully allowing greater loads to be taken on the scaffold.

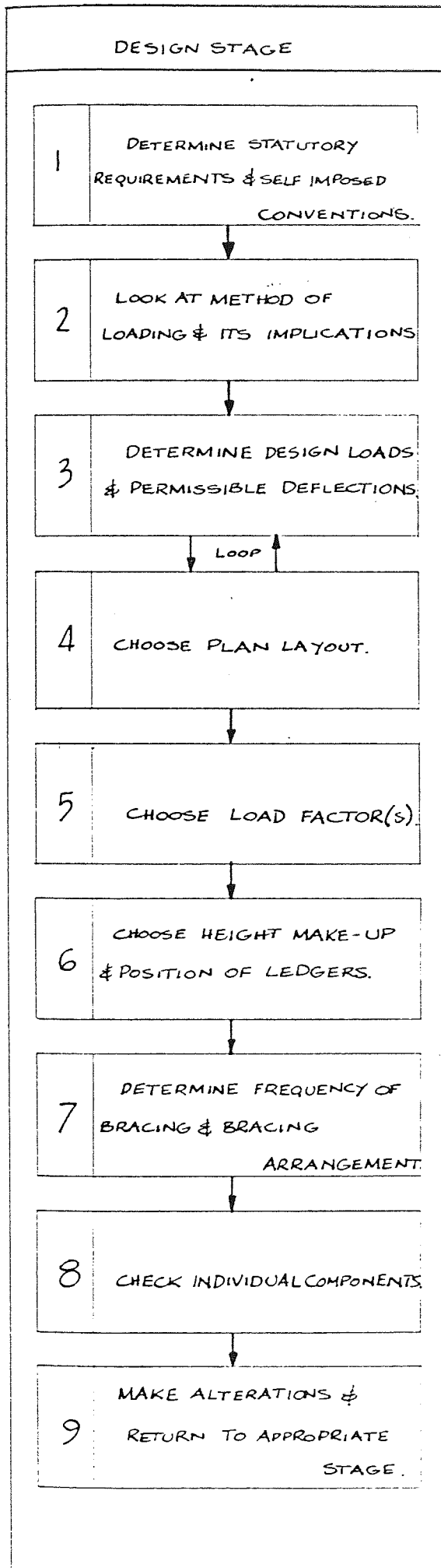
## 8.1 RECOMMENDATIONS FOR A DESIGN PROCEDURE

A general form of the procedure for designing a load bearing falsework is given overleaf in Fig. 8.1. It takes the form of a flow chart although the sequence is not rigid and may vary. For example, the ultimate load-carrying capacity of a vertical may be dependant upon the strength of a base or forkhead in which case item 8 should be immediately after item 2. Alternatively, the load factor used may be dependant on the size of plan grid if the results of recent research are heeded.

## 8.2 THE EFFECTS OF THE PROJECT

This project has already had several effects and, hopefully, these will spread as it is more widely read. The major benefits are :

- a) Since fairly simple analyses have been used, this thesis gives an insight into the behaviour of a scaffold in a manner which the designer can grasp. This is unlike the situation which exists where computer programmes are used to analyse structures and where the designer is often unaware of the implications of design alterations or inbuilt imperfections.
- b) It allows R.M.D. to use their existing equipment more efficiently and with greater confidence. And the greater knowledge that R.M.D. now have about their equipment could provide a market advantage. Furthermore, the fact that they have been seen to be concerned about the safety of their equipment is a definite advantage when dealing with the Health



DETAILS OF WORK DONE AT THIS STAGE.

FOR EXAMPLE:-

- MINIMUM HORIZONTAL LOAD WHICH SCAFFOLD MUST BE ABLE TO RESIST
- METHOD OF BRACING & MAXIMUM FREQUENCY
- WHETHER TO ALLOW FOR DETERIORATION OF MATERIAL
- WHETHER TO ALLOW FOR BAD ERECTION
- ETC.

FOR EXAMPLE:-

- IMPACT LOADS DUE TO DROPPING CONCRETE FROM SKIP
- HORIZONTAL LOADS FROM CONCRETE PUMP
- ETC.

THE LOADS MAY BE FOUND IN A DESIGN BRIEF BUT WILL MORE LIKELY HAVE TO BE CALCULATED (BOTH VERTICALLY AND HORIZONTALLY). AS IN NORMAL STEELWORK DESIGN THEY WILL BE THE ACTUAL IDENTIFIABLE LOADS (SUBJECT TO STAGE 1). AT THIS STAGE THE FORMWORK WILL ALSO HAVE TO BE DESIGNED.

THIS WILL DEPEND ON THE GEOMETRY OF THE SOFFIT AND ALSO THE TYPE OF DECK (i.e. WAFFLE, TROUGHS, PROPRIETARY SYSTEM OR TIMBER & PLYWOOD). ALSO UPON THE MAGNITUDE OF LIVE & DEAD LOADS.

AT THIS POINT IN TIME THIS WILL PROBABLY BE A UNIVERSALLY APPLICABLE FIGURE OF 2.0. HOWEVER, RESEARCH CURRENTLY IN PROGRESS ON THE MEASUREMENT OF SITE LOADS MIGHT WELL SHOW THAT IT IS PRUDENT TO USE DIFFERENT FACTORS FOR SAY SIMPLY-SUPPORTED & CONTINUOUS HEADER BEAMS.

THIS ENABLES THE DESIGNER TO CHECK THE ULTIMATE VERTICAL LOAD-CARRYING CAPACITY USING STANDARD CHARTS. THIS MAY BE DIVIDED BY THE LOAD FACTOR TO OBTAIN SAFE WORKING LOADS. THESE MAY BE COMPARED WITH THE DESIGN LOAD

- CHECK STABILITY AGAINST OVERTURNING OF BRACED BAY
- CHECK ULTIMATE HORIZONTAL LOAD CARRYING CAPACITY
- CHECK DEFLECTION AT WORKING LOAD (IF NECESSARY)
- CHECK VERTICAL LOADS IN MEMBERS ON COMPRESSION SIDE OF BRACED BAY.

FOR EXAMPLE:-

- BASES
- FORKHEADS
- FOUNDATIONS
- SPECIAL DETAILS.

and safety Executive and would be a positive boon in the case of a court action. At the time of writing this thesis the design method shown in Fig. 8.1 is used in an informal way but still using the traditional analysis of section 7.1. But, hopefully, a more formal system can be introduced as soon as the design charts have been produced.

- c) Should R.M.D. ever wish to produce a new system then the information produced during this project would be of use in building additional strength or greater economy into the new system. But since most systems have to be suitable for both access scaffolds and falsework, then it would be advantageous if the work contained in this thesis were extended to include the former.

### 8.3 RECOMMENDATIONS FOR FURTHER WORK

Below is listed a series of topics whose investigation would be beneficial in improving the suggested design method either by increasing its sophistication or by rectifying certain deficiencies. In saying this, the method outlined in this thesis is very useful in giving a qualitative understanding of how the scaffold behaves. The recommendations below would give more quantitative information regarding the use of the scaffold, particularly in adverse circumstances.

1. Assessing the effect of imperfections;
  - a. Determination of the effect of eccentricity of loading on the deflection characteristics and ultimate load-

carrying capacities.

- b. Investigate the effects of omission or bad positioning of bracing. This is important in the study of access scaffolds or badly braced falsework.
- c. Study the variations in scaffold tube physical and mechanical properties.

2. Questions thrown up by the project :

- a. What is the beneficial effect of positional fixity at ledger level on the buckling load of a standard?
- b. Investigate the vertical deflection characteristics.
- c. Investigate the effects of plan rotation.

## REFERENCES

### CHAPTER 1. INTRODUCTION

1. Falsework - Report on the Joint Committee : The Concrete Society, The Institution of Structural Engineers : July 1971.
2. Scaffolding Collapses : G.H. Sprackling : D.O.E. Construction No.2 : June 1972.

### CHAPTER 2. RESEARCH PAST AND PRESENT

3. Tubular Scaffolding (Parts 1, 2 and 3) : R.E. Brand : Concrete and Constructional Engineering : Commencing March 1966, (P107, 149, 439).
4. Falsework and Access Scaffolds in Tubular Steel : R.E. Brand : McGraw-Hill.
5. The Design of Scaffolding Falsework to Support Concrete Bridge Deck Shuttering : Capt. R.C. Obbard : Royal School of Military Engineering : May 1973.
6. Effect of Site Factors on the load capacities of adjustable steel props : C.I.R.I.A. Report No.27 : N. Birch, J.G. Booth and M.B.A. Walker : January 1971.
7. Stability of Tubular Scaffolding : R.E. Brand : Civil Engineering and Public Works Review : Nov. 1973 - Scaffolding Supplement.
8. C.I.R.I.A. Project R.P./179 - Scaffolding : John Laing Research and Development.  
Part 1 - Information Search : February 1973  
Part 2 - Site and Load Surveys, Component Testing : August 1974  
Part 3 - Site measurement of Loads in Scaffolding : Sept. 1975
9. The Behaviour of Scaffold Towers and Assemblies under vertical and under combined and horizontal loading : E. Lightfoot : Stability of Steel Structures. Conference : Liege 13th/15th April 1977.

10. A Test Rig for Couplers : Lightfoot and Bhola : Materiaux et Construction, Vol. 10 - No.57.
11. An Idealization of Scaffold Couplers for Performance Tests and Scaffold Analysis : Lightfoot and Bhola : Materiaux et Construction, Vol. 10 - No.57.
12. Rig for Falsework Tests on Scaffold Towers : E. Lightfoot and D.M. Duggan, Oxford University Report No. 1125/75.
13. The Collapse Strength of Tubular Steel Scaffold Assemblies : Lightfoot and Oliveto : Proc. I.C.E. Part 2 : June 1977 : P311 - 329.
14. Preliminary Investigation of Model Scaffold Towers : Lightfoot and de Villiers : Oxford University Report No. 1035/72.
15. Instability of Space Frames having elastically connected and offset members : Lightfoot and Le Mesurier : 2nd International Conference on Space Structures - University of Surrey : Sept. 1975.
16. Elastic Analysis of Frameworks with Elastic Connections : Lightfoot and Le Mesurier. A.S.C.E. (Structural Division) : June 1974.
17. The Design of Bracing for Scaffolding Falsework using a Deflexion Limit State : Capt. R.E. Obbard : Royal School of Military Engineering : June 1975.
18. R.E.T.N. on Scaffolding Design : Capt. R.E. Obbard.
19. A strain monitoring system for determining forces on falsework : A.R. Price : T.R.R.L. Laboratory : Report 707 (1976).
20. A method of measuring dynamic forces in scaffolding falsework structures : P.C. Ryan : T.R.R.L. Supplementary Report 233 U.C. (1976).
21. Adaption of Perry Formula to Represent the New European Steel Column Curves : J.B. Dwight : Steel Construction, Vol. 9, No.1.



CHAPTER 4. INTRODUCTION TO THEORETICAL ANALYSIS EMPLOYED AND ASSUMPTIONS MADE

22. Adaption of Perry Formula to Represent the New European Steel Column Curves : J.B. Dwight : Steel Construction, Vol. 9, No.1.

CHAPTER 5. THE DEFLECTION OF U.P. SCAFFOLDING UNDER LOAD

23. B.S. 1139. Specification for Metal Scaffolding (1964).

CHAPTER 6. LOAD CARRYING CAPACITY OF A BRACED FRAME

24. Final Report of the Advisory Committee on Falsework : H.M.S.O. : June 1975.
25. Scaffold Falsework Design : M. Grant : A Viewpoint Publication : January 1978.
26. Surface Treatment of High Strength Bolted Joints : G.C. Brookhart, I.H. Siddiqi, D.D. Vasarhelyi : A.S.C.E. (Structural Division) : March 1968, P671.
27. Effect of Surface Coatings and Exposure on Slip : J.H. Lee, C. O'Connor, J.W. Fisher : A.S.C.E. (Structural Division) : November 1969, P2371.

CHAPTER 7. THE BUCKLING OF STANDARDS

28. The Strength of Struts : A. Robertson : I.C.E. Selected Engineering Paper No. 28 (1925).

SUMMARY OF RESULTS OF FULL SCALE ASSEMBLY EXPERIMENTS

Exp. No:	Failure Load		Max. Defn. (mm)	Comments
	V (kN/kg)	(kN)		
1	-	-	2	Scaffold under vertical load only No failure at 88 kN per vertical
2	114	12	Off Scale	Vertical and Horizontal load applied to structure. Failure by buckling of standards B4 then B2, C2.
3	83	28.2	36	Repeat of experiment No.2 with different bracing arrangement. Head jack B4 was found to be 8mm out of plumb. The reason for this was thought to be bad erection so experiment was halted.
4	88	61.0	61	Repeat of Experiment 3. Failure by slipping of couplers. This allowed standards to deform in single curvature over full height. Maximum recorded was 82mm out of straight.
5	88	6.3	75	Repeat of Experiment 4. with eccentricity of load of 25mm. Structure held two layers of concrete + 3% horizontal load but failed before 3rd layer of concrete was positioned. Failure was by slipping of coupler on grid line C.
6	-	-	-	Base/Forkhead extensions reduced to 300mm and unbraced, leaving 2 No.6'6" lifts both cross braced. Concentric loading. Experiment halted when slip of couplers took place at low load. Later discovered some couplers not tightened.
7	88	Unknown	43	Repeat of experiment 6. Failure took place as the last block of third layer of concrete was positioned. Failure was in direction normal to applied load and by slipping of couplers.